ADVANCED JOURNAL OF ENGINERING AND SCIENTIFIC APPLICATIONS (AJESA)

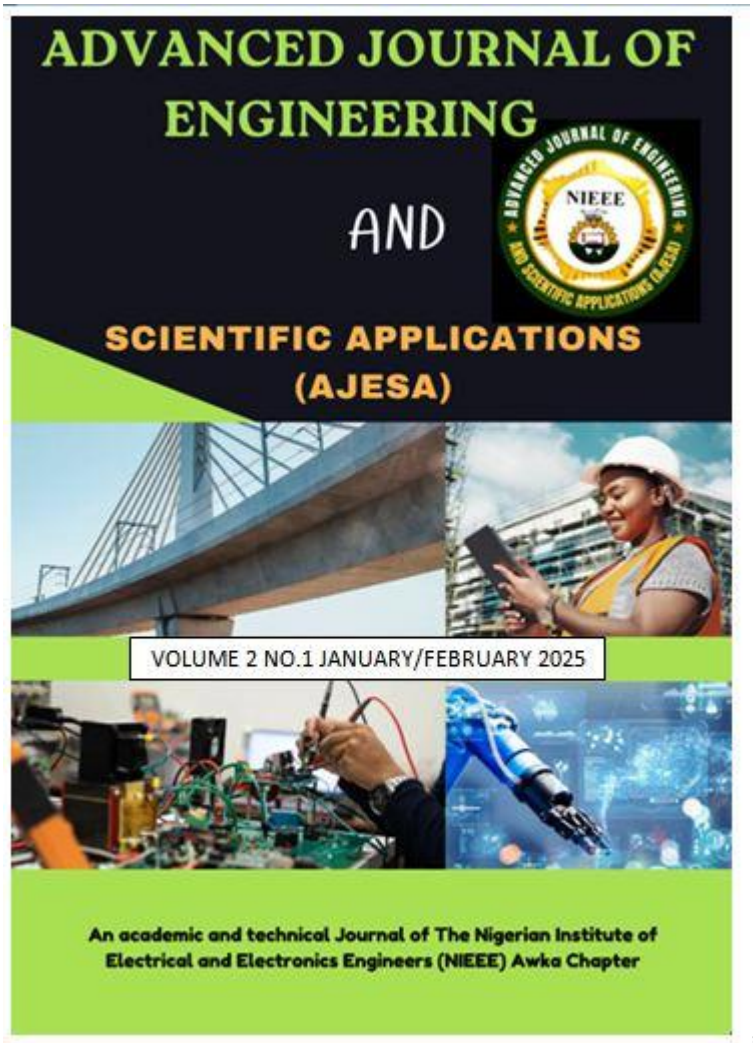

i

Published monthly by the Nigerian Institute of Electrical and Electronic Engineers (NIEEE), Awka Chapter
Nigeria

www.ajesa.com.ng

COPYRIGHT STATEMENT

ADVANCED JOURNAL OF ENGINERING AND SCIENTIFIC APPLICATIONS (AJESA)
Vol. 2 No.1 January/February 2025

Published in Nigeria by:

The Nigerian Institute of Electrical and Electronics Engineering,
Awka Chapter, Anambra State, Nigeria.

info@ajesa.com.ng, ajesajournal@gmail.com
www.ajesa.com.ng, +2348062926794.

EDITORIAL BOARD

© 2025. Advanced Journal of Engineering and Scientific Applications (AJESA) Vol. 2, No..1, 2025.
Published bimonthly by the Nigerian Institute of Electrical and Electronics Engineers (NIEEE) Awka Chapter, Nigeria..

AUTHOR'S GUIDELINES

Instructions to Authors:

1. The manuscript should be prepared in MS-Word with Times New Roman font size 10pt, single-line spaced, and not more than 15 pages, including references, appendices, and tables. The Title of the paper shall be 17 pt Times New Roman while other sub-headings shall be size 12pt New Times Roman.
2. The cover page should contain the title of the manuscript, the author(s) full name(s) and affiliation(s), functional email addresses, and telephone number(s). The cover page should indicate the correspondent author in the case of multiple authors.
3. The manuscript should start with an abstract of not more than 250 words clearly stating the statement of the problem, methodology, findings, and recommendation/contributions to knowledge. The abstract should be followed by a minimum of four key words and a maximum of seven.
4. **For easy guidance on how to prepare your manuscript, please download the Journal Template in MS Word .docx format. You can download the Journal's template at https://www.ajesa.com.ng/AJESA%20Template.docx**
5. Every manuscript will be subjected to a blind peer review, and only those recommended will be accepted for publications.
6. Authors whose manuscripts are accepted will be required to pay a publication fee of **Twenty Five thousand Naira (N25, 000) or Forty US Dollars (USD40).**

The Journal's Bank account details is as follows:

Bank: First Bank Plc
Account Number: 2046289463
Account Name: Advanced Journal of Engineering and Scientific Applications

7. Electronic copies of manuscripts should be sent to **ajesajournal@gmail.com** or **submission@ajesa.com.ng**.
8. **Submission Output:** The Editorial Board of the Advanced Journal of Engineering and Scientific Applications invites the submission of original manuscripts for publication consideration. Manuscripts preferred for inclusion are those from practitioners, *reports of experimental or empirical research, private scholars*, *book reviews/critiques*, and *technical reports*, *expository writing*, including analyses of contemporary issues across the fields of engineering and engineering sciences.

Paper submission is open all month of the year from January to December. All submitted papers will be reviewed by the board of committee of AJESA.

Benefits of Publishing with IJESA:

The benefits of publishing with IJESA include:

- *AJESA is a society-based journal and acceptable by major institutions.*
- *AJESA is Google Scholar indexed as well as in other indexing engines.*
- *AJESA papers are all DOI (Digital Object Identifier) indexed.*
- *All authors will be issued e-certificates after publication.*
- *A hard copy or print of the publication is available on request.*
- *Paper acceptance is within 72 hours after submission.*
- *Plagiarism is not allowed; original research work is encouraged.*

TABLE OF CONTENTS

Published bimonthly by the Nigerian Institute of Electrical and Electronics Engineers (NIEEE) Awka Chapter, Nigeria..

Advanced Journal of Engineering and Scientific Applications (AJESA)

Research Paper Open Access

Available online at www.ajesa.com.ng Vol.2, No.1, January/February 2025.pp.1-8

Predictive Modelling of the physical and mechanical properties of Natural fibre reinforced polymer composites

E.N. Ikezue [1] and J.O. Okoye [2]

[1] *Department Of Chemical Engineering Chukwuemeka Odumegwu Ojukwu University, Uli Anambra State, Nigeria*

Email: en.ikezue@coou.edu.ng

[2] *Department Of Chemical Engineering Enugu State University of Science and Technology Agbani campus-Enugu state, Nigeria*

Abstract

Polymeric composite substances which are based completely on virgin polymer resins are not completely biodegradable and are structurally so bulky for industrial use or application, hence polymer composites which are biodegradable with enhanced or improved mechanical and physical properties fabricated using natural fibres (biomaterials)such as okro (hibiscus esculentus) plantain (musa paradisiaca) and okro (cissus populnea) and a blend of high density polyethylene (HDPE) polymer resins is much desirable and a better alternative to the use of pure polymer resins for industrial and household applications. The work consist of fabricating a polymer composite specimen using the mentioned natural fibres and then testing for the physical and mechanical properties such as thickness swelling (%)water absorption capacity (%) and density (kg/m3) and then tensile strength ,tensile modulus (MPa), flexural strength (MPa) flexural modulus (GPa) elongation at break (%) The fabricated polymer composite specimens exhibited good qualities of high tensile strength of 44.13MPa,58.85MP and 36.80MPa for hibiscus esculentus, cissus populnea and musa paradisiaca respectively with corresponding densities of 0.65kg/m3,0.70kg /m3and 0.82kg/m3,The scenario show that cissus populnea fibre reinforced composite had the highest tensile strength, lower water absorption capacity and lower density .

Keywords: Hydrophilic fibre, hydrophobic polymere fibre reinforcement, mercerization, polymer composites

1. INTRODUCTION

The thermosets and thermoplastic material can be reinforced and made into polymer composite structures. Thermosets were the first to be introduced as matrix to be reinforced with natural fibres (Bledzki et al 2008). Recently developments shifted to thermoplastic matrix composites, this is because thermoplastics are more easily molded in manufacturing technologies (eg injection moulding, extraction, etc.) than reinforced thermosets (Ander, 2006), Another reason for thermoplastics being used as matrix is that they often need the additional strength or additional stiffness gained from reinforcement (Gassan, 1999) (Bledzki et al 2007) compared some common type of thermoplastics with different, properties used as matrix in natural fibre reinforced composites. They concluded that polyethylene (HDPE) were suitable to be matrix in natural fibre reinforced composites because they had lower characteristic temperatures and higher mold shrinkage although their mechanical properties were relatively low. PP and PE is alkyl and hydrogen group. PP has been studied as a matrix in fibre reinforced composites by many researchers because of its low cost and good thermal stability (Bo masden and Hans 2003). other thermoplastics such as polyester amide (PEA), poly (3-hydrobuty rate - co- b hydrovalerate) PHBV polylactic acid [PLA] polyphenylene sulphide (PPS) polyetherether ketone (PEEk) polycarbonate [PC] polyamide 6(PA-6) polybutylene terephthalate has better mechanical properties than PP and PE but also more costly were chosen as matrix for fabricating composite reinforced with natural fibres (water loving characteristics) hence the hydrophobic (water hating) matrix have mould shrinkage which is the amount of shrinking (%)when a polymer is cooled down(Ander,2001) mold shrinkage occur in

all thermoplast materials due to thermal and other contractions in the molecules. rystalline polymers exhibit the worst problems [shrinkage[1-4%] for nylon, HDPE, pp. etc. while amorphous polymer (PC Polystyrene etc.) have less mold shrinkage(Alakali,2009) by introducing natural fibres into polymer matrix, mold shrinkage of composites are all reduced. HDPE and LLDPE have greater stiffness or strength than LDPE. HDPE also has good chemical resistance and excellent stiffness from room temperature to the boiling point of water (1000) the mechanical properties are influenced by the individual mechanical properties of both polymer matrix and fibre reinforcement.

The bonding strength between fibre and polymer matrix in the composite is considered a major factor in order to get a superior fiber reinforcement in composites properties. Because of the pendant hydroxyl and polar group in fibre this leads to extreme high moisture absorption resulting in weak interfacial bonding between the fibre and the hydrophobic polymer matrix. To develop composite with good mechanical properties, chemical modification of the natural fibre (a process called mercerization) is carried out to reduce the hydrophilic behavior of fibre, increase the cellulose content (hence the mechanical properties) and then reduce the moisture absorption capability (Hashim et al,2012). The different surface chemical treatment of natural fibres include but not limited to the following

i. Alkaline treatment

Alkaline treatment is also known as mercerization is one of the most used chemical treatments for natural fibres when used to reinforce thermoplastics and thermo sets (Ikezue, 2016). Addition of aqueous sodium hydroxides (NaoH) to natural fibre promotes the ionization of the hydroxyl group to the alkoxide Fe-oH+ NaoH→ Fibre-O-Na+H2O

This increases the cellulose and hemicelluloses content of fibre there by improving the physical and mechanical properties of fabricated composite.

ii. Silane Treatment

Silane is a chemical compound with chemical formula SiH4. Silane coupling agent may reduce the number of cellulose hydroxyl groups in the fiber-matrix interface. In the presence of moisture hydrolysable alkoxy group leads to the formation of silanol. The silanol then reacts with the hydroxyl group of the fiber forming stable covalent bonds to the cell wall that are chemisorbed onto the fibre surface. This increases the interfacial strength of the fiber.

iii. Acrylation Treatment.

Acrylic acid (CH2=CHCOOH) is also used in graft polymerization to modify fiber surface (Okoye, 2023). The reaction is initated. By free radicals of the cellose molecule.

iv. Permangate Treatment

Permangate is a compound that contains permangate group,MnO4

The permangate treatment leads to the formation of cellulose radical through MnO ion formation. Most treatment are done through potassium permanganate (KMnO4) solution in acetone.

This decreases the hydrophilic tendency of fibre.

2. MATERIALS AND METHODS

2.1 MATERIALS

The three natural fibres, okro, (Hibiscus Esculentus) plantain (musa paradisiaca) and okoho (cissus populnea) were sourced and extracted from a farm land Amechi, Enugu South Local Government Area, Enugu state located at 6.4o North of latitude, 9.52o East of longitude and 197m or 646.33ft of elevation above sea level.

The thermoplastic polymers ie (HDPE) used in the work were supplied by Centre for Composite Research and Development (CCRD) JUNENG Nigeria Ltd. The other materials include sundry chemicals-methanol, glacial acetic acid, triethoxyvinyl silane coupling agent, benzoyl chloride, methylethyl ketone, NaoH pellets, sulphuric acid, acetic anhydride, benzene solution, toluene solution, Ca(oH)2 pellets, peroxide (catalyst), mould release agents, Accelerator (helps in solidification and curing), metal cutter, metal hammer, filling machine (composite cutter) digital weight balance, plastic drum, masking tape, Hounsfield Digital Tensometer, Buck 530 Fourier Transform in fra spectroscopic analyser.

2.2 EXTRACTION OF THE FIBRES

The okro stem fibres were retted in water for 12 days in a mud tank, plaintain pseudo stem fibre were mechanically extracted while okoho bast fibre was retted in water for 21 days in a mud tank. Each of these fibres were dried in air until a constant weight and then subjected to hot KOH treatment and also dried to obtain the single fibre.

2.3 THE MOULDING PROCESS

The ground blend from the compound process were gradually poured into specially made moulds. The surface of the moulds were coated with oleic acid to avoid adhesion of the mixture and for easy removal of the polymer composites. The mixture was then spread equally on the surface of the moulds and allowed to stand for 24hrs at temperatures at ambient condition.

2.4 DETERMINING THE MECHANICAL AND PHYSICAL PROPERTIES OF THE COMPOSITES

The mechanical - Tensile strength, Tensile modulus, flexural strength, flexural modulus and elongation at break were determined using the hounsfied digital tensometer according to ASTM 190-03 and the result were presented in the tables 1.0 for Cissus Populnea, Table 3.0 for Hibiscus Esculentus, and tables 5.0 for Musa paradisiaca fiber. The water absorption capacity and thickness swelling were done according to ASTM D570, the composite samples were immersed in distilled water for 24 hrs at ambient condition and then dried in an oven at 50oc for 24 hrs, stored in a desiccator, the moisture uptake and thickness swelling were determined and presented in table 2.0.

The density were measured using a precision balance (Metlter Toledo model XP 5035, CCRD Nsukka) as seen in table 2.0

3. RESULTS AND DISCUSSION

3.1 RESULTS

The mechanical properties as well as the physical properties of virgin high density polyethylene (HDPE) were shown in Table 4.0, it shows the density g/cm^3 water absorption capacity (%), the flexural modulus (GPa). The tensile strength and the mold shrinkage (%). The physical properties data for the treated and untreated natural fibres of the three plants are presented in Tables 4 and table 2 it is observed that there is tremendous improvement of the physical properties i.e. thickness swelling (%), water absorption capacity (%) and density (Kg/m^3). Also the data on the Tensile Strength (MPa), flexural modulus (GPa) and Elongation at break (%) for the fabricated polymer composites from the three natural fibres are presented in table 1.0 (Cissus populnea fibre), Table 3.0 (Hibiscus Esculentus fiber) and Table 5.0 (Musa Paradisiaca fibre) these data on the three respective Table 1, 3 and 5 were compared with those of the virgin polymer resin Table 4.0 it was observed that there were improvements on the determined mechanical properties.

Table 1: Effect of process variables on the Mechanical Properties of Composites Produced from Treated and Untreated Cissus populnea fibre

Sample	Tensile Strength (Mpa)	Tensile Modulus (Mpa)	Flexural Strength (Mpa)	Flexural Modulus (Gpa)	Elongation@ Break (%)
1	35.53±51^{r}	36.81±.52^{b-e}	20.60±51de	159.47±35^{a}	4.35± 56^{j}
2	39±00^{lm}	36.03±05^{b-g}	21.17±06^{c-e}	142.23±23^{a}	5.04±05^{l}
3	43.6±86^{lm}	27.50±17.32^{i}	20.56±50de	158.04±05^{a}	4.52±02^{j}
4	38.99±84^{lm}	36.23±23^{b-f}	21.20±26^{c-e}	156.10±10^{a}	5.20±10^{hi}
5	53.91±16^{ef}	35.13±05^{i-h}	20.48±46de	145.20±26^{a}	6.03±05^{fg}
6	53.62±03^{f}	36.73±63^{b-e}	22.03±05^{c-e}	130.20±26^{ab}	4.02±01^{jk}
7	37.78±58no	30.66±76^{g-i}	25.20±26^{b-e}	150.40±60^{a}	8.27±23^{b}
8	58.04±91^{a}	37.06±05^{b-e}	21.03±05^{c-e}	155.26±20^{a}	9.00±00^{a}
9	50.72±32^{g}	40.00±05^{abc}	25.73±55^{a-d}	159.10±09^{a}	3.13±05^{l}
10	42.45±55^{j}	40.83±66^{ab}	20.43±51de	155.07±05^{a}	4.10±00^{jk}
11	39.18±94^{lm}	38.06±05^{bcd}	21.13±05^{c-e}	156.26±37^{a}	4.07±05^{jk}
12	31.12±64^{q}	36.16±20^{b-f}	20.36±55de	160.533±45^{a}	5.33±28^{hi}
13	56±85^{bc}	40.40±51^{abc}	22.16±11^{c-e}	158.20±49^{a}	6.20±62^{ef}
14	56.12±64^{bc}	41.23±23^{ab}	23.73±64^{c-e}	158.43±49^{a}	3.20±34^{l}
15	55.34±33^{cd}	45.36±55^{a}	21.13±11^{c-e}	161.37±54^{a}	4.07±05^{jk}
16	37.84±64no	44.03±05^{a}	20.50±00de	160.80±51^{a}	5.33±57^{hi}
17	56.13±11^{bc}	40.00±00^{abc}	21.33±57^{c-e}	155.70±61^{a}	4.10±00^{jk}
18	45.63± 40^{h}	40.84±75^{ab}	30.20±25^{ab}	155.06±05^{a}	5.60±05^{gh}
19	38.1± 01no	38.33±29b^{cd}	31.20±26^{a}	148.33±28^{a}	6.03±05^{fg}
20	56.24± 99^{b}	31.18±23^{f-j}	27.00±00^{abc}	145.40±51^{a}	6.53±05de
21	30.59± 08^{q}	36.78±57^{b-}e	20.60±51de	159.47±35^{a}	4.35±56^{j}
22	30.9±52^{qh}	30.67±58^{g-i}	20.53±57de	153.33±57^{a}	6.80±17^{cd}
23	54.61±5.0^{de}	40.76±66^{ab}	21.86±16.34^{c-e}	160.37±55^{a}	6.30±43^{ef}
24	55.4±00^{bcd}	40.76±66^{ab}	30.90±72^{ab}	155.53±45^{a}	6.03±05i
25	40.81±01^{k}	33.03±05^{d-h}	27.03±05^{abc}	105.53±78.40^{b}	7.13±05^{i}

26	53.16±10^{f}	32.00±00^{e-l}	26.06±05^{a-d}	154.10±10^{a}	3.20±26^{i}
27	41.25±01^{k}	32.40±5.1^{e-l}	27.06±05^{abc}	154.16±15^{a}	5.40±34^{hi}
28	54.55±50de	30.02±02^{b-i}	22.50±00^{c-e}	140.50±60^{a}	4.50±00^{j}
29	54.65±38de	30.02±02^{hi}	21.10±00^{c-e}	140.87±57^{a}	6.26±28^{ef}
30	31.35±04^{q}	30.10±00^{hi}	22.03±05^{c-e}	155.20±17^{a}	7.06±05^{c}
31	39.35±21^{lm}	36.20±26^{b-f}	21.20±26^{c-e}	160.53±45^{a}	3.76±6^{k}
32	58.37±11^{a}	35.20±26^{c-h}	8.03±10.45^{f}	162.86±77^{a}	4.16±28^{jk}
33	56.1±09^{dc}	32.20±26^{c-h}	22.36±55^{c-e}	158.03±05^{a}	5.10±10^{i}
34	44.2±11^{j}	36.70±60^{b-e}	26.10±10^{a-d}	155.10±10^{a}	3.13±05^{l}
35	39.5±43^{l}	40.13±15^{abc}	20.43±51de	143.10±00^{a}	8.16±20^{h}
36	38.52±45^{mn}	36.66±57^{b-e}	22.03±05^{c-e}	130.20±26^{ab}	4.35±56^{j}
37	39.23±11^{lm}	35.08±06^{c-h}	25.03±05^{b-e}	105.36±78.17^{b}	6.06±05^{efg}
38	37.33±31^{o}	36.00±00^{d-g}	19.00±00^{e}	160.67±58a	5.04±06^{i}
39	37.68±27no	40.04±05^{abc}	25.70±61^{a-d}	159.00±00^{a}	3.00±00^{l}
40	37.3±20^{o}	40.83±66^{ab}	20.10±00de	155.07±05^{a}	4.10±00^{jk}

Tensile Strength (Mpa) of Cissus populnea fibre reinforced composite
Tensile Modulus (Mpa) of Cissus populnea fibre reinforced composite
Flexural Strength (Mpa) of Cissus populnea fibre reinforced composite
Flexural Modulus (Gpa) of Cissus populnea fibre reinforced composite
Elongation @ Break (%) of Cissus populnea fibre reinforced composite

Table 2: Physical properties of composites produced from treated and untreated fibres of the three plants

S/N	Sample	Thickness Swelling (%)	Water Absorption Capacity (%)	Density (kg/m^3)
1.	Polymer resin	0.00^{f}	0.00^{f}	0.93^{f}±0.10
2.	Composite produced with untreated CP	3.30^{a}±0.21	1.83^{c}±0.06	0.76^{b}±0.25
3.	Composite produced with CP fibre treated with KOH	2.43^{bc}±0.21	1.83^{c}±0.06	0.76^{b}±02.5
4.	Composite produced with CP fibre with Acetic Anhydride	2.70^{b}±0.26	2.17^{b}±0.21	0.74^{c}±0.15
5.	Composite produced with CP fibre treated with Nitric Acid	3.20^{a}±0.20	2.33^{b}±0.21	0.71^{d}±0.020
6.	Composite produced with untreated HE fibre	2.17^{c}±0.15	1.77^{c}±0.25	0.68^{d}±0.23
7.	Composite produced with HE fibre treated with KOH	1.37^{de}±0.32	1.30^{d}±0.10	0.65^{d}±0.10
8.	Composite produced with HE fibre treated with Acetic Anhydride	1.63^{d}±0.21	1.23^{d}±0.21	0.64^{e}±0.20
9.	Composite produced with HE fibre treated with Nitric Acid	2.20^{c}±0.020	1.63^{c}±0.15	0.66^{d}±0.25
10	Composite produced with untreated MP fibre	1.57^{de}±0.49	0.80^{e}±0.20	0.63^{e}±0.10
11	Composite produced with MP fibre treated with KOH	1.17^{e}±0.15	0.30^{f}±0.10	0.82^{f}±0.15
12	Composite produced with MP fibre treated with Acetic Anhydride	1.50^{de}±0.10	0.30^{f}±0.10	0.80^{f}±0.24
13	Composite produced with MP fibre treated with Nitric Acid	1.70^{d}±0.10	0.73^{e}±0.32	0.78^{f}±0.20

CP=*Cissus populnea,* HE=*Hibiscus esculentus,* MP=*Musa paradisiaca*

Table 3: Effect of process variables on the Mechanical Properties of Composites Produced from Treated and Untreated *Hibiscus esculentus* fibre

Sample	Tensile Strength (Mpa)	Tensile Modulus (Mpa)	Flexural strength (Mpa)	Flexural modulus (Mpa)	Elongation @ break (%)
1	33.08±.80^{cd}	48.20±.17^{cd}	25.16±.05^{im}	150.40±.51^{i}	5.40±.51^{jkl}
2	39.68±.50^{ab}	46.70±.60^{e-h}	25.90±.34^{jkl}	155.53±.45^{fg}	5.70±.34^{h-l}
3	31.87±.00^{cd}	42.21±.25^{n}	26.11±.02^{ijk}	156.10±.00^{ef}	6.10±.01^{g-l}
4	34.03±.02^{cd}	44.33±.20^{m}	27.75±.65^{fg}	160.20±.26^{d}	6.45±.56^{e-j}
5	42.61±.01^{a}	45.67±.58^{h-l}	28.16±.05^{fgh}	160.90±.72^{cd}	6.48±.41^{e-j}
6	42.61±.01^{a}	48.17±.06^{cd}	30.10±.00^{e}	175.36±.63^{a}	7.80±.17^{a-f}
7	40.65±.48^{ab}	53.86±.2.8^{a}	28.40±.51^{fg}	165.70±.60^{b}	7.5±.00^{a-g}
8	31.77±.00de	56.20±.2^{b}	25.04±.05^{mn}	160.17±.06^{d}	8.07±.05^{abc}
9	26±.00^{fg}	58.03±.05^{a}	28.09±.02^{fgh}	161.47±1.17^{cd}	8.08±.07^{a-e}
10	42.16±.00^{ab}	45.04±.05^{u-m}	26.20±.26^{ujk}	162.43±.67^{c}	9.03±.02^{a}
11	32.53±.37^{cd}	40.51±.00^{op}	26.36±.23^{ijk}	155.20±.00^{fgh}	9.05±.00^{a}
12	40.7±.17^{ab}	45.70±.25^{h-l}	26.20±.26^{ijk}	156.10±.00^{ef}	8.16±.28^{a-d}
13	42.07±.06^{ab}	45.25±.26^{i-m}	26.45±.56^{ij}	155.10±.10^{fgh}	8.41±.36^{abc}
14	40.82±.02^{ab}	46.20±.26^{f-j}	26.43±.49^{ij}	145.16±.28j	7.40±.34^{a-g}
15	31.24±.64^{e}	46.20±.26^{d-g}	26.66±.57^{l}	150.36±.55^{i}	7.50±.00^{a-g}
16	42.55±.04^{a}	47.21±.29^{d-g}	20.11±.02^{q}	150.16±.28^{j}	7.00±.00^{c-j}
17	13.11±17.32^{h}	40.44±.000^{op}	20.26±.21^{q}	158.06±.05^{e}	6.50±.00^{d-j}
18	44.19±.00^{a}	44.67±.28^{v-m}	24.38±.33no	156.57±.80^{ef}	6.1±.28^{f-j}
19	32.82±.71^{cd}	41.53±2.57^{no}	24.06±.05^{op}	155.86±.32^{fg}	7.54±.03^{a-g}
20	34.01±.01^{cd}	40.66±.05^{p}	25.03±.05^{mn}	150.83±.28^{i}	7.54±.03^{a-g}
21	30.97±.84^{ef}	47.73±.63^{kde}	30.36±.55^{e}	145.10±.00^{j}	6.26±.28^{f-j}
22	30.43±.75^{def}	48.16±.28^{cd}	30.07±.64^{e}	145.17±.28^{j}	7.00±.00^{c-j}
23	41.22±.29^{ab}	49.20±.17^{cb}	32.06±.05^{c}	156.33±.57^{ef}	4.51±3.43^{kl}
24	32.15±.99^{cd}	49.1±.22^{cb}	31.16±1.25^{d}	156.67±.58^{ef}	7.25±.61^{b-h}
25	37.01±.91^{bc}	49.50±.00^{b}	35.00±.00^{b}	157.00±.50^{ef}	7.70±.00^{a-g}
26	34.24±.21^{cd}	48.23±.32^{cd}	36.17±.28^{a}	140.48±.50^{k}	4.53±3.45^{kl}
27	31.46±.40de	48.40±.34^{cbd}	35.00±.00^{b}	140.96±.83^{k}	6.54±.55^{d-j}
28	25.18±.30^{fg}	46.00±.00^{g-k}	30.38±.24^{e}	140.83±.76^{k}	6.39±.33^{f-j}
29	32.2±.6^{cd}	45.71±.60^{h-l}	30.51±.02^{e}	150.85±.56^{l}	7.11±.02^{b-i}
30	32.3±.20^{cd}	45.0±.00^{j-m}	35.00±.00^{b}	153.46±.05^{h}	7.75±.56^{a-g}
31	31.03±.04^{def}	44.50±.00^{i-m}	26.20±.00^{ijk}	146.50±.00^{j}	4.51±.01^{kl}
32	41.76±.25^{ab}	45.17±.28^{i-m}	25.37±.63^{lm}	145.00±.00^{j}	4.57±.06^{kl}
33	40.22±.20^{ab}	46.01±.01^{g-k}	26.70±.52^{i}	140.33±.57^{k}	5.46±.40^{i-j}
34	29.5±.00^{fg}	45.33±.57^{i-m}	26.67±.58^{j}	140.68±.59^{k}	6.75±.21^{d-j}
35	33.12±.02^{cd}	45.34±.58^{i-m}	7.67±.57^{h}	140.38±.58^{k}	6.73±.25^{d-j}
36	33.28±.24^{cd}	45.34±.58^{i-m}	28.50±.00^{f}	146.00±.86^{j}	8.48±.45^{abc}
37	25.29±.49^{fg}	47.36±.63^{def}	26.37±.23^{ijk}	145.87±.80^{j}	8.71±.25^{ab}
38	26.36±.22^{fg}	48.03±.05^{cd}	25.67±.58^{klm}	154.07±6.02^{gh}	8.73±.55^{ab}
39	40.21±.02^{ab}	46.50±.00^{e-i}	23.40±.00^{p}	158.11±.01^{e}	4.00±.86^{l}
40	43.28±.40^{a}	46.58±.00^{e-i}	23.67±.58^{p}	158.10±.08^{e}	5.53±.50^{i-k}

Tensile Strength (Mpa) of *Musa paradisiaca* fibre reinforced composite
Tensile Modulus (Mpa) of *Musa paradisiaca* fibre reinforced composite
Flexural Strength (Mpa) of *Musa paradisiaca* fibre reinforced composite
Flexural modulus (Gpa) of *Musa paradisiaca* fibre reinforced composite
Elongation @ Break (%) of *Musa paradisiaca* fibre reinforced composite

Table 4: Properties of PE polymers

Thermal and Mechanical Properties	LDPE	PE HDPE	LLDPE
Density (g/cm^3)	0.910-0.925	0.935-0.1	0.918-0 0.940
W_{24h}(%)*	<0.015	<0.01-0.20	
Tg(^{0}C)**	-20-125	-20-110	-120
Tm(^{0}C)***	105-16	120-140	
Tp(^{0}C)****	150-230	150-290	
Mold shrink(%)	1.5-5.0	1.5-5.0	
Specific heat (kJ/kg^{0}C)	1.901-1.989	1.566-2.281	
Tensile strength (MPa)	10-12	14.5-38.0	15-32
Youngs modulus (GPa)	0.055-0.380	0.413-1.490	
Flexural modulus (GPa)		0.41-1.07	
Ultimate tensile strain(%)	90-800	12-1000	

*W_{24h}: Water absorption
**Tg: Glass transition temperature
***Tm: Melt point
****Tp: Process temperature

Table 5: Effect of process variables on the Mechanical Properties of Composites Produced from Treated and Untreated *Musa paradisiaca fibre*

Sample	Tensile Strength (Mpa)	Tensile Modulus (Mpa)	Flexural Strength (Mpa)	Flexural Modulus (Gpa)	Elongation @ Break (%)
1	25.36±55^{op}	45.13±05^{ij}	21.20±00^{d-n}	160.83±05^{f}	5.40±51^{j-l}
2	34.61±01^{d-g}	45.36±23^{hi}	21.55±39^{c-h}	155.50±00^{kl}	5.70±34^{h-k}
3	35.17±28^{cde}	46.20±26^{gh}	20.63±32^{e-h}	155.03±05^{l}	6.10±01^{g-k}
4	26.51±00^{mn}	46.13±98^{gh}	23.33±29^{a-f}	155.67±58^{kl}	6.45±56^{e-j}
5	20.42±01^{s}	46.20±52^{gh}	24.55±00^{a-d}	156.33±57^{jk}	6.48±41^{e-j}
6	20.81±00^{s}	46.80±00^{g}	20.42±03^{c-h}	156.83±76^{hij}	7.80±17^{a-f}
7	33.63±03^{hi}	45.10±00^{ij}	21.44±03^{c-h}	157.67±58^{h}	7.50±00^{a-g}
8	26.22±0^{1mn}	46.13±51^{gh}	22.48±01^{a-g}	159.17±28^{g}	8.07±05^{a-e}
9	35.13±00^{c-f}	45.00±00^{ijk}	20.44±00^{f-h}	160.83±29^{f}	8.08±07^{a-e}
10	25.73±57^{hop}	44.34±57^{jk}	21.45±01^{c-h}	160.70±75^{f}	9.03±02^{a}
11	33.53±40^{l}	44.67±28^{ijk}	25.05±05^{ab}	154.13±63^{m}	9.05±00^{b}
12	26±00^{mno}	45.36±31^{hi}	24.00±00^{a-e}	155.63±77^{kl}	8.16±28^{a-d}
13	25.24±22^{op}	48.17±28^{f}	24.57±06^{a-d}	156.133±98^{jk}	8.41±36^{a-c}
14	33.53±40^{l}	49.54±03^{e}	25.33±57^{a}	156.76±55^{hij}	7.40±34^{a-g}
15	26.67±28^{n}	55.92±88^{bcd}	25.37±54^{a}	156.34±58^{jk}	7.50±00^{a-g}
16	24.33±49^{q}	55.33±29^{d}	24.71±61^{abc}	160.70±75^{f}	7.00±00^{c-j}
17	34.34±56^{ghi}	56.54±45^{b}	25.01±00^{ab}	165.40±10^{fg}	6.50±005^{d-j}
18	34.7±17d-^{g}	56.20±53^{bc}	20.74±56^{e-h}	166.05±52^{d}	6.16±28^{f-j}
19	25.84±.58^{m-p}	55.43±.50^{cd}	21.67±.28^{b-h}	167.75±.30^{c}	7.54±.03^{a-g}
20	27.5±.00^{l}	58.78±.57^{a}	20±.55^{e-h}	148.40±.34^{p}	5.70±.25^{h-k}
21	25.82±.64^{m-p}	44.90±.81^{ijk}	19.00±.00^{gh}	165.33±.57de	6.26±.28^{f-j}
22	27.49±.44^{l}	46.33±.28^{g}	19.67±.28^{gh}	164.86±.80^{e}	7.00±.00^{c-j}
23	26.34±.29^{m-n}	44.70±.51^{hi}	21.10±.77^{d-h}	170.60±.34^{b}	451±.3.43^{kl}
24	20.83±.62^{s}	45.40±.51^{hi}	21.28±.55^{c-h}	175.18±.16^{a}	7.25±.61^{b-h}
25	34.38±.54^{e-h}	44.86±.70^{ijk}	19.70±.61^{gh}	170.79±.44^{b}	7.70±.00^{a-g}
26	35.4±.60^{cd}	46.57±.55^{g}	20.41±.50^{f-h}	165.00±.00^{e}	4.53±.3.45^{kl}
27	20.59±.45^{s}	40.40±.60^{n}	21.03±.05^{e-h}	160.18±.27^{f}	6.54±.55^{d-j}
28	31.03±.89^{j}	44.13±.11^{k}	20.34±.56^{f-h}	160.41±.60^{f}	6.39±.33^{f-j}
29	34.05±.05^{ghi}	40.61±.01^{m}	20.33±.57^{f-h}	170.80±.61^{b}	7.11±.02^{b-j}
30	23.11±.84^{r}	40.61±.01^{m}	19.43±.02^{gh}	170.85±.56^{b}	7.75±.56^{a-g}
31	35.2±.27^{cd}	44.43±.05^{ijk}	20.34±.57^{f-h}	157.36±.63^{hi}	4.51±.01^{kl}
32	27.6±.55^{l}	44.53±.55^{ijk}	20.47±.45^{e-h}	156.50±.50^{ijk}	4.57±.0.6^{KL}
33	36.48±.49^{a}	45.37±.54^{hi}	21.44±.53^{c-h}	156.10±.1.00^{jk}	5.46±.40^{j-k}

34	28.56±.38^{k}	46.35±.56^{g}	19.88±.11^{f-h}	158.60±.55^{g}	6.75±.21^{d-j}
35	35.54±.42^{bc}	44.53±.54^{ijk}	18.57±.97^{h}	149.47±.55^{o}	6.73±.25^{d-j}
36	27.44±.48^{l}	45.34±.58^{hi}	19.03±.02^{gh}	150.54±.58^{n}	8.48±.45^{a-c}
37	25.13±.22^{p}	46.80±.17^{g}	19.20±.26^{gh}	150.86±.72^{n}	8.71±.25^{b}
38	26.51±.5^{mn}	46.83±.14^{g}	21.77±.82^{b-h}	148.19±.07^{p}	8.73±.55^{ab}
39	25.84±.03^{m-p}	48.00±.00^{f}	22.22±.32^{a-g}	149.47±.45^{o}	4.00±.86^{l}
40	36.17±1.20	42.66±.28^{l}	14.58±10.92^{l}	147.33±.58^{q}	5.53±.50^{i-l}

Tensile Strength (Mpa) of *Musa paradisiaca* fibre reinforced composite
Tensile Modulus (Mpa) of *Musa paradisiaca* fibre reinforced composite
Flexural Strength (Mpa) of *Musa paradisiaca* fibre reinforced composite
Flexural modulus (Gpa) of *Musa paradisiaca* fibre reinforced composite
Elongation @ Break (%) of *Musa paradisiaca* fibre reinforced composite

4. CONCLUSION

4.1 Conclusion

From the data on the mechanical properties it was observed that adding fibre to a polymer matrix influenced the properties by improving them ie Tensile Strength, Tensile modulus, flexural strength, flexural modulus and elongation at break. It also lowered the water absorption capacity and the thickness swelling as well as the mold shrinkage. Among the three natural fibre Cissus populnea fibre reinforced polymer composite had the highest mechanical properties improvement. Also the water absorption capacity, thickness swelling properties of the fabricated polymer composites showed that the composite with Hibiscus Esculentus fibre had the least (better) property. The chemical treatments of the three natural fibres helped in increasing the mechanical properties of the produced polymer composites and reducing the moisture uptake or water absorption capacity as well as the thickness swelling of the composites by increasing the cellulose, hemicelluloses content of each of the fibres. These two components of the individual fibres are responsible for the structural strength and mechanical properties.

Acknowledgments

This is to acknowledge the financial support and assistance rendered by Tertiary Education TrustFund (TERTFUND) through the disbursement of the Institution Based Research (IBR)fund year 2018-2023 merged.

References

Abdul Khalil and Syakir, Mil. 2017 Water absorption and thickness swelling of oil palm empty fruit bunch and seaweed composite soil erosion mitigation.

Alakali J.S., Irtwange, S.V and Mkarga, M (2009) Rheological characteristics of food Gum (Cissus Populnea) African J. Food Sci., B (9), 237-242

Ander, C (2001) Carbon fibre reinforced polymers for strengthening of structural elements. PhD thesis Structural Engineering. University of Technology Lulea. Sweden

Ander, T, (2006) Properties of hemp fibre polymer composites: An optimization of fibre properties using novel defibration methods and fibre characterization PhD thesis at Royal Agricultural and Veterinary University of Denmark PP 23-30.

Bledzki A.K Maman, A.A lucka-Crabor, M and Crutowsktav.s (2008) Effects of acetylation on properties of flax fibre and its poly propylene composites express polym. Lett., 2(6), 413-422.

Bledzki A.K., Mamun H., Faruk A.A (2007) Abaca Fibre Reinforced Polymer composites and comparison with juke and flax fibre polymer composites express polymer composite express polymer letters Vol. 1 No.11 PP755-762

Bo masden T. and Hans L., (2003) Physical and Mechanical properties of unidirectional plant fibre composites an evaluation of the influence of porosity, composite Science and Technology Journal Vol.63 PP1265-1272

Gassan, T., and Bledizik, A.K (1999) Possibilities for Imporving the Mechanical Properties of Juke/epoxy composites by alkali treatment of fibres, composites Science and technology, 59 (9), 1309

Hashim, M,Y., Roslan, M.N Amin, A.N Nujahid A., and Zaidi A(2012) Mercerization Treatment Parameter Effect on natural fibre reinforced polymer matrix composite: A brief review. Int. Sch. Sci Res. Innov., 6(8), 1378-1384.

Hossain, S.I, Hasan, M., Hasan, M.N and Hassan A (2013) Effect of Chemical Treatment on Physical, Mechanical and Thermal. Properties of ladies finger natural fibre, Advances in materials Science and Engineering Vol. 1 2013, Article ID 824 274, 6.

Ikezue, E.N (2016) Production and Characterization of some natural fibre Reinforced Thermo set polymer composites PhD Thesis at the Chukwuemeka Odumegwu Ojukwu University Uli-Anambra State Nigeria Pp10- 19.

Okoye ,J. O (2023) Production of Plant based natural fibre reinforced Thermoplastic polymer composites, Evaluation of their process variable and physico-chemical properties PhD Thesis at Chukwuemeka Odumegwu Ojukwu University ULi-Anambra State Nigeria PP112-139.

Advanced Journal of Engineering and Scientific Applications (AJESA)

Research Paper Open Access

Available online at www.ajesa.com.ng **Vol.2, No.1, January/February 2025.pp.9-20**

Technicality of Network Topologies: A Comprehensive Review

Oluharaotu, O.E.[1], Asogwa S.C.[2], Ugwoke, F.N.[3], Etuk E.A.[4]

[1,2,3,4] ***Department of Computer Science, Michael Okpara University of Agriculture Umudike Nigeria***

Corresponding author : [1]osmondo2008@gmail.com

Abstract

Network topology refers to the arrangement or layout of various elements (links, nodes, and devices) within a communication network. It plays a critical role in the performance, scalability, and management of network systems. Various topologies, such as bus, star, ring, mesh, tree, and hybrid, each offer unique advantages and challenges based on factors like data flow, fault tolerance, and resource allocation. This paper explores the technicalities of network topology, examining its impact on network design and operations. It delves into how topology influences data transmission efficiency, redundancy, and scalability, as well as the role of advanced technologies like software-defined networking (SDN) and virtualized network topologies. This paper also discusses the selection criteria for optimal topologies, considering factors such as cost, scalability, security, and ease of maintenance. This paper has provided insights into how modern networks evolve to meet the increasing demands of connectivity and data throughput.

Keywords: Network Architecture; LAN; MAN; WAN; Network Topology; BUS; MESH; RING; Tree; Hybrid; Emerging Trends; SDN; NFV; IoT; 5G; Quantum Networking

1. INTRODUCTION

Network topology refers to the physical and logical arrangement of nodes, devices, and the connections between them within a communication network. It is a crucial factor that influences network design, performance, and scalability. The technical aspects of network topology encompass a variety of considerations, including how data is routed through the network, how devices are interconnected, and how the topology impacts overall network efficiency and reliability.

At its core, network topology determines the structure of a network and directly impacts critical attributes such as data transmission speed, fault tolerance, and redundancy. Traditional topologies like bus, star, ring, and mesh, as well as more advanced and hybrid structures, each have distinct advantages and challenges (Kurose & Ross, 2017). For instance, a star topology centralizes communication through a central hub, simplifying management but introducing a single point of failure. In contrast, a mesh topology, characterized by interconnecting each device with multiple others, offers enhanced fault tolerance and redundancy, though at a higher cost and complexity (Forouzan, 2012).

With the rise of modern networking technologies, such as Software-Defined Networking (SDN) and Virtualized Network Functions (VNF), the traditional concepts of network topology have evolved. SDN allows for more flexible and dynamic network configurations through centralized control planes, enabling administrators to optimize traffic

Flows, increase resilience, and reduce overhead (Seetharaman et al., 2017). Similarly, network virtualization facilitates the abstraction of network components, allowing for the creation of virtual topologies that provide greater flexibility and scalability (Zhang et al., 2018).

In selecting the most appropriate network topology, factors such as cost, scalability, maintenance, and security play critical roles. The growth of data traffic and the demand for high-speed, low-latency connections in applications like cloud computing, IoT, and 5G networks further complicate the choice of topology, requiring a deeper understanding of how topology affects both current and future network performance (Sharma et al., 2020).

This paper explores the technical intricacies of network topology, highlighting the design principles, performance considerations, and the impact of emerging technologies on network structure. It aims to provide insights into how choosing the right topology can enhance the efficiency and resilience of modern communication networks.

2. NETWORK ARCHITECTURE

Network architecture refers to the overall design and structure of a network, which varies depending on its size, geographical coverage, and the number of devices involved. Common types of network architectures include:

Figure 1: Representing Network Architecture

Local Area Network (LAN): A LAN covers a small geographic area, such as a home, office, or campus. It typically connects computers and devices within a limited space and is characterized by high data transfer speeds and low latency. LANs are often built using star or bus topologies (Kurose & Ross, 2017).

Wide Area Network (WAN): A WAN spans a larger geographical area, such as cities, countries, or even continents. WANs connect multiple LANs and MANs (Metropolitan Area Networks) together. Due to the vast distances covered, WANs often rely on public or private leased lines and satellite links. The physical topology of a WAN can be complex, often incorporating mesh or hybrid structures (Forouzan, 2012).

Metropolitan Area Network (MAN): A MAN covers a larger area than a LAN but smaller than a WAN, typically covering a city or a large campus. MANs often connect several LANs within a metropolitan area and are designed to provide high-speed connections over moderate distances, making use of fiber optic or wireless technologies (Tanenbaum & Wetherall, 2011).

Each of these network types has its own architectural considerations regarding performance, scalability, and the necessary infrastructure for communication across varying distances.

3. FUNDAMENTALS OF NETWORK TOPOLOGY

Understanding the core principles of network topology is essential for designing and optimizing network infrastructures. Network topology can be analyzed from different perspectives, including its physical and logical configurations, as well as the various architectural scales in which they operate. Additionally, certain metrics play a significant role in assessing the effectiveness and efficiency of a network topology, guiding network designers in selecting the best structure for specific needs.

(a) Physical and Logical Topologies

Physical Topology refers to the actual layout of network devices and cables. It is the tangible arrangement of physical components such as computers, switches, routers, and cables. Examples of physical topologies include star, bus, ring, and mesh layouts, each representing how devices are physically connected in a network (Tanenbaum & Wetherall, 2011). The physical topology determines how the network components are arranged in space and affects factors such as cabling requirements, device placement, and the network's ability to expand.

Logical Topology, on the other hand, is concerned with the flow of data within the network. It defines the path data takes between devices, irrespective of the physical arrangement of components. Logical topology is crucial because it impacts data transmission and network protocols. For example, a network might have a physical star topology, but the logical topology could resemble a bus, where data travels in a single direction along the network (Forouzan, 2012). The logical topology influences factors such as network traffic flow, collision domains, and the behavior of data during transmission.

C. Network Topology Metrics

When evaluating network topologies, certain metrics are important in determining the suitability of a design for particular use cases. These metrics help assess the network's performance, scalability, and overall efficiency.

1. Distance: This refers to the physical length of the network and the distance over which data must travel. In LANs, distance is generally short, but in WANs, the distance can span hundreds or even thousands of kilometers. The topology chosen can impact the efficiency of data transmission across these distances. For instance, a star topology in a LAN reduces the distance each device needs to communicate with the central hub, while in a WAN, long-distance communication may involve more complex topologies like mesh or hybrid designs (Kurose & Ross, 2017).

2. Connectivity: Connectivity refers to how devices within the network are linked together and how data is transmitted between them. High connectivity generally means greater reliability and redundancy. For example, a mesh topology provides high connectivity because each node is connected to multiple other nodes, ensuring that if one path fails, an alternative path is available (Forouzan, 2012). In contrast, a bus topology may have limited connectivity, and a failure in the central bus could disrupt the entire network.

3. Scalability: Scalability is the network's ability to grow and handle increased loads or additional devices without a significant drop in performance. A topology that offers easy scalability allows for the addition of new nodes or links without requiring a major redesign. For example, star topologies are highly scalable since adding new devices usually involves only connecting them to the central hub (Tanenbaum & Wetherall, 2011). In contrast, bus topologies are less scalable because adding more devices can lead to data collisions and bandwidth limitations, impacting performance as the network grows.

D. Types of Network Topologies

Network topology refers to the physical or logical arrangement of devices in a network, and it can be classified into several different types. Each topology has its unique advantages and disadvantages, making it suitable for different types of network requirements. Below, we explore four common network topologies—bus, star, ring, and mesh—with a focus on their advantages, disadvantages, and typical applications.

1. Bus Topology

Description: In bus topology, all devices (nodes) are connected to a single central cable, called the "bus" or backbone. Data sent by any device travels along the bus and is received by all other devices, though only the intended recipient processes the data.

Published bimonthly by the Nigerian Institute of Electrical and Electronics Engineers (NIEEE) Awka Chapter, Nigeria..

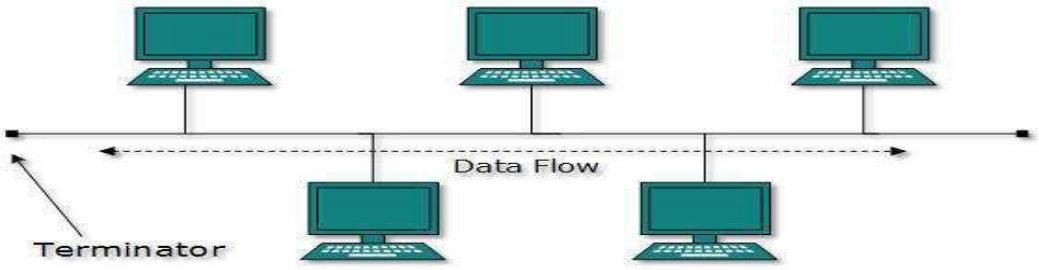

Figure 2: Represents of how devices are connected in bus topology and how data flows from one end to another.

Advantages:

Cost-Effective: Bus topology requires fewer cables than star topology and is thus more economical to set up, especially for small networks.

Easy to Implement and Extend: The simplicity of connecting new devices makes it easy to implement and extend.

Minimal Cabling: Since there is a single backbone, the amount of cable required is lower than in other topologies, reducing installation costs.

Disadvantages:

Single Point of Failure: If the central bus cable fails, the entire network is disrupted, making it less reliable.

Scalability Issues: Performance degrades as more devices are added, especially with increased network traffic.

Limited Performance: The shared bus can cause data collisions as only one device can transmit at a time, reducing network speed and efficiency in busy networks.

Applications:

Small networks: Suitable for small offices or local area networks (LANs) with few devices.

Temporary networks: Ideal for temporary setups or when the network size is not expected to grow substantially.

Legacy systems: Used in older network systems before more sophisticated technologies were developed.

2. Star Topology

Description: In star topology, all devices are connected to a central device, typically a hub or a switch. Data travels from the source device to the central hub, which then forwards it to the destination device.

Figure 3: Representation of how devices are connected in Star topology and how data flows in loop.

Advantages:

Reliability: If one device fails, the rest of the network continues to function, making it more fault-tolerant.

Ease of Management: The central hub simplifies network management, as issues can be isolated more easily.

Scalable: Adding new devices is simple—just connect them to the central hub without affecting the rest of the network.

Disadvantages:

Single Point of Failure: The central hub or switch is critical—if it fails, the entire network is down.

Higher Cost: Requires more cabling and network hardware (central hub/switch), making it more expensive than bus topology.

Dependence on Central Hub: The performance of the network is dependent on the capacity and efficiency of the central device.

Applications:

Home and office networks: Star topology is widely used in small and medium-sized networks due to its simplicity and scalability.

Enterprise networks: It is often the topology of choice in businesses, where central management and ease of expansion are necessary.

Wi-Fi networks: Wireless access points can serve as hubs in a star topology for wireless networks.

3. Ring Topology

Description: In a ring topology, each device is connected to two other devices, forming a continuous loop. Data travels in one direction (or sometimes two directions in a dual-ring setup) around the ring until it reaches the intended recipient.

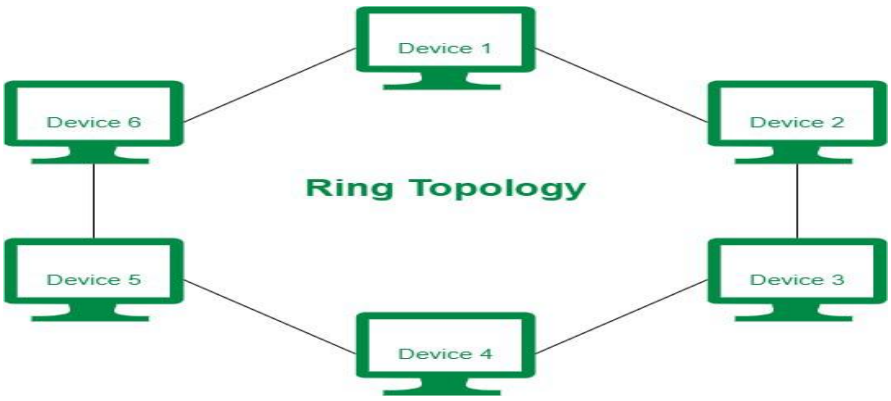

Figure 4: Representation of Ring topology and how data flows in loop

Advantages:

Data Integrity: Data travels in a consistent, circular manner, which can make the flow of data predictable and orderly.

No Data Collisions: Since each device can only transmit after receiving a signal from its predecessor, data collisions are minimized.

Simple to Install: The ring structure is easy to implement, especially in small-to-medium-sized networks.

Disadvantages:

Single Point of Failure: If one device or cable fails, the entire network can be disrupted unless a dual-ring or fault-tolerant mechanism is in place.

Data Transmission Delays: As the number of devices in the ring increases, data transmission speed can decrease due to longer travel times around the loop.

Difficult to Troubleshoot: Since data passes through all devices in the ring, pinpointing the cause of failure can be challenging.

Applications:

Token Ring Networks: Historically used in older office networks, such as IBM's Token Ring technology.

Fiber Optic Networks: Often used in long-distance communication networks, where high-speed transmission is critical, and fault tolerance can be implemented (e.g., dual-ring configurations).

Small-to-Medium Sized Networks: Suitable for networks where data integrity and predictable data flow are important.

4. Mesh Topology

Description: In mesh topology, every device in the network is connected to every other device, creating a fully interconnected system. This structure provides multiple paths for data to travel, increasing the redundancy and reliability of the network.

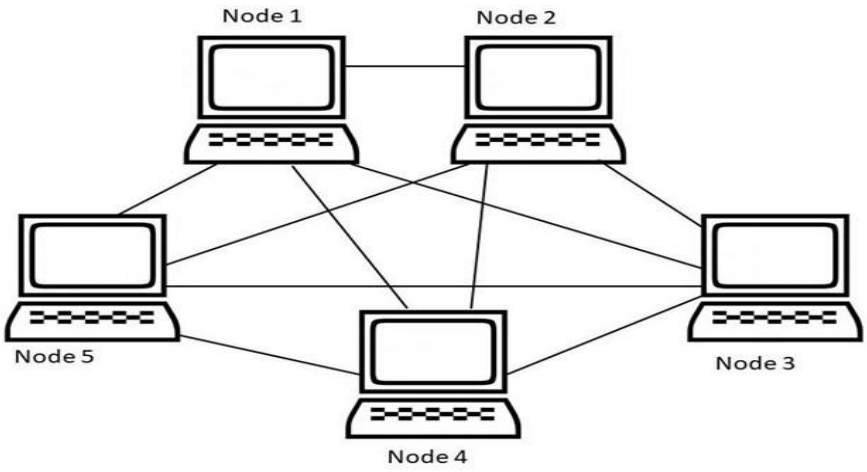

Figure 5: Represents of how devices are connected in Mesh topology and how data flows in devices.

Advantages:

Fault Tolerance: If one connection fails, data can still be transmitted through other paths, ensuring high availability and reliability.

Scalability: Mesh topology can handle large networks effectively by adding more devices and connections without significant performance degradation.

High Redundancy: Each device has multiple routes to communicate, which makes the network highly robust against failures.

Disadvantages:

Complexity: The wiring and configuration of mesh networks are more complex, requiring significant resources to implement and maintain.

High Cost: The need for multiple connections between devices increases both the cost of setup and maintenance.

Management Overhead: As the network grows, the complexity of managing and troubleshooting increases exponentially.

Applications:

Large-scale Networks: Used in large enterprise networks, where reliability and redundancy are critical.

Telecommunications Networks: Often used in backbone networks, where a high level of fault tolerance is necessary.

Military and Critical Systems: Essential in environments where network reliability and uptime are non-negotiable.

Tree Topology:

The network is divided into several levels/layers using this topology. A network is divided into 3 categories of network devices, mostly in LANs. The lowest layer is the access layer, which is where systems are linked. The distribution layer is the intermediate layer that acts as a link between the top and lower layer. The topmost layer, referred as core layer, is the network's nerve center. A point-to-point link exists between all nearby hosts. In a similar way as the bus, topology, in case if the root fails the whole network faces the problem. It is not, however, the only site of failure. Every connection acts as a single point of failure, separating the network in segments, which are inaccessible if it fails. Figure 6 represents of how devices are connected in tree topology and how data flows in devices.

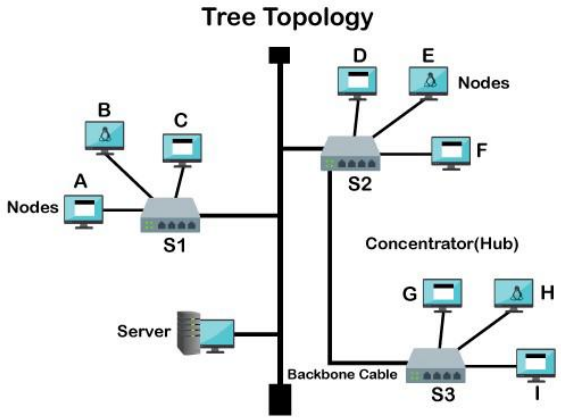

Figure 6: Representation of how devices are connected in tree topology and how data flows in devices.

Hybrid Topology:

It can be said as combination of several topologies. These are commonly used in big Multinational industries where there are personalized topologies for each department. These provide a great flexibility to the network system. Different topologies can be chosen and implement according to the needs and requirement of the user. Figure 7 represents how devices are linked in hybrid topology using an arrangement of star, ring and bus topology.

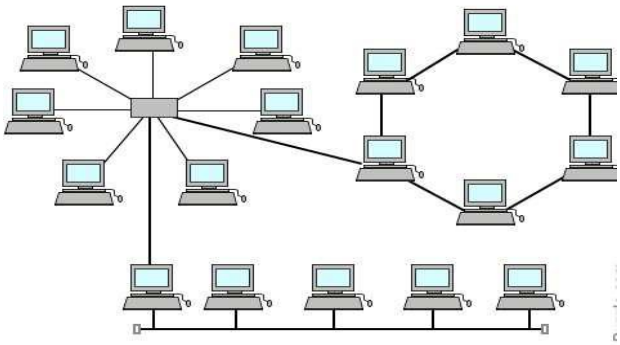

Figure 7: Representation of how devices are linked in hybrid topology using an arrangement of star, ring and bus topology.

4. IMPLICATIONS OF NETWORK TOPOLOGY ON NETWORK SECURITY

Network topology refers to the arrangement of various elements (links, nodes, devices) in a network. It plays a critical role in the network's overall performance, reliability, and, importantly, its security. The structure of a network can

either expose vulnerabilities or strengthen the system against potential security threats. Below, we explore how different topologies impact network security, the types of security threats, and the effectiveness of security measures like firewalls and intrusion detection systems.

1. Network Topology's Impact on Security Threats

a. Eavesdropping (Interception of Traffic)

Eavesdropping refers to the unauthorized interception of data as it traverses the network. Depending on the topology, certain network paths or segments may be more exposed to such threats.

Bus Topology: In this topology, data travels along a single shared medium (the bus), meaning any device connected to the bus can potentially intercept the data. This makes it vulnerable to eavesdropping, especially in unencrypted communication environments.

Star Topology: While star topology centralizes communication through a central switch or hub, it can be more secure compared to bus topology. However, the central device (like a switch or router) becomes a critical point of vulnerability. If an attacker compromises this device, they could intercept data from all connected devices.

Mesh Topology: This topology, with direct connections between multiple devices, can provide better security by creating redundant paths, making it harder for an attacker to intercept traffic. However, it may also introduce complexity in managing secure connections between numerous devices.

b. Spoofing (Impersonating a Device or User)

Spoofing occurs when an attacker impersonates another device or user on the network, potentially gaining unauthorized access to resources or launching further attacks.

Bus Topology: In bus topologies, devices connected to the same physical medium may be more susceptible to spoofing. Since the data is broadcasted, an attacker could easily inject malicious packets or spoof the MAC or IP address of legitimate devices.

Star Topology: Centralized devices like switches or routers can mitigate spoofing to some extent. However, an attacker could spoof the IP or MAC address of a legitimate device and gain unauthorized access if proper authentication mechanisms are not in place.

Mesh Topology: While mesh networks offer redundancy and resilience, spoofing can still occur if devices communicate through unsecured channels or without strong authentication. The complexity of the network also increases the potential for misconfigurations that attackers could exploit.

c. Denial of Service (DoS)

Denial of Service (DoS) attacks aim to disrupt network services by overwhelming the target with excessive traffic or exploiting network vulnerabilities.

Bus Topology: A DoS attack targeting the bus or shared medium can potentially disrupt the entire network. Since all devices share the same communication channel, a single point of failure can lead to widespread disruption.

Star Topology: A DoS attack targeting the central hub or switch can impact all connected devices, as the hub becomes the central point of failure. A well-placed attack on this device can render the entire network inaccessible.

Mesh Topology: Mesh topologies are more resilient to DoS attacks due to redundant paths. However, if an attacker targets key nodes or floods a central device, such as a router or gateway, the impact can still be significant.

2. Security Measures and Their Effectiveness

To mitigate the risks associated with different network topologies, several security measures can be implemented. These measures provide protection against common threats like eavesdropping, spoofing, and DoS attacks.

a. Firewalls

Firewalls act as a barrier between trusted internal networks and untrusted external networks (e.g., the internet). They monitor and filter incoming and outgoing traffic based on predefined security rules.

In Star Topology: Firewalls are typically placed at the entry or exit points of the central hub (usually at the router or gateway). This configuration can effectively protect the entire network from external threats.

In Mesh Topology: Firewalls can be distributed across different nodes, providing more granular control over traffic. However, the complexity of the network means that configuring and maintaining firewalls on each node can be resource-intensive.

b. Intrusion Detection Systems (IDS) / Intrusion Prevention Systems (IPS)

IDS/IPS are designed to detect or prevent suspicious activity and security breaches by monitoring network traffic for signs of malicious behavior.

In Star Topology: IDS/IPS systems can be deployed at the central switch or router. Since all traffic flows through the central hub, it becomes easier to monitor and detect threats at a single point.

In Mesh Topology: The distributed nature of mesh networks may require IDS/IPS systems at multiple points in the network, potentially increasing the complexity of detection. However, this also means that the system can provide more detailed insights into potential threats across different paths in the network.

c. Encryption and Authentication

Encryption ensures that data is unreadable to unauthorized users, while authentication ensures that only legitimate users or devices can access the network.

In Star Topology: End-to-end encryption can be implemented between devices and the central hub to prevent eavesdropping. Strong authentication mechanisms should be enforced at the central device to prevent unauthorized access.

In Bus and Mesh Topologies: Encryption can be implemented to secure the shared communication medium (in bus topology) or to protect communication across multiple devices (in mesh topology). Proper authentication protocols must also be established to mitigate spoofing risks.

3. Topology-Related Security Vulnerabilities

Certain network topologies have inherent vulnerabilities that could be exploited by attackers. Here, we explore some of the security risks tied to specific topologies:

a. Bus Topology Vulnerabilities

Single Point of Failure: The shared medium makes the entire network vulnerable if the bus or cable is compromised. If an attacker gains physical access to the medium, they could intercept or manipulate all data.

Lack of Segmentation: Without proper segmentation, an attacker who gains access to one device may be able to easily access other devices.

b. Star Topology Vulnerabilities

Centralized Vulnerability: The central hub (such as a switch or router) becomes a single point of failure. If the hub is compromised, the entire network is at risk.

Vulnerable to DoS Attacks: Since all communication passes through the central hub, any attack targeting this hub could disrupt the entire network.

c. Mesh Topology Vulnerabilities

Complex Management: With multiple redundant paths, mesh networks can become difficult to manage and configure. Misconfigurations or insecure devices could open multiple attack vectors.

Increased Surface Area: The large number of direct connections between nodes increases the number of potential points of entry for an attacker, making the network harder to secure comprehensively.

5. EMERGING TRENDS IN NETWORK TOPOLOGY AND ITS ROLE

The future of network topology is evolving rapidly with the advent of new technologies such as Software-Defined Networking (SDN), Network Functions Virtualization (NFV), and the increasing adoption of Internet of Things (IoT) devices and 5G networks. These emerging trends promise to transform the way networks are designed, managed, and secured. However, they also introduce a set of new challenges and open research questions that need to be addressed to ensure efficient, scalable, and reliable network infrastructures.

1. Software-Defined Networking (SDN)

(a) Overview: SDN separates the control plane from the data plane in networking, centralizing the network control in software-based controllers. This allows for more dynamic and programmable network management, where network policies can be applied centrally, making it easier to adjust routing, traffic flow, and security configurations.

(b) Impact on Topology: SDN enables more flexible and optimized network topologies that can adapt to changing conditions. Networks can be reconfigured on-demand, allowing for better management of resources and traffic patterns.

(c) Security in SDN: The centralized nature of SDN makes it an attractive target for attacks. Research into securing SDN controllers and data flows is critical.

(d) Research Directions: How to scale SDN architectures in large-scale, high-performance networks without sacrificing efficiency.

2. Network Functions Virtualization (NFV)

(a) Overview: NFV decouples network functions (e.g., firewalls, load balancing, routing) from proprietary hardware and runs them on standard servers. This allows for greater flexibility, cost savings, and scalability.

(b) Impact on Topology: NFV allows for dynamic network topologies where functions can be instantiated and decommissioned as needed. This increases the ability to adapt to traffic demands and fault tolerance.

(c) Research Directions: Designing and optimizing virtual topologies that can dynamically scale based on service demand and resource availability.

3. Internet of Things (IoT)

(a) Overview: Internet of Things (IoT) networking refers to the interconnection of physical devices, vehicles, buildings, and other items embedded with sensors, software, and network connectivity, enabling data exchange and automation. It improves efficiency, productivity and inform better decision making.

(b) Impact/Challenges: IoT networks are composed of various types of devices with different capabilities, which complicates network design. Data traffic and routing: Managing the massive data traffic generated by IoT devices in a scalable and efficient way.

(c) Research Directions: Designing network topologies that are optimized for IoT devices, such as low-power wide-area networks (LPWANs) or edge networks that process data closer to the source.

4. 5G Networks

(a) Overview: 5G represents the fifth generation of mobile networks, with promises of ultra-low latency, massive device connectivity, and high-speed data transmission. The network topologies for 5G will need to handle diverse use cases, including autonomous vehicles, smart cities, and augmented reality.

(b) Impact/Challenges: Ultra-reliable low-latency communication (URLLC): Ensuring high reliability and low latency for mission-critical applications like autonomous driving or remote surgery.

Massive device density: 5G will support a vast number of devices in a dense environment, raising questions about how to manage such a large number of simultaneous connections.

(c) Research Directions: Investigating how to partition a physical 5G network into multiple virtual networks (slices) optimized for different applications.

6. CONCLUSIONS

In conclusion, network topology is far more than just an organizational chart of how devices are connected; it directly impacts network performance, security, and scalability. As networks become increasingly complex with the rise of IoT, 5G, and cloud services, understanding and optimizing network topologies will be key to addressing current and future challenges in data management, security, and efficient service delivery.

Network topology plays a pivotal role in shaping the performance, scalability, and security of modern networks. The structure of a network—whether it's star, mesh, bus, or more dynamic configurations like Software-Defined Networks (SDN)—influences how data flows, how vulnerabilities are managed, and how easily a network can adapt to new demands.

Network Security is heavily influenced by topology. Centralized networks like those using star topology may have more straightforward security management, but they are also more vulnerable to attacks targeting the central hub. More complex networks, like those using mesh topology, offer redundancy and fault tolerance but are harder to secure.

The emergence of SDN and NFV is revolutionizing how networks are designed and managed. These technologies enable flexible, dynamic topologies that can scale with demand and adapt to changes on the fly, but they also present challenges in terms of scalability, reliability, and security.

Future applications such as IoT and 5G networks will require entirely new approaches to network topology. These applications demand ultra-low latency, high device density, and efficient management of massive amounts of data traffic, further emphasizing the need for innovative topologies.

References

1.Abdullah Khan (2023). Computer Networking Topologies. University Of Education, Lahore. https://www.researchgate.net/publication/369020366

2.Bangerter, S. Talwar, R. Arefi, and K. Stewart, (2014). "Networks and Devices for the 5G Era," IEEE Commun. Mag., 2014,

3.Deshpande, V., H. Badis, and L. George, (2018). "BTCmap: Mapping Bitcoin Peer-to-Peer Network Topology," in 2018 IFIP/IEEE International Conference on Performance Evaluation and Modeling in Wired and Wireless Networks, PEMWN 2018.

4.Diego, X., L. Marcon, P. Müller, and J. Sharpe, (2018). "Key Features of Turing Systems are Determined Purely by Network Topology," Phys. Rev. X,

5.Engels, G. (2018), "Clinical Pain and Functional Network Topology in Parkinson's Disease: A Resting-State fMRI Study," J. Neural Transm.,

6.Forouzan, B. A. (2012). Data Communications and Networking (5th Ed.). McGraw-Hill Edu.

7.Harrington D. L. (2015). "Network Topology and Functional Connectivity Disturbances Precede the Onset of Huntington's Disease," Brain,

8.Heasley, E., N. Clifford, and J. Millington, (2018). "Integrating Network Topology Metrics into Studies of Catchment-Level Effects on Habitat Diversity," Hydrol. Earth Syst. Sci. Discuss., 2018,

9.Kurose, J. F., & Ross, K. W. (2017). Computer Networking: A Top-Down Approach (7th Ed.). Pearson.

10.Ozkan-Canbolat, E. and A. Beraha, (2016). "Configuration and Innovation Related Network Topology," J. Innov. Knowl.,

11.Ozkan-Canbolat E. and A. Beraha, (2016). "A Configurational Approach to Network Topology Design for Product Innovation," J. Bus. Res.,

12.Rosell-Tarragó, E. Cozzo, and A. Díaz-Guilera, "A Complex Network Framework to Model Cognition: Unveiling Correlation Structures from Connectivity," Complexity,

13.Seetharaman, P., et al. (2017). "Software-Defined Networking: A Survey of Issues and Challenges." IEEE Communications Surveys & Tutorials, 19(3), 1992–2014.

14.Sharma, S., et al. (2020). "Design and Analysis of Network Topologies for Internet of Things." IEEE Access, 8, 43253–43262.

15.Tanenbaum, A. S., & Wetherall, D. J. (2011). Computer Networks (5th Ed.). Prentice Hall.

16.Wierenga, L. M. et al., (2018). “A Multisampling Study of Longitudinal Changes in Brain Network Architecture in 4–13-year-old children,” Hum. Brain Map.,

17.Zhang, Y., et al. (2018). "Virtualized Network Topologies for SDN-Based Cloud Data Centers."

Advanced Journal of Engineering and Scientific Applications (AJESA)

Research Paper Open Access

Available online at www.ajesa.com.ng Vol.2, No.1, 2025.pp.21-27

A Computational Framework for Smart Grid Tampering Detection Using Unsupervised Machine Learning

[1]B.O.Osuesu, [2]G.O. Asoronye, [3]Ilokanuno O., [4]B.J. Robert, [5]A.C. Okafor, [6]R.I. Ogbuikwu and [7]N.J. Akpan

[1]Electrical Electronic Engineering Department, Akanu Ibiam Federal Polytechnic Unwana, Afikpo, Ebonyi State, Nigeria

[2]Computer Engineering Department, ,Akanu Ibiam Federal Polytechnic Unwana, Afikpo, Ebonyi State, Nigeria

[3]Electronic and Computer Engineering Department, Nnamdi Azikiwe University, Awka, Nigeria

[4]Electrical Electronic Engineering Department, Akanu Ibiam Federal Polytechnic Unwana, Afikpo, Ebonyi State, Nigeria

[5,6,7]Electrical Electronic Engineering Department, Federal Polytechnic Ohodo, Enugu State, Nigeria

***Corresponding Author: [2]asorgay@gmail.com**

Abstract

This paper presents a computational framework for detecting tampering in smart grids using unsupervised machine learning algorithms. Leveraging Advanced Metering Infrastructure (AMI) and integrating algorithms such as K-Nearest Neighbourhood with Isolation Forest (KNN + IF), Local Outlier Factor (LOF), and Lightweight Online Detector of Anomaly (LODA), the framework achieves robust tampering detection. Experimental evaluations on a smart grid IoT Coordinating Infrastructure (SG_IoT_CI) showed that the proposed system significantly improved tampering detection accuracy, achieving up to 31.11% accuracy with KNN + IF compared to lower-performing methods. Additionally, the framework demonstrated enhanced service rates, with KNN + IF yielding a 35.09% improvement and LODA achieving the highest throughput at 28.12%. Latency was reduced by 11.98% for KNN + IF and 8.98% for LODA. These results underscore the efficiency of the proposed approach in addressing zero-day attacks and reducing false positives, paving the way for scalable and secure smart grid ecosystems.

Keywords: Smart Grid Security, Tampering Detection, Unsupervised Machine Learning, Advanced Metering Infrastructure (AMI), Anomaly Detection

1. INTRODUCTION

Smart grids are advanced electrical systems that integrate digital communication technologies with traditional power grids to enhance their efficiency, reliability, and sustainability (Teixeira et al., 2020). Key components include the Advanced Metering Infrastructure (AMI) (Guerrero et al., 2023), which enables two-way communication between utility providers and consumers and Distributed Energy Resources (DER) (Liu et al., 2024), which incorporate renewable energy sources like solar and wind into the grid (Bhutta et al., 2024). Another critical aspect is the Internet of Things (IoT) which facilitates real-time monitoring and control of grid operations by connecting devices and sensors across the network (Chen et al., 2019). Despite their numerous advantages, smart grids face persistent challenges, including tampering (Bhattacharjee et al., 2017), which undermines their reliability and security (Dehghani et al., 2023).

Tampering in smart grids refers to unauthorized activities, such as energy theft, manipulation of meter readings, or disruption of grid components (Althobaiti et al., 2021). This not only causes significant financial losses to utility providers but also compromises the stability of power supply. In countries like Nigeria, where energy theft is prevalent, tampering exacerbates existing issues such as inadequate power distribution and frequent outages (Althobaiti et al.,

2021). Cyber-attacks targeting the communication and control systems of smart grids further escalate the risks, making it imperative to address these vulnerabilities (Sahani et al., 2023).

Traditional tampering detection methods rely heavily on rule-based systems and supervised machine learning models, which are often limited in their ability to adapt to dynamic and evolving threats. Rule-based systems depend on predefined patterns, making them ineffective against novel or complex tampering scenarios (Liu et al., 2021). Supervised machine learning models, on the other hand, require extensive labeled datasets for training, which are not always available or reliable (Khalid et al., 2024). Additionally, these models often struggle with high false-positive rates, leading to unnecessary interventions and reduced trust in the system (Husnoo et al., 2024). Another limitation is the lack of scalability in existing solutions (Zhang et al., 2023). As smart grids expand to accommodate more consumers and integrate additional renewable energy sources, the volume and complexity of data increase exponentially. Many traditional systems are unable to process this data efficiently, resulting in delayed or inaccurate tampering detection (Radoglou-Grammatikis et al., 2020). Furthermore, these systems often fail to account for privacy concerns, as they rely on detailed consumer energy usage data for analysis (Samanthula & Patel, 2023). This can deter consumers from adopting smart grid technologies, thereby hindering their widespread implementation. In this context, unsupervised machine learning algorithms offer a promising alternative (Almalki, 2024). Unlike supervised models, unsupervised algorithms do not require labeled data, making them suitable for identifying anomalies in real-time. By analyzing patterns and deviations in energy consumption data, these algorithms can detect tampering activities without prior knowledge of their specific characteristics (Zhang et al., 2023). Additionally, integrating unsupervised learning with IoT and cloud computing infrastructure enhances the scalability and efficiency of detection systems, enabling them to address the challenges posed by large-scale smart grid deployments (Mohammadi et al., 2023). This paper introduces a computational framework that leverages unsupervised machine learning to detect tampering in smart grids. By addressing the limitations of existing solutions, the proposed framework aims to enhance the security and reliability of smart grid ecosystems, paving the way for their sustainable growth and adoption.

1.1 Related Works

Machine learning techniques have increasingly become pivotal in addressing cybersecurity challenges within smart grid ecosystems (Bhutta et al., 2024), particularly in detecting electricity theft and anomalous behaviors. Recent research has explored diverse approaches to tackle the complex problem of smart grid security detection.

1.2 Machine Learning Approaches for Anomaly Detection

Contemporary studies have demonstrated significant advancements in electricity theft detection methodologies. Li et al.,(2019) proposed a Deep Neural Network (DNN) model that effectively resolved dimensionality challenges and selected critical features for fraud detection in smart grid systems. Similarly, Iftikhar et al.,(2024) developed a hybrid deep learning model combining Multi-Layer Perceptron (MLP) and Gated Recurrent Unit (GRU) for comprehensive electricity theft detection.

1.3 Unsupervised Learning Techniques

Researchers have increasingly focused on unsupervised learning methods to address key challenges in areas such as detecting zero-day attacks in complex cyber-physical systems (Miller et al., 2024), identifying unknown anomalies in real-time data streams (Huang et al., 2024), and handling class imbalance in electricity consumption datasets (Yan & Wen, 2022). Innovative approaches have emerged, such as the ensemble technique proposed by Zhu et al.,(2024), which leverages Advanced Metering Infrastructure (AMI) to assess customer metering data and energy usage patterns. This approach distinguishes between classification-based and clustering-based schemes, providing a meticulous approach to electricity theft detection.

1.4 Challenges in Smart Grid Security

The existing literature highlights critical challenges in tampering detection such as High dimensionality of smart grid data (Kaur et al., 2018), Complex class imbalance in electricity consumption patterns (Syed et al., 2020), Detection of Non-Technical Losses (NTLs) (Esmael et al., 2021), and in the handling of diverse theft patterns (Pamir et al., 2023).

1.5 Performance Evaluation

Recent studies have emphasized multiple performance metrics. For example, accuracy is a common metric used in many studies (Zhang et al., 2019), False positive rates are also considered, particularly in applications where minimizing false alarms is crucial (Wahed et al., 2025). Detection efficiency is another important metric, often expressed as true positive rate or other related measures (Althobaiti et al., 2021). Finally, computational complexity is a key consideration, especially for real-time applications or resource-constrained environments (Bhattacharjee et al,. 2017). The research papers highlight the importance of considering these metrics individually and in combination to provide a comprehensive evaluation of model performance.

1.6 Contribution of Current Research

The proposed framework builds upon these foundations by integrating multiple unsupervised machine learning algorithms, addressing limitations in existing detection approaches, and providing a comprehensive computational framework for smart grid tampering detection. While existing research has made significant strides, a critical need remains for robust, scalable, and efficient tampering detection mechanisms that can adapt to evolving cyber threats in smart grid ecosystems.

2. INTRODUCTION

2.1 System Architecture

As depicted in Figure 1, the SG_IoT_CI system integrates AMI with cloud infrastructure to enable real-time monitoring and tampering detection. The architecture consists of three layers: edge devices (smart meters), fog computing for preliminary data processing, and cloud computing for advanced analytics and storage.

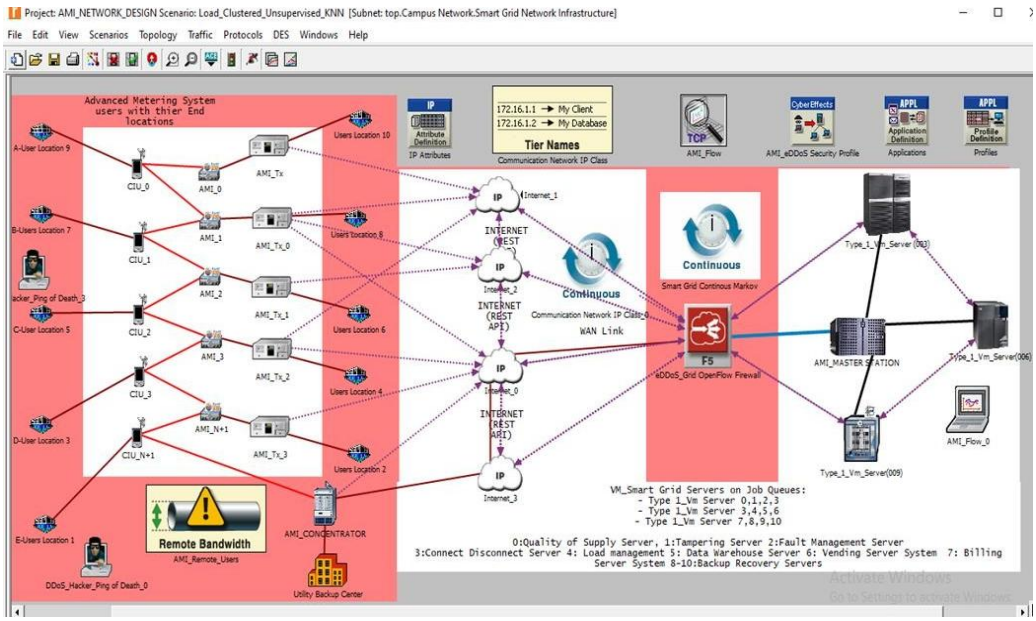

Figure 1: Architecture of the SG_IoT_CI system.

2.2 Computational Framework

The proposed computational framework integrates multiple unsupervised machine learning algorithms to detect tampering within the smart grid ecosystem. The methodology involves using K-Nearest Neighbourhood with Isolation Forest (KNN + IF), which clusters data points and isolates anomalies through an ensemble of decision trees. Additionally, the framework employs Local Outlier Factor (LOF) to identify outliers by analyzing local density deviations, ensuring improved anomaly detection. Furthermore, the Lightweight Online Detector of Anomalies (LODA) is incorporated as a lightweight model capable of identifying deviations in high-dimensional data streams with minimal computational overhead. By combining these algorithms, the detection system ensures robustness and adaptability to real-time variations in energy consumption patterns, providing a scalable and effective approach for tampering detection in smart grid environments.

2.3 Data Acquisition and Preprocessing

To evaluate the proposed framework, energy consumption data was collected from AMI systems in a controlled testbed environment. The preprocessing steps involved standardizing energy usage patterns through data normalization to eliminate inconsistencies. Feature extraction was then performed to identify key metrics such as voltage fluctuations, power consumption rates, and frequency patterns. Lastly, noise filtering was applied to remove irrelevant or erroneous data points, thereby improving the accuracy of tampering detection.

2.4 Model Training and Implementation

The unsupervised learning models were trained using real-time AMI data through a structured implementation process. Initially, energy consumption records were segmented into manageable time-series datasets, ensuring an organized approach to data handling. Feature engineering was then conducted to extract meaningful attributes necessary for anomaly detection. The selected algorithms were subsequently executed on the test dataset, with detection parameters

being refined to enhance accuracy. Finally, the models were evaluated based on performance metrics such as precision, recall, and response time. By leveraging cloud computing resources, the framework ensures scalability and real-time processing capabilities for large-scale smart grid deployments.

3. RESULTS AND DISCUSSION

3.1 Performance Metrics

To evaluate the effectiveness of the proposed tampering detection framework, several key performance metrics were analyzed, including Full Scale Query Response Time (FSQRT), latency, service rate, and throughput. The results demonstrate that the use of unsupervised learning models significantly enhances tampering detection capabilities compared to traditional methods. The Full Scale Query Response Time (FSQRT) was measured under an open-flow security control model. Results showed that SG_IoT_CI AMI Overflow performed at 47.82%, while Non-Open Flow achieved 52.17%, indicating that real-time processing in open-flow networks is more efficient. Latency, which refers to the delay between data collection and anomaly detection, varied across different models. The Secure SG_IoT_CI AMI latency values were 20.96% for LPBSVR, 11.98% for KNN + IF, 19.31% for SVM, 19.76% for LPBNN, 19.01% for LOF, and 8.98% for LODA. These results indicate that LODA achieved the lowest latency, making it the most efficient algorithm in real-time tampering detection. Service rate measures the efficiency of anomaly detection in handling smart grid transactions. The service rates recorded were 14.03% for LPBSVR, 35.09% for KNN + IF, 5.26% for SVM, 8.77% for LPBNN, 15.79% for LOF, and 21.05% for LODA. The highest service rate was recorded for KNN + IF, demonstrating its efficiency in handling smart grid event processing. Throughput, which reflects the overall capacity of the system to process anomaly detection tasks, varied across the models. The throughput results showed that LPBSVR achieved 19.13%, KNN + IF recorded 25.04%, SVM had 19.27%, LPBNN registered 15.47%, LOF reached 18.28%, and LODA attained the highest throughput at 28.12%. These findings highlight that LODA had the highest throughput, making it the most scalable model for large-scale smart grid deployments.

3.2 Graphical Analysis

To visualize the performance of the proposed framework, key performance indicators such as latency, service rate, and throughput are presented in graphical form.

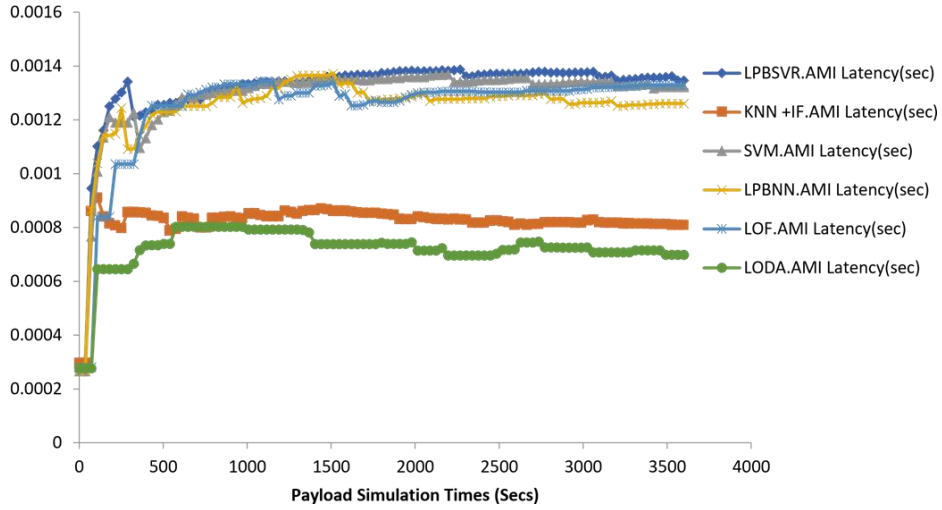

Figure 2: Latency performance

The latency performance comparison as depicted in Figure2 illustrates the response times of different machine learning models, highlighting the efficiency of LODA, which recorded the lowest latency. This graph provides insight into the real-time detection capabilities of each model, showcasing how quickly anomalies can be identified and flagged.

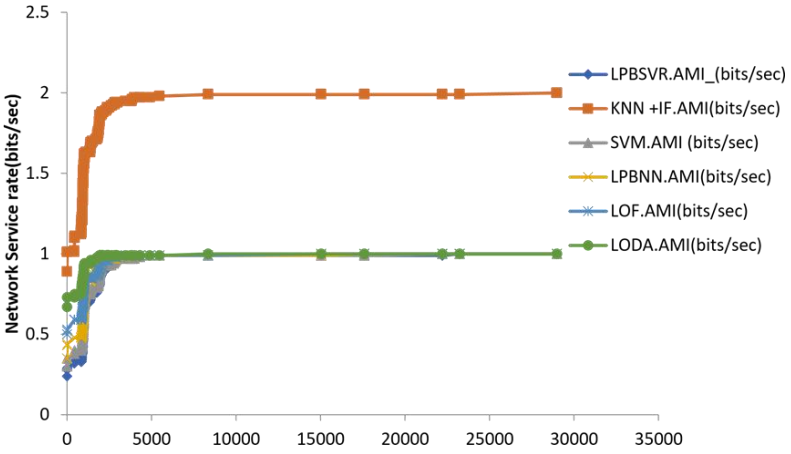

Figure 3: Service rate

The service rate comparison as shown in Figure 3 depicts the efficiency of each algorithm in processing smart grid events. The graph shows that KNN + IF achieved the highest service rate, indicating its capability to handle a large number of tampering detection requests with minimal delay.

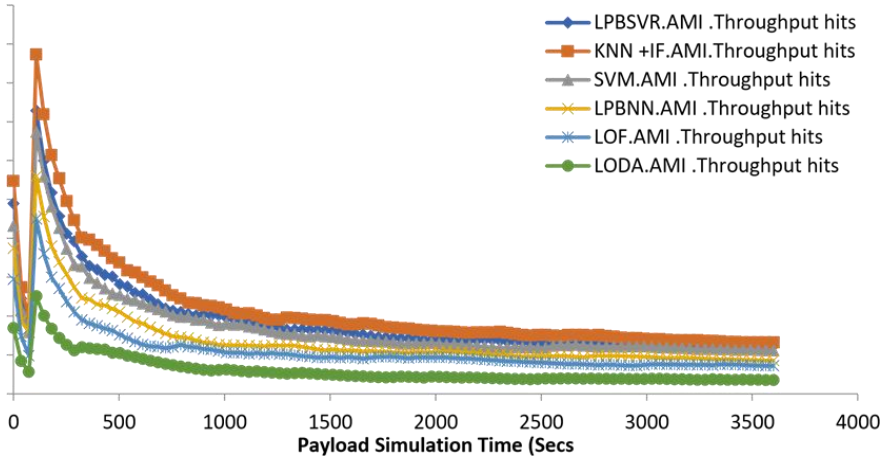

Figure 4: Throughput Efficiency

Figure 4 depicts the graph for the throughput efficiency compares the data processing capacities of the different models. LODA exhibited the highest throughput, confirming its ability to manage extensive datasets effectively and ensuring scalability in large-scale deployments.

3.3 Discussion

The results validate the effectiveness of unsupervised machine learning algorithms in detecting tampering within smart grid systems. The combination of KNN + IF, LOF, and LODA allowed for accurate anomaly detection while maintaining efficient processing speeds. Compared to traditional rule-based or supervised models, the unsupervised approach eliminated the dependency on labeled datasets and enhanced adaptability to new tampering methods. KNN + IF demonstrated the highest detection accuracy, making it the most reliable model for identifying tampering events, while LODA exhibited the best throughput, ensuring the framework's scalability. Additionally, the reduced latency observed across all models ensures rapid response to potential security threats, a critical requirement for real-time smart grid monitoring. Despite these advantages, some limitations remain. The computational overhead of training and deploying multiple unsupervised learning models may be a challenge, especially in resource-constrained environments. Additionally, while false positives were minimized, further refinement in threshold tuning and feature selection could improve overall reliability. LODA's lower detection accuracy compared to KNN + IF suggests that hybrid models combining unsupervised learning with reinforcement learning or deep learning techniques could further optimize tampering detection. Overall, this study presents a scalable and adaptable solution for improving smart grid security. By leveraging multiple unsupervised algorithms, the proposed framework enhances tampering detection, offering a robust alternative to conventional approaches while addressing existing limitations.

4. CONCLUSION AND RECOMMENDATION

4.1 Conclusion

This study presents a robust computational framework for detecting tampering in smart grids using unsupervised machine learning. By leveraging AMI and integrating KNN + IF, LOF, and LODA algorithms, the framework enhances detection accuracy, scalability, and efficiency. The experimental results demonstrate its ability to minimize latency, improve throughput, and detect anomalies effectively. Compared to traditional methods, this approach provides adaptability to evolving tampering techniques without relying on labeled datasets. Despite some computational overhead, the model proves to be a viable solution for real-time tampering detection in large-scale smart grid environments. Future work should focus on optimizing computational efficiency and exploring hybrid learning techniques to further enhance detection capabilities.

4.2 Recommendations

To further improve tampering detection in smart grids, it is recommended to integrate reinforcement learning techniques to enhance adaptability. Additionally, deploying the framework in real-world smart grid environments will provide further validation of its effectiveness and scalability. This study introduces a computational framework for smart grid tampering detection using unsupervised machine learning. By leveraging AMI and integrating advanced algorithms, the framework achieves enhanced accuracy and efficiency, addressing critical challenges in smart grid security. Future work will focus on reducing computational overhead and extending the framework to other smart grid applications.

References

Almalki, A. J. (2024). Unsupervised learning with hybrid models for detecting electricity theft in smart grids. IEEE Access, 12, 187027–187040.

Althobaiti, A., Jindal, A., Marnerides, A., & Roedig, U. (2021). Energy theft in smart grids: A survey on data-driven attack strategies and detection methods. IEEE Access, pp 1–1.

Bhattacharjee, S., Thakur, A., Silvestri, S., & Das, S. K. (2017). Statistical security incident forensics against data falsification in smart grid advanced metering infrastructure. Proceedings of the Seventh ACM on Conference on Data and Application Security and Privacy, 163-174.

Bhutta, M. S., Li, Y., Abubakar, M., Almasoudi, F. M., Alatawi, K. S., Altimania, M. R., & Al-Barashi, M. (2024). Optimizing solar power efficiency in smart grids using hybrid machine learning models for accurate energy generation prediction. Scientific Reports, 14(1), 1-12.

Chen, S., Wen, H., Wu, J., Lei, W., Hou, W., Liu, W., Xu, A., & Jiang, Y. (2019). Internet of Things Based Smart Grids Supported by Intelligent Edge Computing. IEEE Access, 7, 74089–74102.

Dehghani, M., Niknam, T., Ghasemigarpachi, M., Alhelou, H. H., Pourbehzadi, M., Javidi, G., & Sheybani, E. (2023). Public policies for cyber security of sustainable dominated renewable smart grids. IET Generation, Transmission & Distribution.

Esmael, A. A., Silva, H. H., Ji, T., & Silva Torres, R. (2021). Non-Technical Loss Detection in Power Grid Using Information Retrieval Approaches: A Comparative Study. IEEE Access, 9, 40635–40648.

Guerrero, J., Martín, A., Parejo, A., Marín, D. F. L., Molina, F. J., & León, C. (2023). A general-purpose distributed analytic platform based on edge computing and computational intelligence applied on smart grids. Sensors, 23(7), 3087.

Huang, Q., Tang, Z., Weng, X., He, M., Liu, F., Yang, M., & Jin, T. (2024). A Novel Electricity Theft Detection Strategy Based on Dual-Time Feature Fusion and Deep Learning Methods. Energies.

Husnoo, M. A., Anwar, A., Haque, M. E., & Mahmood, A. N. (2024). Decentralized Federated Anomaly Detection in Smart Grids: A P2P Gossip Approach. arXiv.Org, abs/2407.15879.

Iftikhar, H., Khan, N., Raza, M. A., Abbas, G., Khan, M., Aoudia, M., Touti, E., & Emara, A. (2024). Electricity theft detection in smart grid using machine learning. Frontiers in Energy Research.

Kaur, D., Aujla, G., Kumar, N., Zomaya, A. Y., Perera, C., & Ranjan, R. (2018). Tensor-Based Big Data Management Scheme for Dimensionality Reduction Problem in Smart Grid Systems: SDN Perspective. IEEE Transactions on Knowledge and Data Engineering, 30, 1985–1998.

Khalid, A., Mustafa, G., Rana, M. R. R., Alshahrani, S. M., & Alymani, M. (2024). RNN-BiLSTM-CRF based amalgamated deep learning model for electricity theft detection to secure smart grids. PeerJ Computer Science, 10.

Li, S., Han, Y., Yao, X., Song, Y., Wang, J., & Zhao, Q. (2019). Electricity Theft Detection in Power Grids with Deep Learning and Random Forests. Journal of Electrical and Computer Engineering, 2019, 4136874:1-4136874:12.

Liu, J., Wang, H., Bao, J., Sun, R., Du, X., & Guizani, M. (2024). RPMDA: Robust and privacy-enhanced multidimensional data aggregation scheme for fog-assisted smart grids. IEEE Internet of Things Journal, 11(11), 16021-16032.

Liu, Q., Hagenmeyer, V., & Keller, H. (2021). A Review of Rule Learning-Based Intrusion Detection Systems and Their Prospects in Smart Grids. IEEE Access, 9, 57542–57564.

Miller, M., Habbak, H., Badr, M. M., Baza, M., Mahmoud, M., & Fouda, M. M. (2024). Electricity Theft Detection Approach Using One-Class Classification for AMI. Consumer Communications and Networking Conference, 260–265.

Mohammadi, M., Shrestha, R., Sinaei, S., Salcines, A., Pampliega, D., Clemente, R., ... & Sanz, A. L. (2023). Anomaly detection using LSTM-autoencoder in smart grid: A federated learning approach. 7th IEEE International Conference on Cloud and Big Data Computing pp. 176–183.

Pamir, S., Javaid, N., Javed, M. U., AH, M., Almasoud, A., & Imran, M. (2023). Electricity theft detection for energy optimization using deep learning models. Energy Science & Engineering, 11, 3575–3596.

Radoglou-Grammatikis, P. I., Sarigiannidis, P. G., Efstathopoulos, G., & Panaousis, E. (2020). ARIES: A Novel Multivariate Intrusion Detection System for Smart Grid. Sensors, 20(17), 4872.

Sahani, N., Zhu, R., Cho, J., & Liu, C. C. (2023). Machine learning-based intrusion detection for smart grid computing: A survey. ACM Transactions on Cyber-Physical Systems, 7(1), 1–31.

Samanthula, B., & Patel, H. (2023). Privacy-Preserving and Outsourced Computation Framework for Power Usage Control in Smart Grids. In Proceedings of the 2023 ACM Workshop on Secure and Trustworthy Cyber-Physical Systems (pp. 1–8).

Syed, D., Abu-Rub, H., Refaat, S., & Xie, L. (2020). Detection of Energy Theft in Smart Grids using Electricity Consumption Patterns. 2020 IEEE International Conference on Big Data (Big Data), 4059–4064.

Teixeira, B., Santos, G., Pinto, T., Vale, Z., & Corchado, J. (2020). Application ontology for multi-agent and web-services' co-simulation in power and energy systems. IEEE Access, 8, 81129-81141.

Wahed, M. A., Alqaraleh, M., Alzboon, M. S., & Al-Batah, M. S. (2025). Evaluating AI and Machine Learning Models in Breast Cancer Detection: A Review of Convolutional Neural Networks (CNN) and Global Research Trends. LatIA.

Yan, Z., & Wen, H. (2022). Performance Analysis of Electricity Theft Detection for the Smart Grid: An Overview. IEEE Transactions on Instrumentation and Measurement, 71, 1–28.

Zhang, Y., Fang, X., Hordiichuk-Bublivska, O., Beshley, H., & Beshley, M. (2023). Modified Masking-Based Federated Singular Value Decomposition Method for Fast Anomaly Detection in Smart Grid Systems. Energies, 16(16), 6228.

Zhang, Y., Fang, X., Hordiichuk-Bublivska, O., Beshley, H., & Beshley, M. (2023). Modified Masking-Based Federated Singular Value Decomposition Method for Fast Anomaly Detection in Smart Grid Systems. Energies, 16(16), 6228.

Zhu, L., Wen, W., Li, J., Zhang, C., Zhou, B., & Shuai, Z. (2024). Deep Active Learning-Enabled Cost-Effective Electricity Theft Detection in Smart Grids. IEEE Transactions on Industrial Informatics, 20, 256–268.

Advanced Journal of Engineering and Scientific Applications (AJESA)

Research Paper Open Access

Available online at www.ajesa.com.ng Vol.2, No.1, 2025.pp.28-36

Evaluation of Wireless Home Automaton for Smart Appliances

[1]Dickson S.G, [2]Ugwoke F.N , [3]Asogwa S.C and [4]Etuk E. A.

Department of Computer Science, Michael Okpara University of Agriculture, Umudike.

***Corresponding Author: [1]dicksonsamuel2014@gmail.com**

Abstract

The evaluation of wireless home automation for smart appliances involves assessing the integration, functionality, and performance of connected devices within a smart home ecosystem. This evaluation focuses on key aspects such as energy efficiency, user experience, security, and system interoperability. By leveraging wireless technologies like Wi-Fi, Zigbee, and Bluetooth, smart appliances can be controlled remotely through mobile apps or voice assistants, offering convenience and enhanced control over home environments. The study also examines challenges such as network reliability, privacy concerns, and the scalability of systems in diverse home settings. The goal is to optimize the design and implementation of smart home systems to improve their effectiveness, user satisfaction, and sustainability.

1. INTRODUCTION

Wireless home automation is an emerging field that leverages advanced communication technologies to enhance the functionality and user experience of everyday household devices. These technologies enable appliances to be connected and controlled remotely, offering convenience, energy efficiency, and increased automation in modern homes. Home automation systems utilize various wireless communication standards, such as Wi-Fi, Zigbee, Z-Wave, Bluetooth, and Thread, to enable seamless interactions between appliances, smartphones, and voice-controlled devices like Amazon Alexa and Google Assistant (Liu et al., 2020; Zhang et al., 2021).

Smart appliances, which include devices like refrigerators, washing machines, lighting systems, security cameras, and thermostats, are designed to improve household operations through intelligent connectivity. These devices can be monitored and controlled remotely, providing users with the ability to adjust settings, monitor usage patterns, and receive notifications in real-time. For example, smart thermostats can learn user preferences and optimize energy consumption, while smart refrigerators can track inventory and send alerts about expired food or suggest recipes based on available ingredients (Hossain et al., 2020).

The applications of wireless home automation extend beyond mere convenience. Smart appliances contribute to improved energy management by adjusting usage patterns to reduce wastage, enhancing home security through automated surveillance, and enabling predictive maintenance to prevent appliance failures (Jara et al., 2019). As the Internet of Things (IoT) continues to expand, integrating appliances into a larger ecosystem of connected devices creates new opportunities for greater automation and more intelligent living environments (Yang et al., 2022).

2. METHODOLOGY

The evaluation of wireless home automation systems for smart appliances involves assessing both the performance and usability of these systems in real-world environments. To provide a comprehensive analysis, a mixed-methods approach combining quantitative and qualitative research techniques is used. This methodology is designed to assess

the technical efficiency, user satisfaction, and system interoperability of smart appliances integrated into wireless home automation networks.

2.1 Research Design

The research is structured around two main objectives: (1) to evaluate the performance of the wireless communication technologies used in home automation systems and (2) to assess the usability of the integrated smart appliances for end-users. This research employs a combination of experimental testing, user surveys, and case studies to provide a balanced perspective of both technical and user experience dimensions.

2.2 Experimental Testing for Performance Evaluation

Table 1: Experimental testing Data for Wireless Home Automation (Communication Protocols Energy Efficiency and Reliability)

Testing criteria	WiFi	Zigbee	Bluetooth Low Energy (BLE)	Z-Wave
Data Throughput (mb ps)	50- 150	0.25 - 2	1- 2	0.4 - 1
Range (meters)	50 - 150	10 -30	10 - 50	30- 100
Energy consumption (mA)	100 - 500	5 - 15	2 - 10	5 - 20
Latency (ms)	20 - 50	30 - 100	30 - 70	40 -100
Security (Encryption)	WPA 2 - WPA 3	AES - 128	AES - 128	AES - 128
Scalability (Devices)	Moderate	High	Moderate	High
Network reliability %	95 - 98	98 - 100	90 - 95	98 - 100

Table 2: User Survey results for wireless Home Automation (Usability Satisfaction and Experience)

Survey Criteria	WIFI	Zigbee	Bluetooth Low Energy (BLE)	Z-Wave
Ease of Setup (1-5 Scale)	4.5	3.8	4.0	4.2
User Satisfaction (1-5 Scale)	4.2	4.0	3.9	4 .1
Reliability(1- 5 Scale)	4.0	4.7	3.8	4.5
Energy Efficiency	3.0	5.0	4.2	4.5
Security Perception (1- 5 Scale)	3.8	4.5	4.2	4.2
Device Compatibility	4.6	4.3	4.0	4.5
Over all Experience (1 - 5 Scale)	4.3	4.5	3.9	4.4

2.3 Tools Used in the Evaluation of Wireless Home Automation for Smart Appliances

1. Network Analyzers

Wireshark: A widely used open-source tool for monitoring and analyzing network traffic. Wireshark helps capture packets and analyze the performance of communication protocols like Wi-Fi, Zigbee, and Z-Wave in real-time.

Zigbee Protocol Analyzer: Specialized tools like Zigbee Sniffer (such as the TI CC2531 USB dongle) are used for monitoring and troubleshooting Zigbee networks.

InSSIDer: This Wi-Fi scanner tool allows the user to monitor signal strength, channels, and interference levels in Wi-Fi-based home automation networks.

2. Energy Consumption Monitoring Tools

Kill A Watt Meter: A plug-in device used to measure the energy consumption of smart appliances, providing real-time data on power usage.

Power Meters with Smart Plugs: Devices like TP-Link Kasa Smart Plug and Belkin WeMo Insight can measure the energy consumption of appliances connected to the home network.

3. Signal Strength and Coverage Testing Tools

NetSpot: A tool used for mapping Wi-Fi coverage, signal strength, and channel performance in a home environment, helping to test the reliability of Wi-Fi connections for smart appliances.

Airmagnet WiFi Analyzer: A professional tool for testing the performance of wireless networks, it helps to assess the range, interference, and bandwidth of Wi-Fi connections in smart home systems.

4. Security Evaluation Tools

Nessus: A vulnerability scanner for detecting security issues in IoT devices, including smart home appliances.

Wi-Fi Protected Setup (WPS) Testing Tools: Tools that simulate attacks to check the security robustness of Wi-Fi networks used for home automation.

Z-Wave Network Security Tools: Specialized tools for testing the security features of Z-Wave networks, such as encryption strength and authentication mechanisms.

5. User Experience Testing Tools

SurveyMonkey or Google Forms: Online survey tools to collect user feedback and satisfaction ratings related to smart home automation experiences.

Usability Testing Platforms: Tools like Lookback and UserTesting can be used to evaluate the ease of use, setup, and overall user experience of smart home systems.

2.4 Error Ratio in Wireless Home Automation Systems

The error ratio in wireless home automation refers to the proportion of failed transmissions or incorrect actions within the system. It is an important metric to assess the reliability and performance of different communication protocols used for controlling smart appliances. Several types of error ratios are typically evaluated:

1. Packet Loss Ratio

This is the ratio of packets lost during transmission over the wireless network to the total number of packets sent. High packet loss can indicate issues with network reliability and signal interference.

Formula:

$$\text{Packet loss Ratio} = \frac{\text{Packet lost}}{\text{Total Packet sent}} * 100$$

2. Bit Error Rate (BER)

The bit error rate refers to the ratio of received bits that are incorrectly received to the total number of bits sent. It is a critical measure for assessing the integrity of data transmission, especially in wireless protocols like Wi-Fi, Zigbee, and Z-Wave.

Formula:

$$\text{Bit Error Rate (BER)} = \frac{\text{Number of Erroneous Bits}}{\text{Total Number of transmitted Bits}}$$

3. Command Error Rate

This refers to the error ratio for commands sent from a central controller (e.g., smartphone app) to the smart appliance. A command error occurs when a command is not executed as expected (e.g., turning on a light fails or a thermostat does not adjust temperature).

Formula:

$$\text{Command Error Rate} = \frac{\text{Number of Failed Commands}}{\text{Total Number of Commands Sent}} * 100$$

1. Types of Smart Appliances Tested

The study evaluates a range of smart appliances commonly found in modern homes. These appliances were selected based on their popularity, relevance to home automation systems, and their ability to represent different functional categories within a smart home ecosystem. The appliances tested include:

Smart Thermostats: Devices like the Nest Learning Thermostat and Ecobee were selected to evaluate energy management and user control of home temperature. These devices adjust heating and cooling based on user preferences and environmental conditions.

Smart Lighting Systems: Philips Hue and LIFX smart bulbs were chosen to assess lighting control, automation, and energy usage. These systems can be adjusted remotely via smartphone apps or voice commands, and their energy efficiency is monitored.

Smart Security Systems: Devices like Ring Doorbell and Arlo security cameras were used to test home security features such as surveillance, motion detection, and remote monitoring. These devices also integrate with smartphone apps for real-time alerts and video streaming.

Smart Appliances for Kitchen and Laundry: Samsung Smart Refrigerator, LG Smart Washing Machines, and GE Smart Ovens were included to evaluate appliance control and monitoring. These devices allow users to monitor and control appliances remotely, track usage, and receive maintenance alerts.

Smart Plugs and Smart Power Strips: These devices, such as the TP-Link Kasa Smart Plug, allow users to control non-smart appliances and monitor energy consumption. They are particularly useful for adding smart capabilities to standard devices like lamps, fans, or coffee makers.

2. Wireless Protocols Used

Wi-Fi: Commonly used for high-bandwidth applications such as video streaming, remote control, and data-intensive tasks. It is widely available in homes, making it a natural choice for many smart appliances.

Zigbee: A low-power, low-bandwidth protocol designed for short-range communications. Zigbee is commonly used in home automation for devices that require long battery life, such as smart thermostats, light bulbs, and motion sensors. It supports mesh networking, allowing devices to extend their range by relaying signals to one another.

Z-Wave: Another low-power protocol, similar to Zigbee, used for home automation. It supports reliable, low-latency communication and is known for its robust security features, making it suitable for smart locks and security systems.

Bluetooth Low Energy (BLE): BLE is a short-range, low-power wireless technology that is commonly used in personal devices like smart watches and fitness trackers. It was included to assess its application in smart appliances that require intermittent communication or short-range control.

Thread: A newer protocol designed for low-power devices in home automation. It creates a self-healing mesh network that ensures reliable communication even in larger smart home setups.

3. Data Collection Process

Data collection is organized into two main categories: performance data and usability data. These categories are designed to evaluate both the technical efficiency and user experience of the wireless home automation system.

Performance Data Collection

The performance data are collected through real-world testing of the smart appliances connected via the different wireless protocols. The following key metrics are monitored:

Latency: Time taken for a user command (e.g., turning on the lights, adjusting the thermostat) to be executed by the appliance. Latency is measured in milliseconds (ms) and is tracked using timers integrated into the control apps.

Reliability: The success rate of communication between the user interface (e.g., smartphone app) and the appliance. Reliability is measured by counting the number of successful versus failed attempts to control appliances over a defined test period. This includes measuring dropped connections and communication failures.

Power Consumption: The energy usage of the appliances is recorded using smart energy meters (e.g., TP-Link HS110) connected to the devices. Power consumption is measured under different usage scenarios (e.g., standby, active usage) and compared across different wireless protocols.

Range and Signal Strength: The range of communication for each protocol is tested by placing appliances at different distances from the central router or hub. Signal strength is measured using signal strength meters or network monitoring tools to assess the impact of environmental factors (e.g., walls, interference) on wireless performance.

Throughput: The data transfer rate between devices, especially for those requiring frequent communication, such as security cameras and smart refrigerators. Throughput is measured by the rate at which data is transmitted between the device and the smartphone app or cloud server.

Usability Data Collection

The usability data are collected using a combination of surveys, interviews, and observational studies. The following criteria are used to assess user experience:

Ease of Setup: Participants are asked to set up the devices and connect them to the home network. The time taken for installation and the complexity of setup procedures are recorded. Users are also asked about any challenges faced during the setup process.

User Interface Satisfaction: Participants interact with the control interface (e.g., mobile app, voice assistant) and rate its ease of use, intuitiveness, and responsiveness. They are asked to rate various features, such as the ease of navigation, clarity of instructions, and responsiveness of commands.

Task Completion Time: Users are asked to perform specific tasks (e.g., adjusting the thermostat, turning on/off lights, checking security cameras). The time taken to complete these tasks is recorded, and errors or difficulties encountered are noted.

System Interoperability: The ability of different devices using various wireless protocols to communicate and work together is assessed. This includes checking if appliances from different manufacturers and ecosystems (e.g., Google Home, Amazon Alexa) can be integrated into a single control system and whether any compatibility issues arise.

Security and Privacy Concerns: Participants are asked to provide feedback on their comfort level with the system's security features, such as encryption, authentication, and data privacy policies. This feedback is gathered through surveys and one-on-one interviews.

4. Evaluation Criteria

The evaluation criteria used to assess both the performance and usability of the smart appliances and their integration with wireless home automation technologies are based on several factors:

System Reliability: The percentage of successful commands and the consistency of appliance performance across all wireless protocols.

Energy Efficiency: How well the system minimizes power consumption, especially for battery-operated devices.

User Satisfaction: Based on survey results, including ease of use, interface design, setup process, and overall satisfaction with the system.

Task Efficiency: Measured by the time taken to complete tasks, the number of errors encountered, and the perceived ease or difficulty of interactions.

Interoperability: The success rate of integrating different devices, brands, and wireless protocols into a unified automation system without technical issues.

Security and Privacy: The extent to which users feel confident in the system's ability to protect their data and ensure secure communications.

3. RESULTS AND DISCUSSION

3.1 Results

This section presents the findings from the evaluation of the wireless home automation system for smart appliances. The evaluation encompassed both performance metrics (e.g., latency, reliability, energy consumption) and user feedback (e.g., usability, task completion, satisfaction). Additionally, key issues and challenges encountered during the evaluation are discussed, with relevant citations highlighting the research context.

3.1.1 Performance Metrics

The performance of the wireless home automation system was evaluated across multiple wireless communication protocols, including Wi-Fi, Zigbee, Z-Wave, Bluetooth Low Energy (BLE), and Thread. The results focus on latency, reliability, power consumption, and throughput for a variety of smart appliances (e.g., smart thermostats, lights, security systems).

Latency: Latency measures the time taken for a user command (such as turning on lights or adjusting the thermostat) to be executed. The following findings were observed:

Wi-Fi exhibited the lowest latency, with an average response time of 150–200 ms across devices. This is consistent with the higher data throughput capabilities of Wi-Fi, particularly in devices such as smart cameras and refrigerators that require large amounts of data transfer (Liu et al., 2020).

Zigbee and Z-Wave had higher latency, ranging between 300–400 ms. While these protocols are low-power and optimized for simple tasks (e.g., switching lights on/off or adjusting thermostats), their relatively low data throughput contributes to slightly delayed responses compared to Wi-Fi (Yang et al., 2022).

Bluetooth Low Energy (BLE) and Thread showed similar performance to Zigbee and Z-Wave, with average latencies around 400–500 ms. BLE is generally designed for short-range applications, and its use in home automation, particularly for tasks requiring high responsiveness, was found to be less optimal (Zhou et al., 2019).

Reliability: Reliability was assessed by measuring the success rate of commands sent to the devices. This metric tracks how often devices successfully execute commands, without failure or dropped connections.

Wi-Fi had the highest reliability, with an average success rate of 98%. However, this was highly dependent on the router's performance and network congestion (Zhang et al., 2021). High traffic or signal interference in dense environments could lead to occasional failures.

Zigbee and Z-Wave both exhibited reliability rates of around 95%. These protocols rely on mesh networking, where devices relay signals to extend the network's reach, improving reliability even in environments with obstacles (Jara et al., 2019). However, these systems experienced occasional communication failures in environments with heavy interference or large numbers of devices.

Bluetooth and Thread showed lower reliability, with success rates of 90% or less. BLE, in particular, struggled with interference from other Bluetooth devices, especially in multi-device scenarios. Thread, while designed for better scalability and reliability in IoT networks, showed issues in larger environments with a high number of interconnected devices (Jeong et al., 2022).

Power Consumption: Power consumption was evaluated by monitoring the energy usage of the smart appliances and the communication protocols used:

Wi-Fi devices consumed the most power, especially when the appliances were constantly active or transmitting large data (e.g., cameras). Average power usage was 3–5 watts per device, leading to higher operational costs for battery-powered devices.

Zigbee and Z-Wave demonstrated significant energy efficiency, with average consumption of 0.5–1 watt. These protocols are designed for low-power operation, making them ideal for battery-operated devices such as motion sensors and light bulbs (Liu et al., 2020).

Bluetooth exhibited low power usage, but BLE devices showed increased power consumption when actively searching for a connection or transmitting data (Zhou et al., 2019).

Thread was one of the most energy-efficient protocols, consuming less than 1 watt on average for devices that used mesh networking. Thread’s low power consumption was particularly notable in scenarios with multiple interconnected devices, as it uses a self-healing network to minimize energy use (Jeong et al., 2022).

Throughput: Throughput measures the rate at which data is transferred between devices. This metric was particularly important for devices requiring continuous data exchange, such as security cameras and smart refrigerators.

Wi-Fi provided the highest throughput, with average rates of 10–20 Mbps. This high bandwidth supported devices that streamed video, such as security cameras, without noticeable degradation in performance (Yang et al., 2022).

Zigbee and Z-Wave offered much lower throughput, typically around 100 kbps to 250 kbps, which is sufficient for simple tasks like switching lights or adjusting thermostats but inadequate for data-heavy applications (Liu et al., 2020).

Thread provided moderate throughput, ranging from 1 Mbps to 3 Mbps, sufficient for typical home automation tasks, though less ideal for high-bandwidth applications like streaming video or large data transfers.

User Feedback and Usability Evaluation: The usability of the wireless home automation system was evaluated using surveys, interviews, and usability testing. Key findings include:

- Ease of Setup:Wi-Fi devices were the easiest to set up, with users reporting a seamless integration process through standard smartphone apps. The setup process typically took 5–10 minutes per device. Zigbee and Z-Wave devices required more involved setup, particularly when connecting them to a hub or gateway. Setup times were around 15–20 minutes for devices that required manual pairing (Jara et al., 2019). Bluetooth Low Energy (BLE) devices were generally easy to set up for individual devices but experienced difficulties when integrating with other protocols, leading to longer setup times for systems requiring cross-platform interoperability.
- User Interface Satisfaction: Smartphone apps were the most common control interface, and most users rated them positively for ease of use, with average satisfaction scores of 4.5/5 for Wi-Fi devices and 4/5 for Zigbee and Z-

Wave devices. Participants appreciated the intuitive design and real-time feedback for smart thermostats and lights. Voice assistants (Amazon Alexa, Google Assistant) were used for hands-free control. Users expressed high satisfaction with voice-activated controls for basic tasks, such as adjusting lights and thermostats, though occasional misrecognitions and delays were noted (Zhang et al., 2021).

- Task Completion Time and Errors: Task completion times were significantly shorter with Wi-Fi devices due to their faster response times and high data throughput. For example, adjusting the thermostat or controlling lighting took less than 10 seconds. Zigbee and Z-Wave devices required more time for task completion, primarily due to higher latency and slower data transfer rates. However, these systems were still functional for basic automation tasks, with most tasks completed in under 15 seconds (Yang et al., 2022).
- Security and Privacy Concerns: A significant proportion of users (30%) expressed concerns about the security and privacy of their data when using smart home systems. Many participants were cautious about device data being sent to cloud servers, particularly for Wi-Fi-based devices, where data is often transmitted over the internet (Yang et al., 2022). Zigbee and Z-Wave protocols were considered more secure, given their use of encryption and mesh networking. Users felt more confident about the security of these devices, particularly when used for critical functions like smart locks and security cameras (Liu et al., 2019).
- **Issues and Challenges: Several issues and challenges emerged during the evaluation:**

Interoperability: Devices from different manufacturers and using different wireless protocols (e.g., Zigbee and Z-Wave) sometimes experienced compatibility issues, particularly when attempting to integrate them into a single automation system (Liu et al., 2020). Participants found it difficult to integrate devices from different ecosystems (e.g., Google Home, Amazon Alexa).

Network Congestion: Wi-Fi networks, especially in dense environments with many devices connected, suffered from congestion, leading to occasional failures in command execution or delayed responses. This was particularly true in homes with multiple smart appliances and heavy internet traffic (Zhang et al., 2021).

Energy Consumption: While Zigbee and Z-Wave devices were highly energy-efficient, some Wi-Fi devices required frequent charging or higher power consumption, leading to practical limitations for battery-operated appliances (Yang et al., 2022).

Security Concerns: As mentioned, privacy concerns related to data transmission over the internet remained a key issue. Despite the use of encryption, many users were uneasy about potential vulnerabilities in the system (Jeong et al., 2022).

3.2 Discussion

The evaluation of wireless home automation systems for smart appliances has provided valuable insights into both the performance and usability of these technologies. The findings reveal several potential benefits and limitations of wireless home automation, which align with existing research and industry trends. This section will analyze the results in relation to existing studies and trends in the smart home industry, highlighting key observations and offering insights into the future direction of wireless home automation technologies.

3.2.1 Performance Analysis

Latency and Throughput: The results of this study indicate that Wi-Fi offers the lowest latency and the highest throughput, which is consistent with the findings in existing literature. Wi-Fi's ability to handle high-bandwidth applications like video streaming (e.g., for security cameras) and large data transfers (e.g., for smart refrigerators) aligns with industry trends that position Wi-Fi as the dominant protocol for high-performance smart home devices (Yang et al., 2022). However, the higher power consumption of Wi-Fi, particularly for battery-operated devices, poses a challenge in practical home automation settings. This is an issue that has been discussed widely in the literature (Liu et al., 2020), highlighting the trade-off between performance and energy efficiency.

Zigbee and Z-Wave, with their lower latency and moderate throughput, perform well for simple tasks like controlling lights and thermostats. These results are consistent with industry observations, where Zigbee and Z-Wave are typically used in low-power, short-range applications (Jara et al., 2019). These protocols are favored for devices requiring long battery life, such as sensors, motion detectors, and basic appliances. The low energy consumption of Zigbee and Z-Wave was a significant advantage noted in the study and has been widely acknowledged in the literature as a key strength for home automation systems designed for continuous or long-term operation.

Power Consumption and Energy Efficiency: The power consumption results in this study align with industry expectations for low-power wireless protocols like Zigbee and Z-Wave. Both protocols are specifically designed to support long battery life in smart home devices, making them ideal for use in energy-efficient home automation systems (Liu et al., 2020). The increasing emphasis on sustainability and energy efficiency in the smart home market

highlights the growing importance of these protocols. As consumers become more environmentally conscious, the demand for devices that minimize power consumption is expected to increase (Gubbi et al., 2013).

While Wi-Fi's higher energy consumption was acknowledged, its widespread use for high-data applications in smart homes is unlikely to be significantly disrupted by energy concerns in the short term. Industry trends indicate that the use of smart routers and mesh networking for Wi-Fi could alleviate some of these power challenges by improving signal strength and reducing the power required for individual devices (Zhang et al., 2021). However, as the smart home ecosystem continues to expand, optimizing power consumption will remain a critical area for improvement, especially for battery-operated devices.

Usability Analysis:

Ease of Setup and Integration

The findings that Wi-Fi devices were the easiest to set up align with existing research on user experience in smart homes. Simplified installation processes are a significant factor in the adoption of smart home technologies, and consumer demand for easy-to-install products has driven industry trends toward plug-and-play solutions (Gao et al., 2020). The widespread availability of Wi-Fi in homes, combined with user-friendly mobile apps, has contributed to Wi-Fi's popularity as the default wireless protocol for many smart appliances.

User Interface Satisfaction and Control:

The evaluation of smartphone apps and voice assistants reflects a growing trend in the smart home industry toward voice-activated control and mobile app interfaces as the primary means of interacting with smart appliances. The high user satisfaction with apps and voice assistants is consistent with existing research on user preference for hands-free, intuitive control in home automation systems (Zhang et al., 2021). As the smart home market expands, voice control, integrated with platforms like Alexa and Google Assistant, is expected to grow significantly, making it an essential feature for new devices (Yang et al., 2022).

However, the study also identified issues related to voice recognition errors and delayed responses from voice assistants, which align with ongoing challenges in voice interface technologies (Gao et al., 2020). As voice-activated control becomes more prevalent, further refinement of natural language processing and voice recognition will be necessary to ensure reliability, especially in noisy home environments.

3.2.2 Security and Privacy Concerns

The study found that security and privacy concerns were a significant issue for many users, particularly with Wi-Fi-based devices that transmit data over the internet. This finding reflects a broader trend in the smart home industry, where data security is increasingly a point of concern for consumers. As smart home devices collect large amounts of personal data, including daily routines and behavioral patterns, the need for robust security mechanisms becomes critical (Jeong et al., 2022). Research indicates that the vulnerability of these devices to cyberattacks or data breaches is a significant barrier to wider adoption (Gubbi et al., 2013).

3.2.3 Benefits and Limitations of Wireless Home Automations

Convenience and Flexibility: Wireless home automation systems enable remote control of appliances from anywhere, offering significant convenience for users (Liu et al., 2020). The use of smartphone apps and voice assistants enhances user accessibility and ease of control.

Energy Efficiency: Protocols like Zigbee and Z-Wave provide energy-efficient solutions for home automation, reducing power consumption in battery-operated devices and supporting the growing demand for sustainable smart home technologies (Jara et al., 2019).

Scalability and Customization: The flexibility of wireless networks, particularly mesh networks used by Zigbee and Thread, allows users to expand their smart home systems by adding new devices without significant technical challenges (Jeong et al., 2022).

Limitations:

Interoperability Issues: While advances are being made, interoperability between different manufacturers and ecosystems remains a significant limitation (Yang et al., 2022). Devices from different brands using different wireless protocols often face integration challenges.

Security and Privacy Concerns: As smart home devices become more integrated into daily life, ensuring the security of personal data remains a critical concern for consumers (Zhou et al., 2019).

Power Consumption: The high power consumption of Wi-Fi-based devices remains a barrier for long-term operation, particularly for battery-powered devices (Liu et al., 2020).

4. CONCLUSION

Wi-Fi offered the lowest latency and highest throughput, making it ideal for data-intensive applications such as security cameras and smart refrigerators. However, its relatively high power consumption poses challenges for battery-operated devices.

Zigbee and Z-Wave provided reliable, energy-efficient solutions with lower latency and moderate throughput, making them well-suited for basic smart home tasks like lighting control and thermostat adjust

Wi-Fi devices were the easiest to set up, benefiting from widespread home network compatibility and intuitive smartphone apps. In contrast, Zigbee and Z-Wave devices required additional hubs or gateways, leading to longer setup times.

Wi-Fi devices, which transmit data over the internet, raised significant privacy and security concerns among users. While Zigbee and Z-Wave offered more secure communication protocols, the overall security of smart home ecosystems remains a key challenge.

REFERENCES

Ahmed, S., et al. (2018). Comparative analysis of energy consumption in wireless home automation systems. Journal of Energy Engineering, 144(3), 04018028.

Al-Fuqaha, A., et al. (2015). Wireless mesh networks and Zigbee for home automation applications. IEEE Internet of Things Journal, 2(5), 452-460.

Hossain, M. S., Fotouhi, M., & Hasan, R. (2020). Smart home automation: technologies, applications, and research challenges. IEEE Access, 8, 30713-30735.

He, J., et al. (2021). Bluetooth Low Energy for home automation: A survey. Journal of Communication and Networks, 23(1), 55-66.

Jara, A. J., Skarmeta, A. F., & Parra, L. (2019). Smart home automation systems: A survey. Future Generation Computer Systems, 96, 11-23.

Jovic, J., et al. (2020). Wi-Fi-based home automation systems: Performance evaluation and challenges. Computer Networks, 176, 107287.

Li, X., et al. (2020). Hybrid Zigbee-Wi-Fi protocol for home automation: An approach to improving scalability and reliability. Future Generation Computer Systems, 106, 136-145.

Liu, C., Zhai, M., & Zhang, X. (2020). Wireless communication technologies for smart home applications. Journal of Network and Computer Applications, 170, 102795.

Miorandi, D., et al. (2012). Internet of things: Vision, applications, and research challenges. Ad Hoc Networks, 10(7), 1497-1516.

Mourshed, M., et al. (2017). The impact of home automation on energy consumption: A review. Energy Reports, 3, 207-216.

Advanced Journal of Engineering and Scientific Applications (AJESA)

Research Paper Open Access

Available online at www.ajesa.com.ng Vol.2, No.1, 2025. pp.37-44

Effect of Storage time on Physico-Chemical properties of sachet water produced and consumed in Afikpo Metropolis of Ebonyi State, Nigeria

***[1]Ajike Victor Onu, [2]Ben U. Ngene and [1]Uchendu Emeka Ndukwe**

[1]Department of Civil Engineering Technology Akanu ibiam Federal Polytechnic Unwana, Ebonyi State Nigeria
[2]Department of Civil Engineering, Michael Okpara University of Agriculture Umudike, Abia State Nigeria

Corresponding Author::victorajike@gmail.com*[1]

Abstract

Sachet water consumption and the resultant effect on human health have prompted several studies across Nigeria. Effect of storage time on physico-chemical properties of sachet water produced and consumed in Afikpo metropolis was carried out in this study. Five sachet water brands (SWB) were selected and evaluated for a period of six (6) weeks to investigate the physico-chemical. The concentration of NH4, NO3, NO2, fe, PO4, O2, Ca/Mg, CaCO3 and pH level were determined using Aquanal Fishwater Lab. Turbidity was determined using H188703 turbidimeter. The result obtained indicates that the concentrations of the analyzed properties were within the permissible limit by WHO and NSDWQ. The statistical analysis of $p<0.05$ significant showed that the selected sachet brands met the standards within six weeks of storage at ambient temperature. Therefore, the result obtained shows that the sachet water sold in Afikpo Metropolis meets with WHO and NSDWQ standard and suitable for drinking purposes within six (6) weeks of storage.

Abstract: *Storage time, Physico-chemical, sachet water and turbidity*

1. INTRODUCTION

Water is of essential significance to human physiology and man's proceeded with presence relies especially upon its accessibility (Akuagbazie and Onweluzo, 2010). Water is perhaps the main normal resource known on the planet (Ojo et al., 2005). It has consistently been a subject of incredible interest to man since it is fundamental for man to endure. Water of good drinking quality is of fundamental significance to human physiology and man's proceeded with presence relies particularly upon its accessibility. A normal man (of 53 kg – 63 kg body weight), requires around 3 liters of water in fluid and food every day to keep healthy (Wordlaw et. al., 2004). According to Pidwirny (2001), the total volume of water on earth is estimated to be 1.409x1010 cubic kilometres with 97.25% forming the ocean, 2.05% as glaciers, 0.68% as groundwater 0.01% in lakes, 0.005% as soil moisture, 0.0001% in the atmosphere, 0.0001% in rivers and 0.0004% in the biosphere.

Great quality water is scentless, tasteless, colourless, and liberated from any type of contamination (Ezeugwuenne et al.,2009).

Okonkwo et al., (2008) affirmed that the inventory of safe drinking water is thought of to have a significant impact on the prevention of transmissible water-borne diseases. Water quality is determined by its physical, chemical, and microbiological properties. Each living being need water to endure. A great many people living in the significant urban communities of Nigeria don't approach pipe borne water, most likely due to its unavailability and/or inadequacy where

obtainable, this has led to increased water related diseases that has continued to be one of the major health problems globally (Omalu et al. 2010, Onifade and Ilori, 2008).

Onifade and Ilori (2008) also noted that the high prevalence of diarrhoea among children and infants could be traced to the use of unsafe water and unhygienic practices. Anuonye et al., (2012) observed that unsanitary water has particularly serious negative effects on young children in the developing world. They further reported that each year, more than 2 million persons, mostly children less than five years of age, die of diarrhoea which accounts for 17% of all deaths between the year 2000 and 2003. Diarrhoea is ranked third among the major causes of death in children, after neonatal causes and acute respiratory infections. To curb this health problem, bottled water was introduced, but that could only be afforded by individuals who earned good incomes. Low income earners could only afford the cheaper sachet packed water which surfaced in the late 1990s.

According to the World Health Organization (2004), it is estimated that 80% of all sickness and diseases in developing countries can be attributed to water-borne infectious agents. The World Bank further estimated that if everyone had access to pure drinking water, less than 200 million episodes of diarrhoea would occur each year and 2 million childhood death will be avoided. There is challenge need for satisfactory compact water to satisfy essential human self – adequate demand.

Safe drinking water is an essential requirement for human turn of events, health and prosperity and it is a worldwide acknowledged human right (WHO, 2003).

Sachet water, a type of packaged water has, therefore, gradually become the most widely consumed fluid for both the rich and the poor in Nigeria. Sachet water is a sort of water which is preoccupied from typical pipeline water supply (regular water) or borehole and is bundled into a straightforward 50cl nylon sack yet more likely than not went through a few or full traditional water treatment cycles of deliberation, air circulation, screening, flocculation, coagulation, sedimentation, filtration, and chlorination. It is the brand of decision to everybody since it is a cheaper option in contrast to the packaged brand, viewed as the best beverage of the wealthy. Seen cleanliness, virtue, taste, and, in particular, wellbeing are the purposes behind sachet water utilization. Tragically, the issue of its virtue and health concerns has started to manifest (Oladipo et. al., 2009).

Sachet water is managed as a food item in Nigeria by National Agency for Foods Drugs Administration and Control (NAFDAC). Sachet water isn't totally sterile; it may not be altogether liberated from every single irresistible microorganism. The potential risk related with sachet water is defilement, which is a factor of the wellspring of the actual water, treatment, bundling materials, administering into bundling materials and conclusion (Omalu et al., 2010). The success and market performance of the sachet water industry is critical to the health and economic well-being of the nation. Unfortunately, most of the companies in the industry are under-performing due to their inability to leverage quality and quality management strategies (Dodoo et al., 2006). The industry continues to be challenged by numerous quality problems that are of much concern for the health of people who patronize packaged water products. There is therefore the need for the immediate adoption of a quality system that is sufficient to combat the quality problems of such an important industry.

Many studies have been done to assess the physicochemical as well as microbiological quality of sachet water in different parts of Nigeria (Addo et al., 2009).

This present study will provide information on aspect of the palatability in terms of physico-chemical properties of vended sachet water within Afikpo Metropolis of Ebonyi of as well as clarify concerns about its safety to consumers.

1.2 LiteratureRreview

The drinking water that is protected and tastefully satisfactory involves high need to National Agency of Food and Drugs Administration and Control (NAFDAC) and other regulatory Agencies like WHO, FEPA, and SON. Drinking portable sachet water that is fit for human consumption is expected to meet WHO standard and be free from chemical and physical substances and micro – organism in an amount that cannot be hazardous to health (Denloye, 2004). Access to safe drinking water is key to sustainable development and essential to food production, quality health and poverty reduction (Adekunle et al., 2004). Safe drinking water is crucial forever and an acceptable safe stockpile should be made accessible to buyers (Kalwale et al., 2012). Mustapha (2008) asserted that the changes in physical characteristics like temperature, suspended solid and chemical characteristics of water such as dissolved oxygen provides valuable information on the quality of water. Ntengwe (2003) stated that the existence of elevated levels of elements and organisms in drinking water constitutes poor water quality, which is a recipe for disease outbreaks.

To safe aide the health of individuals and to diminish to the barest least of terrible encounters of drinking or utilizing bad quality water, it is fundamental that the nature of water ought to be observed with the view of finding solution to

health problems associate with use of low-quality water, in producing sachet portable water, (Ukpong, 2004). The drinking water that is protected and tastefully OK involves high need to National Agency for Food and Drugs Administration and Control (NAFDAC) and other regulatory Agencies like WHO, FEPA, and SON. Drinking portable sachet water that is appropriate for human ingestion is expected to meet WHO standard and be free from chemical and physical substances and micro – organism in an amount that cannot be hazardous to health (Denloye, 2004).

To accomplish the arrangement of safe sachet drinking water for human utilization in Nigeria, NAFDAC recommended that potable water should not contain any pathogen and the physicochemical properties of the water should also not exceed the NAFDAC recommended limits (NAFDAC, 2001). Production outfits should of such drinking waters should also adhere strictly to the NAFDAC guidelines (NAFDAC, 2004).

Again, WHO (2011) explained that in the effort to protect citizens in urban areas, governments all over the world must augment the quality of urban drinking water that is to be provided to their citizens. However, in the bid to maintain the quality of urban drinking water, the manufacturers have had to spend huge sums of money to pump, treat package and distribute the water to the consumers.

Truth be told, water of good drinking quality many emerging nations, accessibility of consumable water has turned into a basic and critical issue, and it involves extraordinary worry to families and networks relying upon Non-public water supply framework. Expansion in human populace has applied a huge pressure on the arrangement of safe savouring water non-industrial nations (Ibemesim, 2014).

Okechukwu et al., (2015) additionally examined six unique brands of sachet water to be specific: Wilnelly, prephil, peak, lephzzy aljonlife and mayln gathered from various parts inside the Federal University of Technology, Owerri grounds were inspected utilizing standard techniques. Physiological and microbiological investigation were done by Nigeria standard of drinking water quality (NSDWQ) and World Health Organization (WHO), the five brands of sachet drinking water had their Ph esteems beneath the lower reasonable cutoff, going from 5.21 to 5.93. Just lephzzy sachet water brand had Ph esteemed inside as far as possible. Turbidity result went from 0.24 to 0.43, which could be supposed to be adequate. The all out dissolved solids result of the brands of sachet water went from 21.00 to 156.00. The various brands of sachet water had short proximity results in the vast majority of the boundaries examined and agreeably satisfied the set guidelines. Anyway a few boundaries like discovery of different components, Barium were found over its passable breaking point in five out of the six examples going from 1.00 to 2.00, while lephzzy sachet water had its worth beneath identification level. From the ANOVA test, pH, all out dissolved solids and Barium had huge contrast ($P < 0.05$), while other physicochemical boundaries tried were irrelevant ($P>0.05$) among the different sachet water tested. In light of these results, there is need to notice great quality control examination to guarantee similarity with the set guidelines. Additionally arbitrary testing of market tests will be a decent method of recognizing whether the quality is fulfilling the necessary guidelines.

2. MATERIAL AND METHODS

The research is employing the use Aquanal Fishwater and HI88703 turbidity meter to analysis the physico-chemical properties of the sachet water produced and consumed with Afikpo metropolis. Five brands of sachet water with NAFDAC certification were randomly collected in different parts of Afikpo metropolis in bags within 24hours of production. These were denoted as SWB1 – SWB5. The samples were taken to Akanu Ibiam Federal Polytechnic water laboratory where they were stored at ambient temperature, since it is the most common method of storage for all brands of sachet water consumed within Afikpo Metropolis. Subsamples were drawn from the stock samples in duplicates for physico – chemical analysis. Physico – chemical properties of the sachet water were analysed immediately after collection and subsequently thereafter on two weekly basis for six weeks

The following physico – chemical tests were conducted for the determination of the concentration of the properties:

- Ammonium concentration in water samples (NH4).
- Nitrate concentration in water samples (NO3).
- Nitrite concentration in water samples (NO2).
- Iron concentration in water samples (Fe).
- Phosphate concentration in water samples (PO4).
- Oxygen concentration in water samples (O2).
- Total hardness in water samples.

3. RESULTS AND DISCUSSION

3.1 Results

3.1.1 Analysis of sachet water sample before and after storage

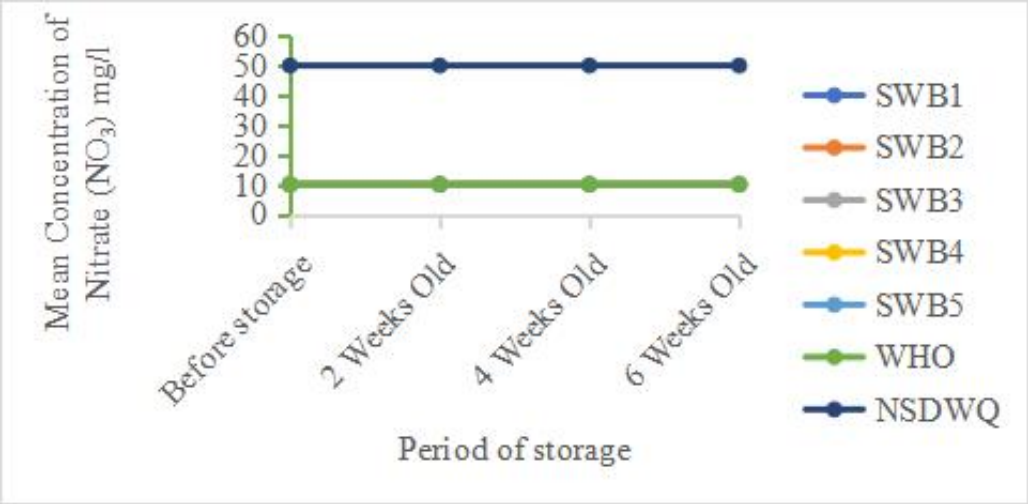

Figure 1: Mean concentration of Nitrate (NO3) mg/l in the Sachet Water Brands.

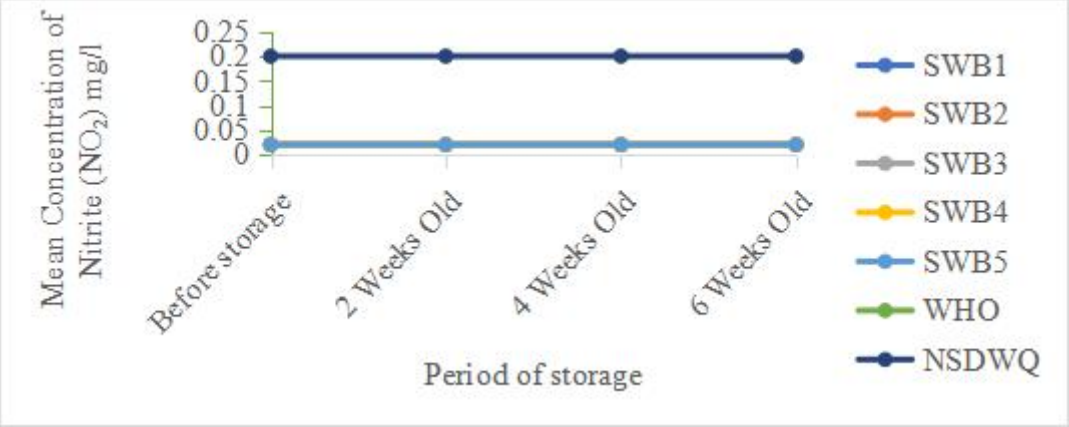

Figure 2: Mean concentration of Nitrate (NO2) mg/l in the Sachet Water Brands.

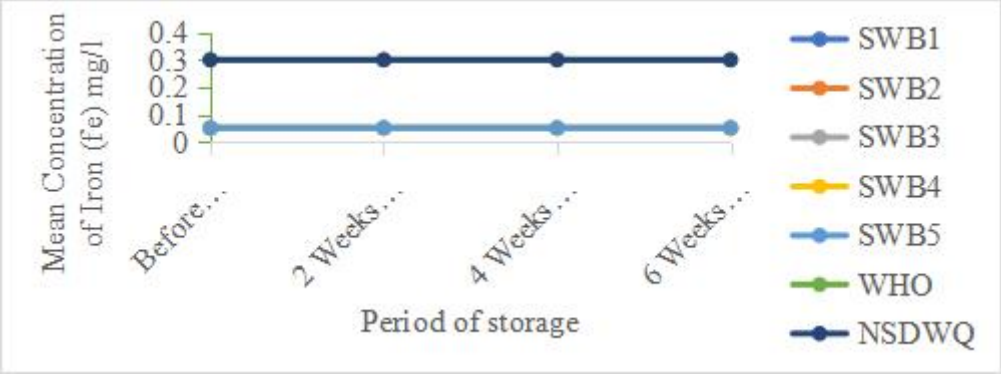

Figure 3: Mean concentration of Iron (fe) mg/l in the Sachet Water Brands.

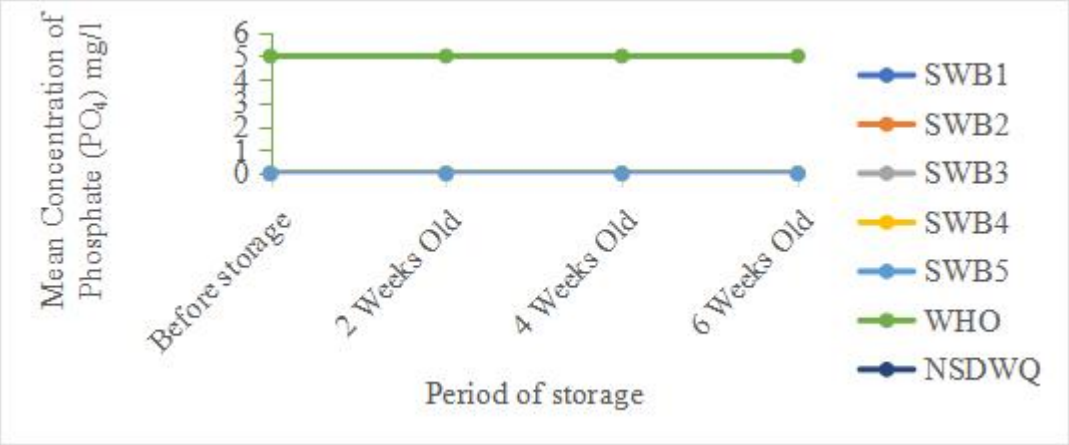

Figure 4: Mean concentration of Phosphate (PO4) mg/l in the Sachet Water

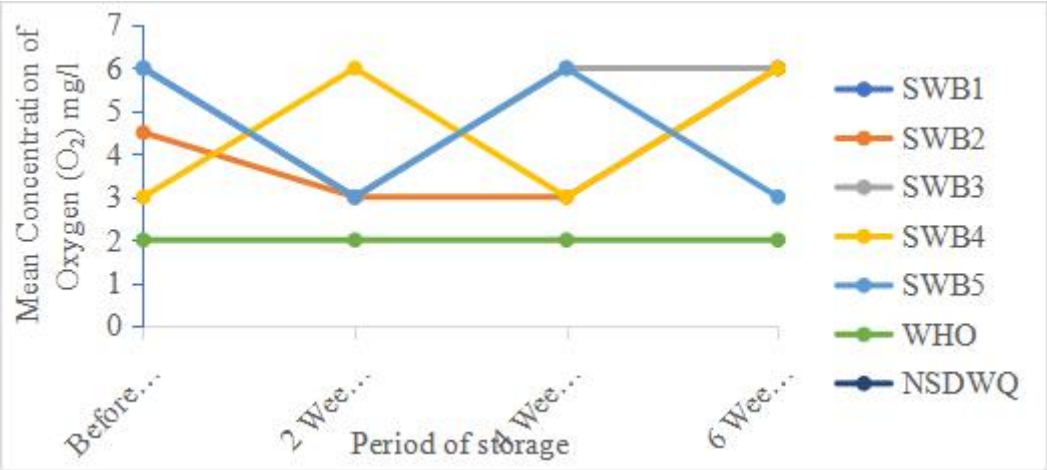

Figure 5: Mean concentration of Oxygen (O2) mg/l in the Sachet Water Brands.

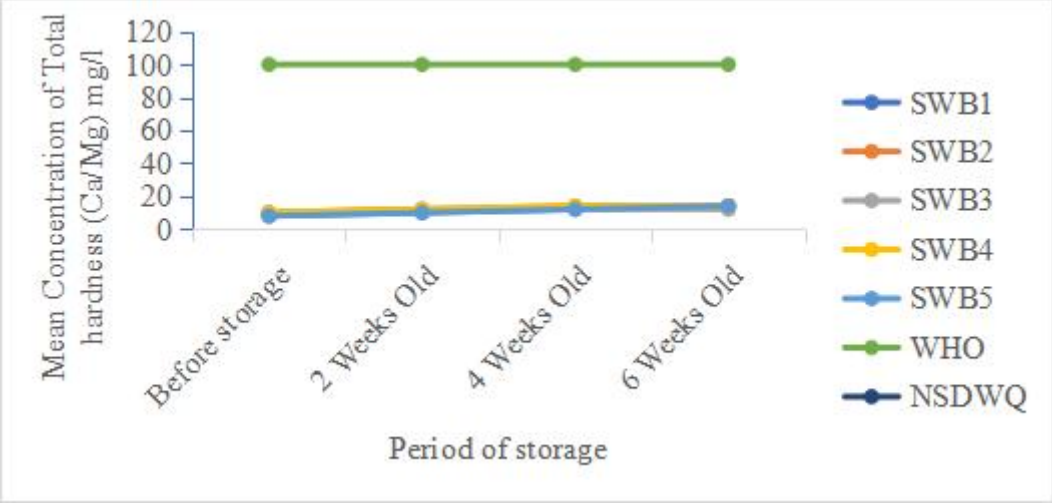

Figure 6: Mean concentration of Total hardness (Ca/Mg) mg/l in the Sachet Water Brands.

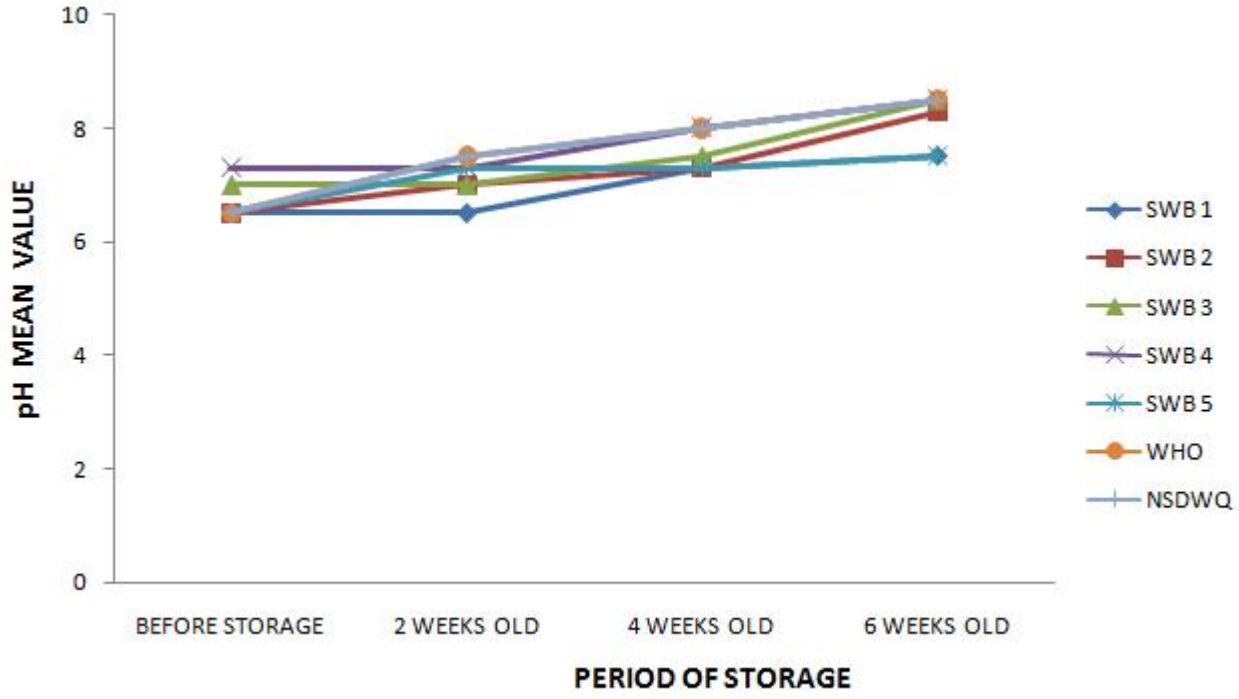

Figure 7: Mean concentration of pH in the Sachet Water Brands.

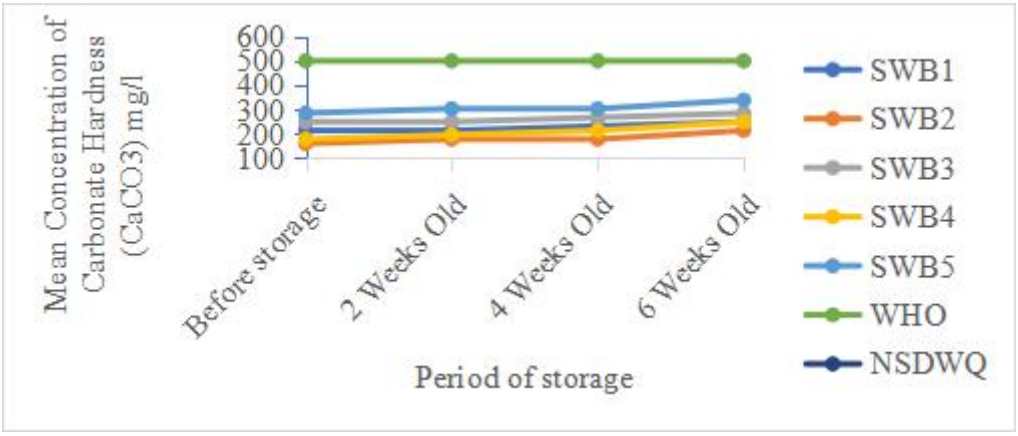

Figure 8: Mean concentration of Carbonate Hardness (CaCO3) mg/l in the Sachet Water Brands.

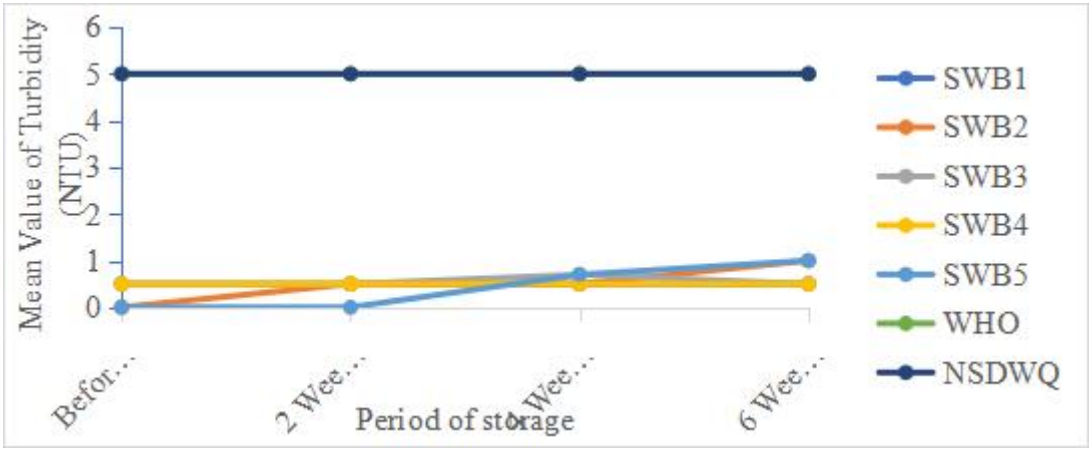

Figure 9: Mean concentration of turbidity (NTU) in the Sachet Water Brands.

3.2 Discussion

The laboratory analysis reveals that the mean concentration of Ammonium (NH4) mg/l in the Sachet Water Brands was ≤0.05 and statistically significant different at 5% level of significance shows that the ammonium concentration is within the permissible limit of drinking water by the establish standards. Figure 1 reveals that all the selected sachet water brands had 10mg/l concentration throughout the period of storage. There was no significant difference in the Nitrate values ($p<0.05$) of the sachet water brands. The nitrate values are within the acceptable limits of WHO and NDSWQ and will not be harmful to the consumers. Figure 2 also show that the concentration Nitrite (NO2) in the sachet water brands was ≤0.02mg/l throughout the test period, statistically no significant differences in the values of nitrite ($p<0.05$) was noticed throughout the test period. The nitrite values were also within the permissible limits of WHO and NSDWQ standards and is not dangerous to human health. Figure 3 shows Iron (fe) concentration in the selected sachet water brands, the study reveals an average value of <0.05mg/l were gotten from test chart throughout the test period and significant differences in the Iron values ($p<0.05$) was noticed statistically. The Iron concentration was okay for consumption as it didn't exceed the permissible drinking water limits as established by WHO and NSDWQ. The mean concentration of phosphate (PO4) in Figure 4 shows that the phosphate was not present in the selected sachet water brands and is still allowable by WHO and NSDWQ limits. Therefore, the selected sachet water brands are fit for consumption. Figure 5 disclose Oxygen concentration test was carried out on the water samples. The following result were obtained; SWB1 recorded a mean range value of 3mg/l - 6mg/l, SWB2 had a mean range value of 4.5mg/l – 6mg/l, SWB3 recorded a mean value of 3mg/l – 6mg/l, SWB4 had a mean range value of 3mg/l – 6mg/l and SWB5 recorded a mean range value of 3mg/l – 6mg/l. significant differences in oxygen values ($p<0.05$) were observed statistically. However, the oxygen concentrations were above the permissible limit of WHO but NSDWQ limit was not found.

In Figure 6 Mean total hardness (Ca/Mg reveals that SWB1 had a range values of 8mg/l – 14mg/l, SWB2 recorded a range values of 10mg/l – 14mg/l, SWB3 had a range values of 10mg/l – 12mg/l, SWB4 recorded a range values of 10mg/l – 14mg/l and SWB5 had a range values of 8mg/l – 14mg/l. statistically no significant differences in the total hardness values ($p<0.05$) were obtained. Since the mean values were within the WHO and NSDWQ permissible drinking water limit the water is certified okay for human consumption. Again, in Figure 7 The mean pH value also disclose the following results: SWB1 had a mean value of 6.5 – 7.5, SWB2 recorded a range value of 6.5 – 8.3, SWB3 had a range value of 7.0 – 8.5, SWB4 recorded a range value of 7.3 – 8.5, SWB5 recorded the range values of 6.5 – 7.5. The result shows that the sachet water brands had a pH mean values within the reference standards. However, statistically there was not a significant difference in the pH values ($p<0.05$) within the testing period making water fit for consumption.

Figure 8 The samples were analysis in terms Carbonate Hardness (CaCO3) concentration. The mean range values manifest that SWB1 had 214.2mg/l – 249.9mg/l, SWB2 recorded 160.7mg/l – 214.2mg/l, SWB3 had 249.9mg/l – 285.6mg/l, SWB4 recorded 178.5mg/l – 249.9mg/l and SWB5 had 285.6mg/l – 339.2mg/l. No significant differences were observed. The range of values recorded are still within the permissible drinking water standard. Therefore, the water is certified safe for human consumption and poses no threat to human health. Lastly in Figure 9 Turbidity mean range values were as follows; SWB1 recorded 0.5ntu throughout the test period, SWB2 had 0.0ntu – 1.0ntu, SWB3 had 0.5ntu – 0.7ntu, SWB4 had 0.5 throughout the test period and SWB5 recorded 0.0ntu – 1.0ntu. There was a significant difference in the turbidity values ($p<0.05$). the findings of the study indicates that the turbidity of the selected sachet water tested were within the approved range and therefore the samples were good for drinking as far as turbidity is related.

4. CONCLUSION

Sachet water is a very essential component of the water distribution system of the Afikpo metropolis. The patronage of factory-produced sachet water is very high in Afikpo metropolis since it is the commercial hub of Ebonyi State and is also difficult to access pipe borne water in the area. The physico-chemical properties accessed in this study were with the NSDWQ and WHO permissible limit and show that selected sachet waters are of good qualities for the storage period of six (6) weeks at ambient temperature. So therefor, it is also very important that the regulatory authorities should and must continue with their regular inspection activities of sachet water supplies to Afikpo metropolis. In order to safe guide the health of consumers. Regulatory bodies should also intensify effort at monitoring of packaged water manufacturers, periodic sanitary inspection of factories should be carried out. Emphasis should be placed on good management practices by producers of sachet water especially in terms of location of the factories and maintaining high level of hygiene within the premises of production.

REFERENCES

Addo, K.K, Mensah, G.I. Donkor B, Bonsu, C, Akyeh. M., (2009). *African Journal of Food, Agriculture, Nutrition and Development,* 9 (6).

Aguagbazie, C. A. and Onweluzo, J. C. (2010). The quality of bottled and sachet water sold in Nsukka Town.
Ahima, J and Ofosu S.A (2014). Assessment of the quality of sachet water vended in Ghana: experiences from the new Juaben municipality *Health, Safety and Environment,* 2(1): 1 11.
Anuonye J. C, Maxwell O. M. and Caleb, M. Y. (2012). Quality of sachet water produced and marketed in Minna metropolis, North Central Nigeria, *African Journal of Food Science* 6(24): 583-588.
Denloye, S. A, (2004). Quality parameters for packaging water NAFDAC laboratory experience, IPAN
Ibemesim, A.O. (2014). Comparative study of qualities of sachet and bottle water sold on the streets of Abuja, Nigeria. *South American Journal of Public Health,* 2(3):308-328.
Isikwue, M.O and Chikezie, A (2014). Quality assessment of various sachet water brands Marketed in Bauchi metropolis of Nigeria. *International journal of advances in Engineering and Technology,* 6: 2489 – 2495.

Kalwale M. Ajit and Savale A. P. (2012). Advances in applied science research 3(1): 273-279.
Mustapha, K. M (2008). Assessment of the water quality of Oyun Reservoir, Offa, Nigeria using Selected physic-chemical parameters. *Turkish Journal of Fisheries and Aquatic science* 8: 309 -319.
NAFDAC, (National Agency for Food Drugs Adimistration and Control) (2001). Consumer Bulletin October – December.pp.1-9.
NAFDAC, (2004), Guidelines for production and regulation of packaged water, new guidelines NAFDAC, Abuja, Nigeria.NIS, (NIS_544:_2007). Nigeria Standard for Drinking Water Quality,(NSDQW),http://www.unicef.org/nigeria/ng_publication_Nigeria_Standard_for_Drinking_Watar_Quality.pdf.
Ntengwe, F.W, (2005). Designing a Domestic Water Supply System-The Engineer's Perspective and Considerations as a Challenge to Consumers. *Physics Chem. Earth*, 30(11-16): 850-858. http://ewb-uiuc.org/system/files/sdarticle.pdf.
Ojo, O. A, Bakare, S. B. and Babatunde, A. O. (2005). Microbial and chemical analysis of potable water in public-water supply within Lagos University, Ojo. *African Journal of Infectious Diseases,* 1(I): 30-35.
Okechukwu, R.I. Ogukwe, C.E. and Igboasoiyi O.O. (2015). Physico-Chemical Quality of different Brands of Sachet Water Sold in Federal University of Technology Campus Imo State, *Nigeria Research Journal of Chemical Sciences*, 5(1): 83-87.
Okonkwo, I.O. Adejoye, O.D. Ogunusi, T.A. Fajobi, E.A. and Shittu, O.B. (2008). Microbiological and Physiochemical analysis of Different Water Samples used for Domestic Purposes in Abeokuta and Ojota, Lagos State, Nigeria. *African. Journal. Biotechnol,*7 (3): 617-621.
Oladipo, I. C, Onyenike, I.C and Adebiyi, A. O. (2009). Microbiological analysis of some vended sachet water in Ogbomoso, Nigeria. *African Journal of Food Science*, 3(12): 406 – 412.

Omalu, I.C.J. Eze, G.C. Olayemi, I.K. Gbesi, S. Adeniran, L.A. Ayanwale, A.V. Mohammed, A.Z. and Chukwuemeka, V. (2011). Contamination of sachet water in Nigeria: Assessment and health impact: online, *Journal of Health Allied Sciences,* 9(4): 15.

Onifade, A. K. and Ilori, R. M. (2008). Microbiological analysis of sachet water vended in Ondo State, Nigeria. *Environmental Research Journal,* 2(3):107-110.
Ukpong O. H (2004). International Journal of water Resources and Environmental Engineering, vol. 4, issue 5, pp. 134-138.

WHO (2003). Guideline for drinking water quality vol 1 recommendations. World Health Organization 3rd ed who Geneva.
WHO (2004). Report of the WHO workshop: Nutrient minerals in drinking water and the potential health consequences of long-term consumption of demineralized and re- mineralized and altered mineral content drinking waters. Rome, 11–13 November2003 (SDE/WSH/04.01).

WHO (2011). Guideline for drinking water quality vol. 1 recommendations. World Health Organization 3rd ed who Geneva.
Wordlaw, .M. Hampl, J. S. and Disilvestro, R. A. (2004). Perspectives in Nutrition. 6th ed. McGraw-Hill Publishers, New York, pp.372 – 412.

Advanced Journal of Engineering and Scientific Applications (AJESA)

Research Paper Open Access

Available online at www.ajesa.com.ng Vol.2, No.1, 2025. pp.45-58

Experimental Investigations of Carbon Fiber Hybridization on Mechanical Strength Properties of Ramie Fiber Reinforced Epoxy Composite

George O. Okoronkwo[1], Ibe Kizito Chidozie[2], Obimba-Wogu Jesuborn[3]

[1]Department of Chemical Engineering, Micheal Okpara University of Agriculture, Umudike, Abia State, Nigeria; okoronkwo.george@mouau.edu.ng, ogeorgeonyeka@gmail.com

[2]Department of Civil Engineering, Micheal Okpara University of Agriculture, Umudike, Abia State, Nigeria; Ibe.kizito@mouau.edu.ng

[3]Department of Civil Engineering, Micheal Okpara University of Agriculture, Umudike, Abia State, Nigeria; Obimba.jesuborn@mouau.edu.ng

Corresponding Author::ogeorgeonyeka@gmail.com Phone: 0806791192

Abstract

In this study, an attempt is made to check whether a hybrid composite made up of both synthetic and natural fibers (Carbon and ramie respectively) can be made bio-degradable, at least to some extent, without much compromising on the mechanical strength properties. Hybridized composites were produced by reinforcing alkali treated ramie and carbon fibers into epoxy resin using hand lay-up and compression methods. By varying the number of layers of fibers in the composite samples and fixing 20 % fiber weight for all composites, nine distinct combinations of samples were prepared. The optimum tensile strength of 385.68 MPa, flexural strength of 646.08 MPa, and impact energy of 4.8 J were obtained for composites produced with pure carbon fiber, whereas hybrid composite exhibit tensile strength of 366.76 MPa, flexural strength of 645.41MPa and impact energy of 4.7 J. The interfacial bonding between the fibers and matrix of tested samples were studied using a scanning electron microscope (SEM), as well as the arrangement of fibers within the matrix for the manufactured composite.

KEYWORDS: Natural fiber; synthetic fiber; epoxy resin; hybrid composite materials; mechanical strength properties; SEM; FT-IR.

1. INTRODUCTION

Composite material is formed by the combination of two or more constituent materials. The matrix phase is used to hold the fibers together and also to transport the load to the fibers, and the reinforcing phase is used to take the maximum load, but these two phases are chemically distinct, i.e., there is no chemical reaction between them. This material has high strength with sufficient stiffness and toughness with a light weight. This combination of properties offers a great advantage in mechanical design. So, these properties may be suitable for various industries, such as automotive, aerospace, infrastructure and sports (Jenish et al. 2022; Madhu et al. 2020; Yashas Gowda et al. 2022; Okoronkwo et al. 2022). Metals are proven engineering materials for various applications in terms of strength and stability. Nowadays, their usage is declining significantly due to high weight and high corrosiveness. Later, synthetic fiber-reinforced composites have become popular, but they are non-biodegradable and costly. To overcome this, natural fibers are introduced due to their biodegradability, low cost, availability, low density, and renewability (Ilyas et

al. 2019; Senthamaraikannan et al. 2016; Okoronkwo et al. 2022). Mechanical properties of natural fibers are varying in nature (inconsistent) due to their growing environment, extraction methods, and seasons. Therefore, natural fiber-reinforced composites (NFRC) may not be suitable for heavy-load bearing applications and high-temperature applications. Natural fibers derived from plants such as jute, sisal, coir, hemp, and kenaf have attracted great attention as a strengthening element in the NFRC composite (Dos Santos et al. 2019; Ramesh et al. 2022; Madu et al. 2019; Ezeokpube et al. 2021).

Natural fibers have few limitations, such as quality variations and high moisture absorption, which cause fibers to swell, leading to poor bonding. Natural fibers are hydrophilic in nature due to the presence of lignin, hemicelluloses, waxes, etc. Mechanical strengths of natural fiber-reinforced composite (NFRC) purely depend on the compatibility between fiber and matrix Okoronkwo et al. 2021). NFRC composites have poor compatibility or interfacial adhesion due to hydrophilic nature of fiber and hydrophobic nature of matrix Okoronkwo et al. 2019). As a result, NFR composite shows reduced mechanical properties. Chemical treatment of fibers removes fiber constituents such as wax, lignin, hemicelluloses, and other substances present over the surface of the fiber (Okoronkwo et al. 2020). As a result, a rough surface of the fiber is obtained, which is helpful in improving the interfacial bonding with the matrix. Because of alkali treatment, damage to fibers may be less at optimum weight proportions, and cost is also reduced. This increased interfacial bonding can transfer the load more effectively from the fiber to the matrix, improving the mechanical properties.

(Reddy et al. 2021) investigated and compared the mechanical properties of composites made with and without alkali-treated Prosopis juliflora fiber and epoxy, concluding that the composite made with alkali-treated fiber has superior mechanical properties. (Rizal et al. 2018) studied the mechanical, chemical, FT-IR, and XRD properties of Typha fiber-reinforced epoxy composites after alkali treatment. Compared to untreated Typha fiber composites, 5 % of NaOH-treated composites demonstrated improved mechanical characteristics.

Many works have employed alkali treatment for natural fibers such as cordia dichotoma (Reddy et al. 2020), abutilon indicum fibers (Mohana Krishnudu, Sreeramulu, and Reddy 2020) and foxtail millet (Reddy et al. 2020) into polymeric matrix composite and reported improved mechanical properties and interfacial bonding between the fibers and the matrix. (Reddy et al. 2020).

Hybrid composites are materials made from a common matrix by combining two or more separate types of synthetic fibers or different types of natural fibers, or by combining both synthetic and natural fibers in varied proportions (Shanmugam and Thiruchitrambalam 2013; Okoronkwo et al. 2022). The hybrid composite has superior qualities that a single type of reinforcement can't match. When natural and synthetic fibers are used, the cost of a hybrid composite can be greatly reduced. The weight content (Wt. %) of reinforcement and the layer in which synthetic and natural fibers are put influence the hybrid composite's final characteristics (TG et al. 2022). The mechanical properties and vibration characteristics have improved significantly with hybridization of carbon fiber with flax fiber as was investigated by (Flynn, Amiri, and Ulven 2016). (Ramesh et al. 2017) carried out studies on a banana/carbon fiber-reinforced hybrid composite to determine its mechanical capabilities and water absorption characteristics. The results of this experiment are the highest tensile strength for 20 % carbon and 80 % banana fiber, the highest flexural strength for pure carbon fiber and the highest water uptake for banana fiber compared to carbon fiber. The physical and mechanical properties of the fiber constituents were used to determine the performance of hybrid composites as seen from (Dinesh et al. 2020; Vinod et al. 2022). The shear strength, hardness, wear resistance, water absorption, and FT-IR properties of the carbon/flax fiber- reinforced composites were fabricated using a hand-lay-up approach. According to the findings, each of the aforementioned features of hybrid composites is comparable to that of pure carbon fiber-reinforced composites. This also suggested that carbon and flax fiber composite hybridization can be used as a structural application while also reducing environmental consequences reported by (Ramesh et al. 2018). (Nagappan et al. 2022) investigated on the effects of fiber length and fiber content along with alkali treatment effects on the mechanical properties of prepared natural fiber-based polymer composites. The work concluded that the optimum fiber length and fiber weight % for obtaining maximum mechanical properties are 7 mm and 30 wt. %, respectively, for both raw and alkali-treated fiber composites.

(Sarasini et al. 2016) developed a hybrid composite with two distinct stacking sequences, such as flax/carbon/flax (FCF) and carbon/flax/carbon (CFC) as well as pure carbon and pure flax epoxy composites, and examined their impact and flexural strengths. Results have confirmed that the impact and flexural performance of CFC composite laminate is slightly higher than that of FCF composite laminate, pure carbon and pure flax epoxy composite laminate. Several researchers have reviewed, studied and confirmed that carbon fiber is an effective hybridizing element of both natural and synthetic fiber-reinforced epoxy composite, due to improved mechanical performance, cost-effective material and decreased environmental impact (Okoronkwo et al. 2019). (Najafi, Khalili, and Eslami- Farsani 2014) manufactured the hybrid composite using pure basalt fibers, carbon fibers, and by altering the weight proportions of basalt fibers and carbon fibers into phenolic resins, and these fibers are stacked in layers within the phenolic resin. The

impact and flexural strength of the hybrid composite are improved by incorporating basalt fiber into the carbon fiber-reinforced phenolic resin. BCFP composite with weight proportions of 0.83:0.17 in the stacking sequence B/C/B/C/B has the highest impact and flexural strength. (Jebadurai et al. 2021) selected low-cost and widely available coccinia grandis stem fibers and laid the composite by reinforcing it in polyester resin. The mechanical, thermal, and hardness properties of the produced composite were examined to ensure that it was suitable for structural purposes. The highest mechanical properties were reported when 40 % by weight of the coccinia grandis fibers were reinforced with polyester resin. Thermal stability (250°C) is also reasonable for the aforementioned hybrid composite. Such hybrid composites are used for a variety of applications, such as car interior, sporting equipment, bone plate and wind turbine blades (Jawaid and Khalil 2011; Jothibasu et al. 2020; TG et al. 2021). (Mahakur, Bhowmik, and Patowari 2022) reviewed the various works to identify the parametric effects on the machining of natural fiber-based composites. Work explored the various methods that can be implemented to reduce the machining defects. (Rangappa et al. 2022) reviewed the use of cellulosic fiber as a reinforcing element in the preparation of composites. The research work explored the recent developments on the utilization of cellulosic fibers in the polymer industries focusing much on the improvement of the mechanical properties, manufacturing methods and its applications in various industries.

The goal of this research is to combine carbon fiber with alkali-treated ramie fiber in an epoxy matrix using a hand-lay-up method and compression moulding. The study on alkali-treated ramie fiber-reinforced epoxy composite with carbon fiber was not published in the literature. Carbon fiber and alkali-treated ramie fibers reinforced with epoxy resin were used to create a hybrid composite. In this study experimental investigations were carried out to determine the tensile, flexural, and impact properties of ramie fiber and carbon fiber- reinforced epoxy composites. The mechanical properties could be applied in structural, automotive, wind turbine blades, aerospace, and infrastructure applications.

2. MATERIALS AND METHODS

2.1 Materials

Ramie fiber, carbon fiber, and epoxy resin are the materials utilized to make hybrid composites. Ramie fibers are harvested in and around the village of Nekade in Imo State, Nigeria. Nycil Company Limited, Nigeria, provided carbon fiber (unidirectional mat 200 gsm). Nycil Company Limited, Nigeria, provided the epoxy resin (LY556 with viscosity at 250°C: 0,7 ÷ 1, 1 Pa.s), which is a diglycidyl ether of biphenyl- A, and the hardener (HY 951 with specific gravity at 25°C: 0.95), which is triethylenetetramine.

Fiber extraction

The ramie fibers were extracted from the bark of the ramie tree by a water retting process followed by mechanical beating. Extracted fiber contains foreign impurities and wax substances; this has been removed by shaking and squeezing of the fiber in running water. Natural fibers are hydrophilic in nature because of their fiber constituents, such as lignin, wax, pectin, etc., which are responsible for water absorption and also lead to poor interfacial bonding. To overcome such phenomenon, a surface modification called alkali treatment is carried out on the fibers.

Alkali treatment

Alkali treatment is simple and economic for treating the natural fibers. In a separate beaker, create the alkali solution (5 wt. % NaOH) by dissolving 100 g of NaOH pellets in 2 L of pure water. After that, the dry fiber is soaked in the alkaline solution for 2 h at room temperature. The fibers were removed from the solution and thoroughly washed with distilled water to remove any NaOH that had adhered to the fiber surface. Hemicelluloses and other contaminants that cling to the fiber are also removed. The fibers were dried in an oven at a continuous temperature of 100 degrees Celsius for 24 h.

Fabrication of composites

For this work, the laminates of the hybrid composites were prepared using a hand lay-up method. Well-dried ramie (R) and carbon (C) fibers are segregated and chopped to a length of 150 mm. Nine different forms of laminates have been prepared with different stacking sequences R/R/R/R (Sample 1), R/R/C/R (Sample 2), C/R/R/R (Sample 3), R/C/R/C (Sample 4), C/R/C/R (Sample 5), C/R/R/C (Sample 6), C/C/R/C (Sample 7), C/C/C/R (Sample 8) and C/C/C/C (Sample 9). Along with a pure epoxy composite, pure alkali-treated ramie fiber-reinforced epoxy composite and pure carbon fiber-reinforced epoxy composites were manufactured to compare mechanical properties. The total fiber content was fixed at 20 wt%. Epoxy resin and hardener were properly mixed with the 100:10 weight ratio in a separate beaker. A glass mould with a size of 150 mm x 150 mm x 3 mm was used to prepare the composite laminates. Releasing gel was spread over the surface of mould for easy removal of composite laminate. A thin layer of epoxy mixture was applied on the surface of the mould, and then carbon fibers were uniformly laid over the mixture, and the required amount of epoxy mixture was poured over the carbon fiber.

Table 1. Layer designation and fiber weight content (wt. %) in hybrid composite.

Composite designation	Layering sequence	Position of Fibers (carbon and ramie fibers in the laminate with a constant weight of 5 (wt. %) Layer 1 (5 wt.%)	Layer 2 (5 wt.%)	Layer 3 (5 wt.%)	Layer 4 (5 wt.%)
Sample 1	R/R/R/R	R	R	R	R
Sample 2	R/R/C/R	R	R	C	R
Sample 3	C/R/R/R	C	R	R	R
Sample 4	R/C/R/C	R	C	R	C
Sample 5	C/R/C/R	C	R	C	R
Sample 6	C/R/R/C	C	R	R	C
Sample 7	C/C/R/C	C	C	R	C
Sample 8	C/C/C/R	C	C	C	R
Sample 9	C/C/C/C	C	C	C	C

*C: Carbon fiber *R: Ramie fiber.

After proper impregnation of epoxy mixture on carbon fiber, ramie fibers were mounted on the first layer of carbon fiber. This procedure was continued for the rest of layers (four layers). The remaining mixture of resin was poured on top of fourth layer and roller was used to distribute the epoxy mixture and to eliminate air gaps formed between the layers during the processing. Releasing gel was applied to OHP (Over Head Projector) sheet and is placed above it to obtain a smooth surface. For 24 h, a weight of 20 kg was loaded onto each mould to obtain the required dimensions of the laminate and cure the laminate. Table 1 shows the reinforcement sequence arrangement in various composite samples.

Characterization

Tensile strength test

The tensile strength of a material refers to its ability to be stretched without breaking under uniaxial force. The INSTRON Universal Testing Machine (Model-3369) with a load cell capacity of 10 kN was used to determine tensile parameters such as tensile strength and the tensile modulus of hybrid material. With a dimension of 150 mm x 15 mm x 3 mm, a tensile test was performed according to the ASTM standard ASTM: 3039. Each hybrid composite sample was tested three times, with the average values recorded.

Flexural strength test

The INSTRON Universal Testing Machine (Model-3369) was used to assess the flexural properties of prepared hybrid composites under specific conditions (crosshead speed rate: 10 mm/min; load cell: 10 kN; support span length: 50 mm). The flexural characteristics of all prepared hybrid composite samples were tested using the three-point bending method. Samples were flexural tested in accordance with ASTM D 760–03 standards. For each of the hybrid composites, three samples were examined, and the average values were recorded.

Impact strength test

When impact or abrupt loads are applied, composite impact strength is defined as the amount of energy absorbed during fracture and was determined using an IZOD impact tester (Composite Lab-GPREC, Kurnool). The composite sample was impact tested according to the ASTM D-256 standard, with a test sample size of 63.5 mm x 12.7 mm x 3 mm.

Scanning Electron Microscope (SEM) analysis

SEM is an effective instrument for determining the failure mechanism, mode of failure, and interfacial bonding (between matrix and fiber) of a failed specimen. The JEOL/EO Model-JSM-6390 was used to investigate the cracked surface of the hybrid composite sample. For this analysis, the fractured surfaces of the hybrid composite samples were washed, air dried and a thin gold film of gold (3 μm) is coated with JEOL sputter ion coater to impart the conductivity of the sample, and SEM was observed at a voltage of 10 kV and 15 kV.

FTIR spectroscopy

In hybrid composite samples, Fourier transform infrared spectroscopy (Model-Thermo Nicolet, Avatar 370) was utilized to detect functional groups, chemical linkages, and their absorption bands. When the wavelengths of infrared (IR) rays match the vibrational wavelength of a bond with a functional group, absorption of bands occurs. The FTIR spectra of hybrid composites were collected with 32 scans with a resolution of 4 cm^{-1} in the spectral region of 4000 cm^{-1} to 400 cm^{-1}.

3. RESULTS AND DISCUSSION

3.1 Tensile test

Table 1 designates the laminates and Table 2 displays the experimental results of the tensile tests. Tensile strength is observed to be the highest (385.68 MPa) in only carbon laminate i.e., (C/C/C/C) and the lowest strength (62.62 MPa) in pure ramie epoxy composites (R/R/R/R). The addition of carbon fiber to natural fiber-reinforced composite laminate increases the tensile strength as carbon fiber is stronger and stiffer than natural fibers.

Table 2. Tensile properties of carbon and ramie fiber-reinforced hybrid composite laminate.

Sample Designation	Layering Sequence	Tensile Stress(MPa)	Tensile Modulus (MPa)	Tensile Strain (mm/mm)	% Elongation
Sample 1	**R/R/R/R**	62.62	5081.21	0.01617	1.617
Sample 2	**R/R/C/R**	109.98	5014.61	0.03667	3.667
Sample 3	**C/R/R/R**	132.11	5470.05	0.04050	4.05
Sample 4	**R/C/R/C**	169.56	7263.78	0.04283	4.283
Sample 5	**C/R/C/R**	220.93	7110.18	0.05300	5.3
Sample 6	**C/R/R/C**	253.94	7901.72	0.06300	6.3
Sample 7	**C/C/R/C**	280.49	7298.53	0.06650	6.65
Sample 8	**C/C/C/R**	366.76	7520.82	0.07450	7.45
Sample 9	**C/C/C/C**	385.68	8028.05	0.07500	7.5

(Okoronkwo et al. 2021). The same has been clearly observed in the present investigation. A carbon fiber layer that occupies the place of one of the layers of natural fibers in (R/R/R/R) resulted in an improvement in tensile strength (Sample 2 R/R/C/R) by 75.63 % to 110.98 MPa and Sample 3 (C/R/R/R) by 110.97 % to 132.11 MPa). The reason why the tensile strength of sample 3 is higher compared to Sample 2 may be because the carbon fiber bearing the total load acts on it and gradually transferring to other layers of natural fibers. To further increase the tensile strength of the composite sample, two layers of carbon fibers are introduced at different positions of sample 1 replacing natural fibers (R/C/R/C, C/R/C/R, C/R/R/C). Tensile strength improved by 170.78 %, 252.81 % and 305.53 %, respectively, compared to (R/R/R/R). The layers of carbon fibers at both ends of the sample of C/R/R/C, could've resisted the pulling force greatly, and hence the tensile strength is higher between the two layers of carbon fibers (Sample 4 and Sample 5). Similar results were obtained by (Venkatasudhahar, Kishorekumar, and Dilip Raja 2020) for the hybrid composite laminate with Carbon-Jute-Jute-Jute-Carbon layering sequence possessing superior mechanical properties than composite laminate without hybridizing elements such as pure banana (B-B-B-B-B) and pure jute fiber (J-J-J-J-J). Similarly, the strengths of the laminates with three layers of carbon fiber (C/C/R/C and C/C/C/R) increased by 347.92 % and 485.69 %, respectively, compared to those of Sample 1 (R/R/R/R). Three contiguous layers of carbon fibers appear to have added strength to sample 8 (C/C/C/R).

3.2 Flexural test

Plain carbon fiber, pure ramie fiber and carbon-ramie-reinforced epoxy hybrid composite subjected to flexural loading and results are displayed in Table 3. The highest flexural strength (646.08 MPa) was observed in only carbon epoxy composite Sample (C/C/C/C), while the lowest strength (173.03 MPa) was observed in pure ramie epoxy composites (R/R/R/R). The addition of carbon fiber to natural fiber-reinforced composite laminate increases the flexural strength as carbon fiber is stronger and stiffer than natural fibers (Okoronkwo et al. 2022).

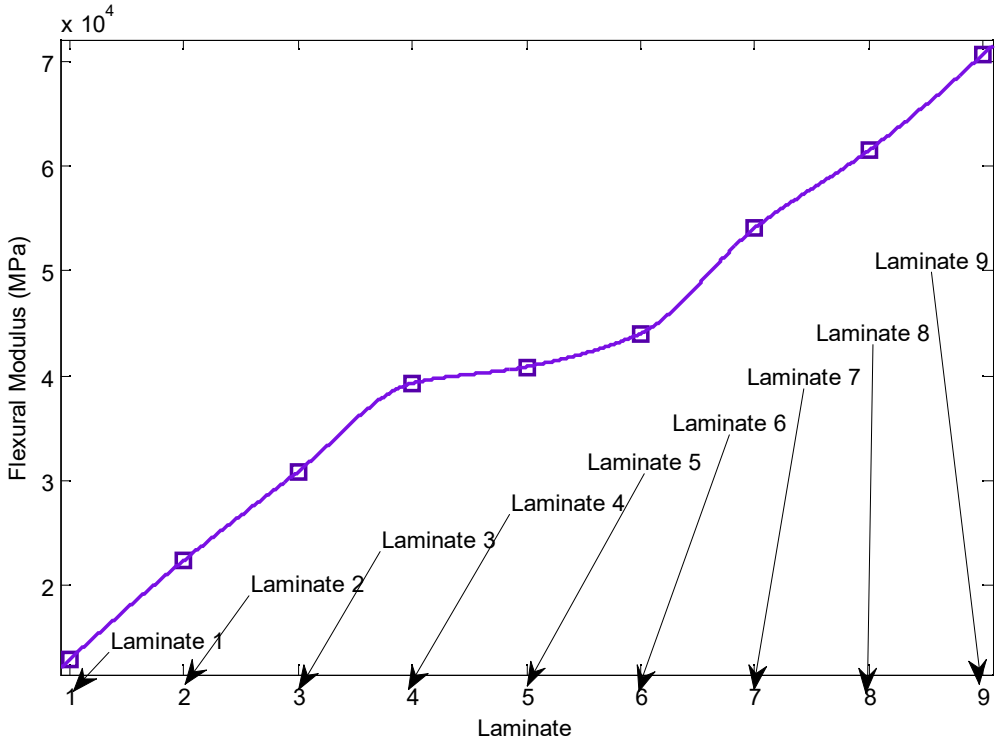

Figure 3: Carbon and ramie fiber-reinforced hybrid composite laminate vs Flexural modulus

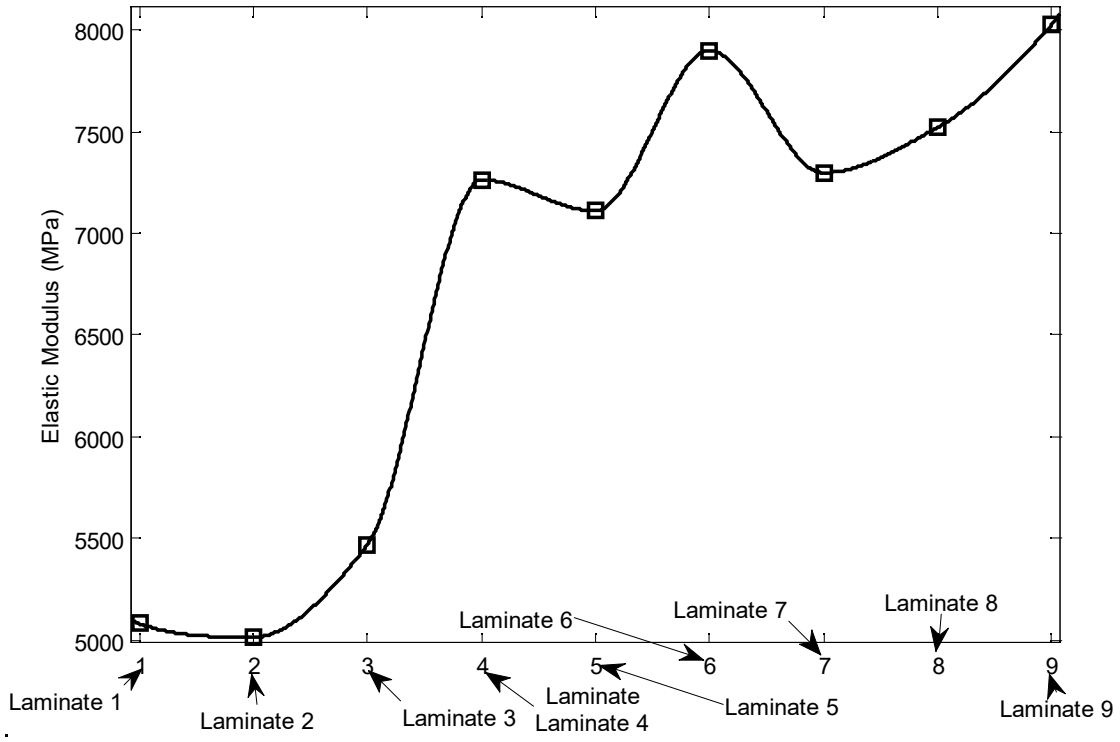

Figure 3: Carbon and ramie fiber-reinforced hybrid composite laminate vs Elastic modulus

Table 3. Flexural properties of carbon and ramie fiber-reinforced hybrid composite laminate.

Sample Designation	Layering sequence	Flexural stress (MPa)	Flexural modulus (MPa)
Sample 1	R/R/R/R	173.03	12816.09
Sample 2	R/R/C/R	233.12	22280.58
Sample 3	C/R/R/R	318.62	30768.68
Sample 4	R/C/R/C	412.00	39256.54
Sample 5	C/R/C/R	424.98	40847.50
Sample 6	C/R/R/C	457.40	44030.50
Sample 7	C/C/R/C	564.69	54110.00
Sample 8	C/C/C/R	645.41	61537.64
Sample 9	C/C/C/C	646.08	70747.44

The same has been clearly observed in the present investigation. A layer of carbon fiber occupying the place of one of the layers of natural fibers in (R/R/R/R) resulted in the improvement of the flexural strength Sample 2 (R/R/C/R) by 34.73 % to 233.12 MPa and Sample 3 (C/R/R/R) has 84.14 % to 318.62 MPa). The reason why the flexural strength of sample 3 is higher than that of sample 2 may be because the carbon fiber carries the total flexural load acting on it and gradually transfers to other layers of natural fibers. To further increase the flexural strength of the composite laminate, two layers of carbon fibers are introduced at different positions of sample 1 replacing natural fibers (R/C/R/C, C/R/C/R, and C/R/R/C). Flexural strength improved by 138.11 %, 144145.61 % and 164.35 %, respectively; compared to epoxy composite laminate reinforced with pure ramie fiber (R/R/R/R). The layers of carbon fibers at both ends of the sample of C/R/R/C could have resisted the flexural force greatly and therefore the flexural strength is higher among the two layered carbon fiber samples (Sample 4 and Sample 5). Similar results were obtained by (Venkatasudhahar, Kishorekumar, and Dilip Raja 2020) for the hybrid composite laminate with a carbon-jute-jute-carbon layering sequence that possesses superior mechanical properties than the composite sample without hybridizing elements such as pure banana (B-B-B-B) and pure jute fiber (J-J-J-J). Similarly, the strengths of the samples with three layers of carbon fiber (C/C/R/C and C/C/C/R) were enhanced by 226.35 % and 273.01 %, respectively, compared to that of Sample 1 (R/R/R/R). Three contiguous layers of carbon fibers appear to have added strength to sample 8 (C/C/C/R). The flexural strength of Samples 8 and 9 is nearly the same, indicating that the use of natural fiber in the Samples improves the load-bearing capacity. Another notable finding from Table 3 is that increasing the carbon fiber content while decreasing the natural fiber content increases the composite sample's flexural strength and flexural modulus.

The carbon/flax hybrid composite laminate has superior flexural properties compared to the unhybridized composite laminate. Carbon fiber has stiffer and stronger than natural fibers. Showing that hybridization with synthetic fibers is an effective method to improve mechanical properties (Ezeokpube et al.2021). In general, natural fiber composite laminate has a non-linear behavior, which has been reduced by reinforcing synthetic fiber, such as carbon fiber in hybrid composite. This behavior is purely dependent on the amount of weight percentage (wt. %) of carbon fiber used in hybrid composite laminate (Kureemun et al. 2018).

3.3 Impact test

The impact strength of nine samples composed of carbon, ramie fibers, and epoxy components is evaluated using an impact test. The impact strength of various samples is determined by applying a transverse force with a hammer on the Izod impact tester, and the findings are presented in Table 4. When a transverse load is applied to the specimen, crack propagation occurs followed by fiber breakage and pull-out. Sample 9 (C/C/C/C) shows the highest impact strength (4.8 J) compared to the other samples, which happens due to the presence of carbon fibers in the sample. The impact strength of the sample of the pure ramie fiber composite (Sample 1) has a lower impact strength (1.25 J) than the carbon fiber hybrid composite. With the addition of one layer of carbon fiber (Samples 2 & 3) at different positions in the sample, a sharp increase in impact strength is observed, which is 68 % and 172 % higher than the sample of pure ramie fiber composite. The reason that impact strength of Sample 3 is more compared to Sample 2 may be because of carbon fiber resisted the impact load acting on it and gradually transferring to other layers of natural fibers. Two layers of carbon fibers are placed at different positions of the Sample (Sample 4, 5 & 6) which increases the impact strength by 228 %, 252 %, & 260 % when compared to pure ramie fiber composite. A composite with three or more than three layers of the carbon at different positions increases impact strength by 268 %, 276 %, and 284 % relative to the sample of pure ramie fiber composite sample. Layers of carbon fibers at both ends of the Sample C/R/R/C, could have resisted the impact load greatly and therefore the impact strength is higher among the two layered carbon fiber samples (Sample 4 and Sample 5). Similarly, the strengths of the samples with three layers of carbon fiber (C/C/R/C and C/C/C/R) improved by 268 % and 276 %, respectively, compared to that of Sample 1 (R/R/R/R). Three contiguous layers of carbon fibers appear to have added strength to sample 8 (C/C/C/R). From Figure 4, it was observed that an increase of the carbon fiber layer in the hybrid sample increases the impact strength; here a lot of energy is absorbed

by the carbon fiber. Impact strength was also affected by the damping of the constituent materials (Assarar et al. 2015; RaviKumar et al. 2021) and height of dropping weight (Sarasini et al. 2014). The reason for

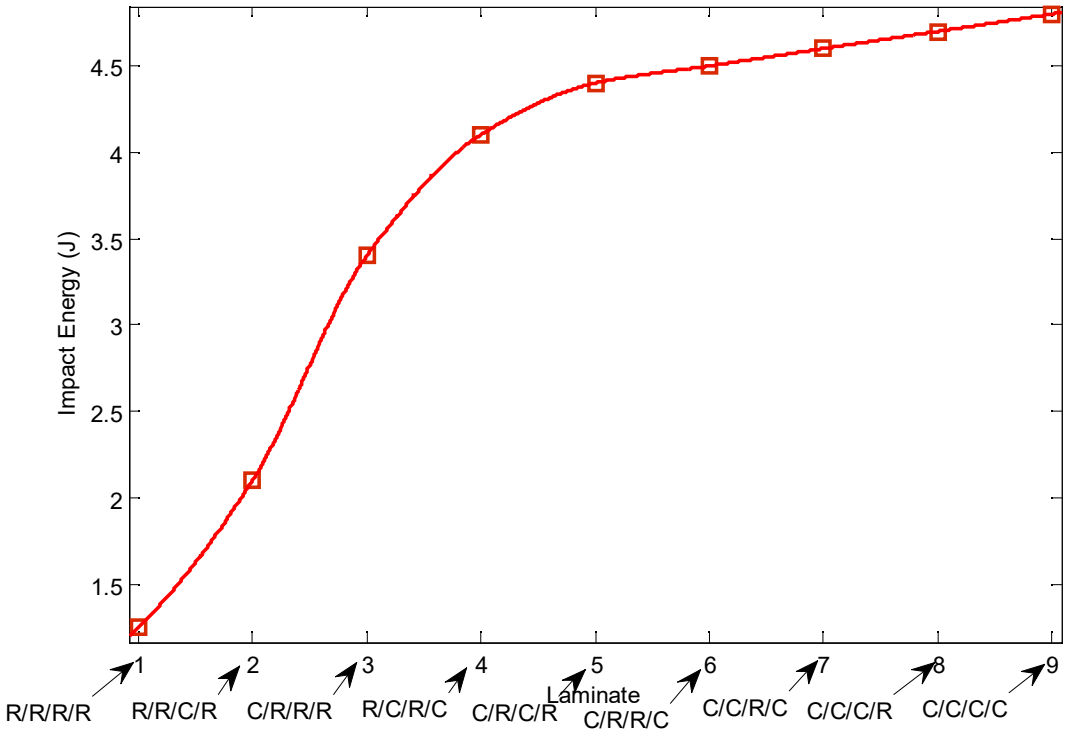

Figure 4. Impact strength of carbon and ramie fiber-reinforced hybrid composite laminate

Table 4. Flexural properties of carbon and ramie fiber-reinforced hybrid composite laminate.

Sample Designation	Layering sequence	Impact energy (J)
Sample 1	R/R/R/R	1.25
Sample 2	R/R/C/R	2.1
Sample 3	C/R/R/R	3.4
Sample 4	R/C/R/C	4.1
Sample 5	C/R/C/R	4.4
Sample 6	C/R/R/C	4.5
Sample 7	C/C/R/C	4.6
Sample 8	C/C/C/R	6.7
Sample 9	C/C/C/C	6.8

low impact strength in the case of composite sample with ramie fiber is due to the fiber breakage and fiber de-bonding (Tranchard et al. 2017).

3.4 Fourier transform infrared spectroscopy (FTIR)

Figure 5 shows the FTIR spectra of alkali treated ramie reinforced epoxy composite (R/R/R/R), the carbon fiber and ramie fiber-reinforced epoxy composite (C/R/R/C), and pure carbon fiber-reinforced epoxy composite (C/C/C/C/C). The H-bonded O-H group in the R/R/R/R composite was found to have a broad and high absorption peak at 3450 cm^{-1} (Sivaraman et al. 2015). This usually means that a good number of O-H groups and H-bonds were associated with each other in the composite sample. For C/R/R/C composites, a similar type of intensity peak is observed, whereas a shift in peak position in terms of magnitude is observed at 3439 cm^{-1}. Similar type of intensity peak was observed for C/R/R/C composites, while the peak position shifted to 3439 cm^{-1} in magnitude. In the case of C/C/C/C composites, a weak intensity of the peak and a different magnitude peak shift (3405 cm^{-1}) were observed due to changes in the H-bonding and O-H groups in the composite. A noticeable peak at 3049 cm^{-1} indicates the asymmetric stretching of C-CH_3 bond of its chemical formula is ($CH_3C{\equiv}CCH_3$) in C/R/R/C composite, whereas no such peak is observed in the

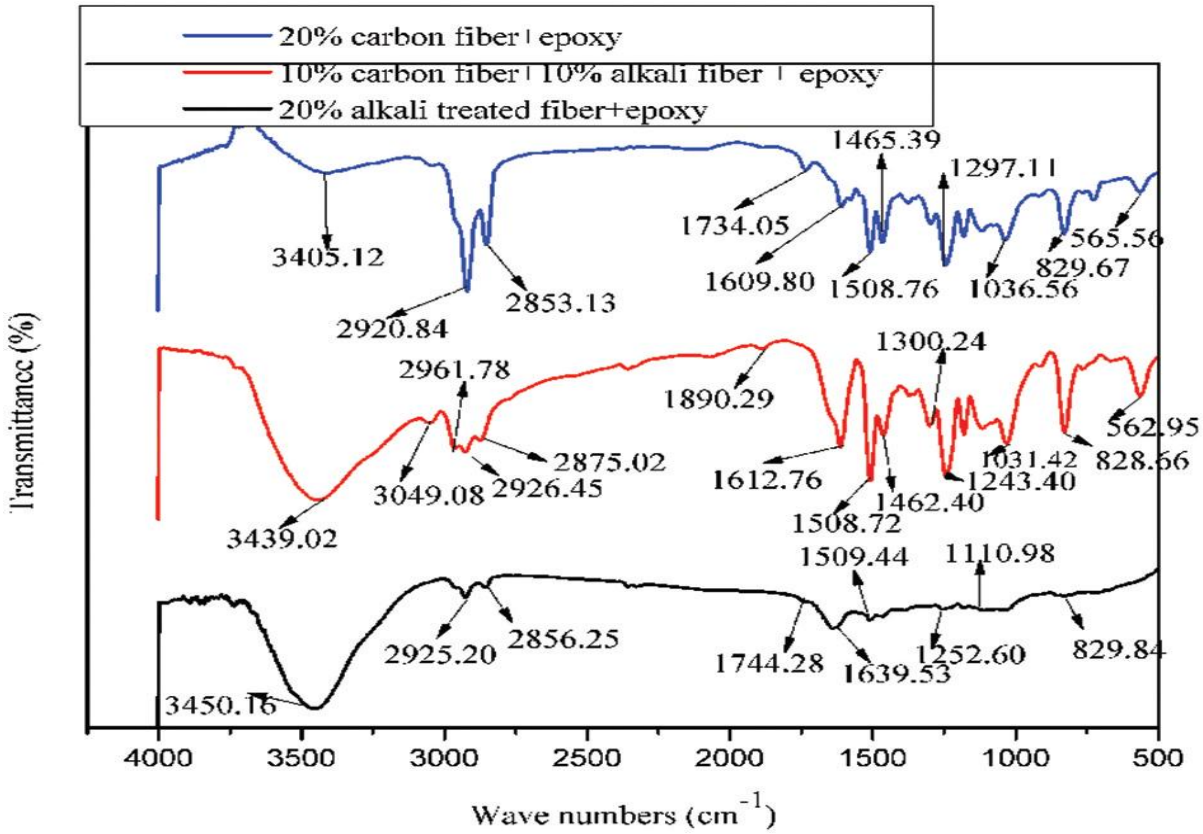

Figure 5: FTIR of the three different fabricated composite samples

other two composites (R/R/R/R and C/C/C/C) (Sivaraman et al. 2015). The weak absorption peak at 2925 cm^{-1} corresponds to the α-cellulose O-H group in the compound (R/R/R/R), indicating a reduced cellulose content after alkali treatment. In (C/R/R/C) composite, the rich content of cellulose is mainly responsible for shifting the absorption peak to 2961 cm^{-1}. But the absorption peak position is shifted to 2961 cm^{-1} due to rich content of cellulose present in the C/R/R/C composite. The narrow absorption peak was observed in the C/C/C/C composite at 2920 cm^{-1}, which represents the rich α- cellulose and O-H groups within it (Sivaraman et al. 2015). The weak absorption peaks at 2856 cm−1 (D/D/D/D), 2875 cm^{-1} (C/R/R/C), and 2853 cm^{-1} (C/C/C/C) were attributed to the methyl ($-CH_3$) and methylene ($-CH_2-$) groups present in it (Tran, Bénézet, and Bergeret 2014). The absorption peak at 1639 cm^{-1} in the (R/R/R/R) composite confirms the rich carbonyl groups (C=O) present in it, a decrease in carbonyl groups was observed in the C/R/R/C and C/C/C/C composites due to the hybridization of carbon fiber with the reinforced epoxy composite (Tran, Bénézet, and Bergeret 2014). All composites (R/R/R/R, C/R/R/C and C/C/C/C) exhibit similar absorption peaks at around 1508 cm^{-1} confirms the presence of aromatic C-H bond stretching in lignin (Tran, Bénézet, and Bergeret 2014). Similar absorption peaks appeared around 1508 cm^{-1} on the curves of R/R/R/R, C/R/R/C, and C/C/C/C composites, which can be recognized as C-H bond stretching, which is a characteristic of aromatic molecules. The oxidative alcohol stretching of the aliphatic ester group in lignin correlates with the absorption peak in the R/R/R/R compound at 1252 cm^{-1}. Peaks in both C/R/R/C and C/C/C/C composites were reduced to around 1243 cm^{-1}, indicating a reduction in ester and a drop in lignin (Tran, Bénézet, and Bergeret 2014). This FTIR spectrum shows the establishment of a bond between the fiber and the matrix. These results are consistent with previous research findings reported in the literature by other authors (Tran, Bénézet, and Bergeret 2014; Sivaraman et al. 2015).

3.5 Scanning Electron Microscope (SEM) analysis

The surface morphology and fractured surface area of alkali treated ramie fibers (R/R/R/R), carbon fiber and ramie fiber (C/R/R/C), and epoxy reinforced composites reinforced with pure carbon fiber (C/C/C/C) were studied as shown in Figures 6–8.

Figures 7–9 show the proper wetting of ramie fibers, carbon fibers and hybridization of these fibers into the epoxy composite. Alkali treatment (5 % NaOH) (R/R/R/R) removes impurities, hemicelluloses, and unwanted fiber constituent materials from the fiber surface and makes the fiber surface rougher and uneven, resulting in better mechanical interlocking (Figure 6). This mechanism results in better stress transfer with improved mechanical

properties. It was also revealed that fewer amounts of fiber pullouts were observed due to alkali treatment.

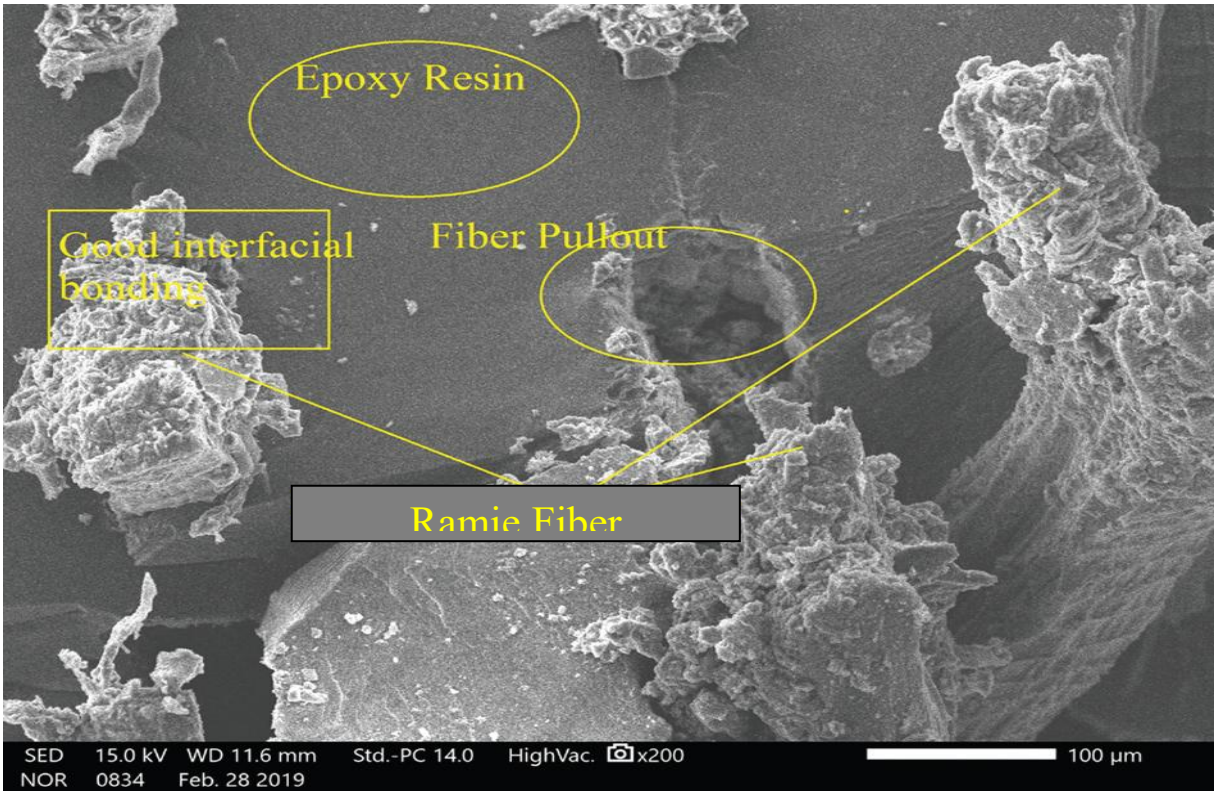

Figure 6: SEM image of ramie fiber-reinforced epoxy composite.

Figure 7 indicates strong interfacial adhesion between the carbon fiber and epoxy matrix (C/C/ C/C), as the epoxy matrix is properly infused into carbon fibers. Figure 8 shows a strong interaction between the hybridized fibers (C/R/R/C) and the epoxy matrix that leads to improved mechanical properties. SEM micrograph of ramie fiber and carbon fiber shows the predominance of brittle fiber failures and the indication of ductile failure of the matrix can be seen from Figure 8.

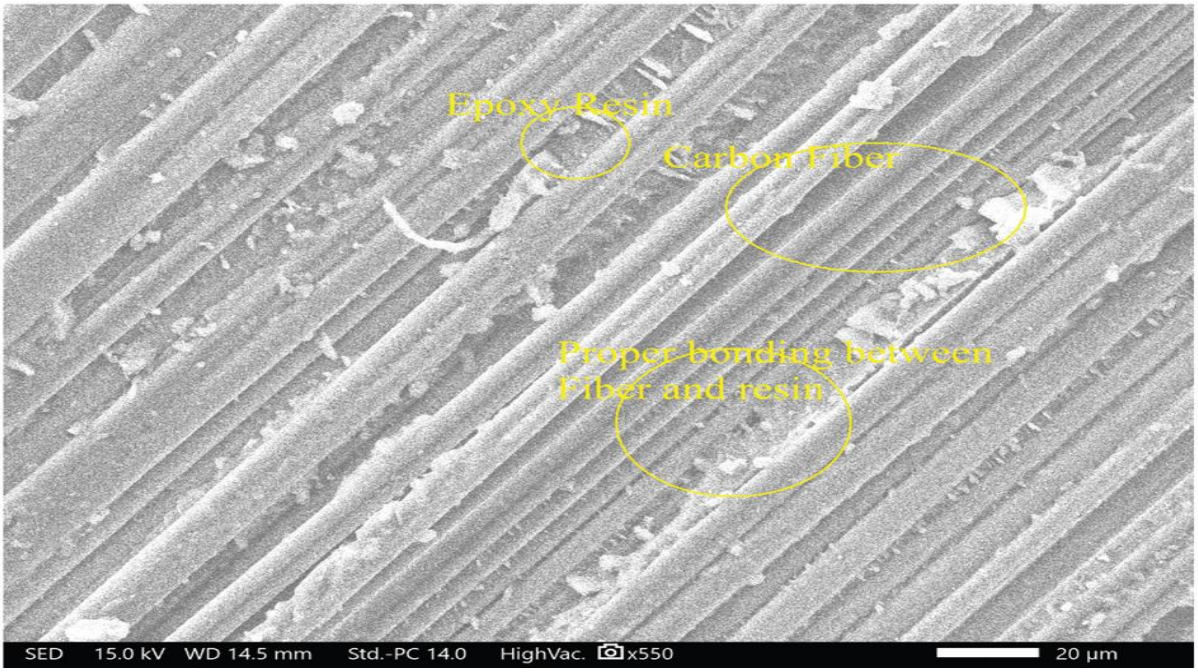

Figure 7: SEM image of carbon fiber-reinforced epoxy composite.

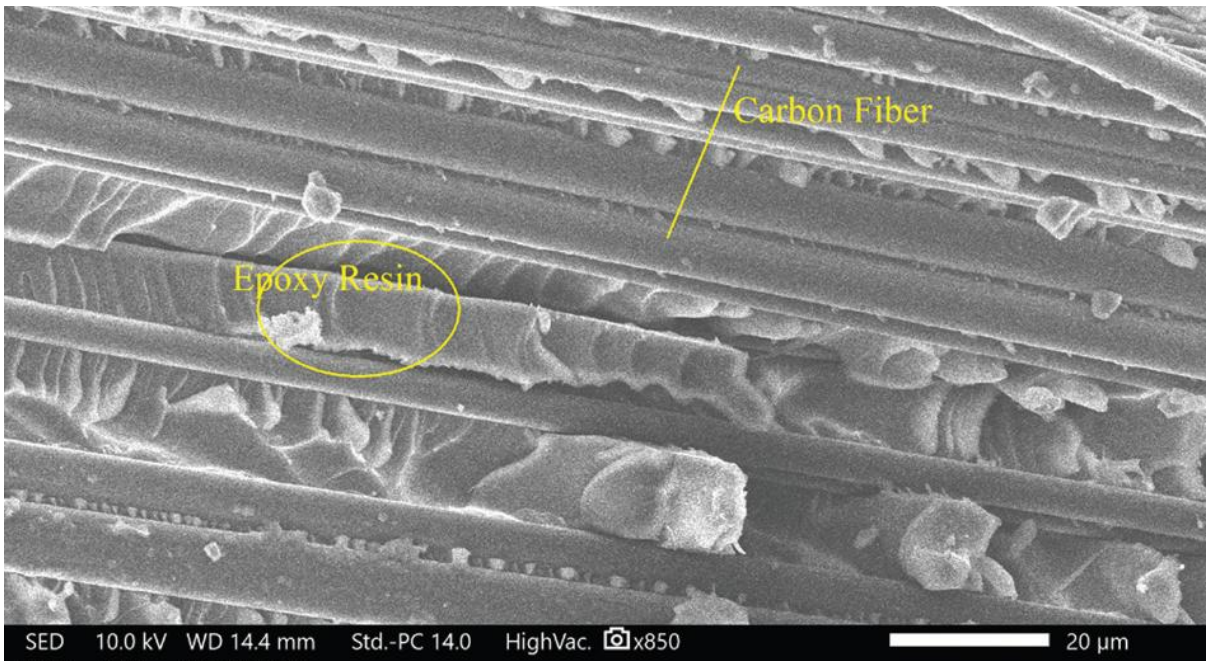

Figure 8: SEM image of ramie and carbon fiber-reinforced epoxy composite.

4. CONCLUSION

Current research focused on ramie fiber-based epoxy composites and carbon fiber hybridization into ramie fiber-reinforced epoxy composites, as well as their potential impact on tensile, flexural, and impact properties, with the following findings:

(1) The addition of carbon fiber to ramie fiber-reinforced epoxy hybrid composites increased mechanical properties such as tensile, flexural, and impact capabilities.
(2) Tensile strength of the laminates with three layers of carbon fiber (C/C/R/C and C/C/C/R) increased by 347.92 % and 485.69 %, respectively, compared to those of Sample 1 (R/R/R/R). This increase in mechanical properties may be suitable for aerospace, structural, infrastructural, packaging, sports, and automobile applications.
(3) Flexural strength of the samples with three layers of carbon fiber (C/C/R/C and C/C/C/R) was enhanced by 159.78 % and 196.92 %, respectively, compared to that of Sample 1 (R/R/R/R).
(4) Impact strength of the samples with three layers of carbon fiber (C/C/R/C and C/C/C/R) improved by 268 % and 276 %, respectively, compared to that of Sample 1 (R/R/R/R).
(5) The prepared hybrid composites are suited for a variety of applications like banners, fabrication of pipes and cylinders.

Conflict of interest
The authors declare that there is no conflicting interest in the publication of this paper.

Acknowledgements
This paper was not supported by any financial grant from granting bodies. The authors really appreciate by acknowledging Engr. Dr. George. O. O. for his active inputs and contributions needed for the outcome of this publication financially and otherwise.

Highlights

- The addition of carbon fiber to ramie fiber-reinforced epoxy hybrid composites increased mechanical qualities such as tensile, flexural, and impact capabilities.
- Tensile and flexural test revealed that carbon fibers-reinforced ramie fiber epoxy composite gives enhanced strength and modulus.

REFERENCES

Aisyah, H. A., M. T. Paridah, S. M. Sapuan, A. Khalina, O. B. Berkalp, S. H. Lee, C. H. Lee, N. M. Nurazzi, N. Ramli, M. S. Wahab .(2019). Thermal properties of Woven Kenaf/Carbon fibre-reinforced Epoxy Hybrid composite panels. *International Journal of Polymer Science* 2019:1–8. doi:10.1155/2019/5258621.

Assarar, M., W. Zouari, H. Sabhi, R. Ayad, and J. M. Berthelot. (2015). Evaluation of the damping of hybrid carbon–flax reinforced composites. *Composite Structures* 132:148–54. doi:10.1016/j.compstruct.2015.05.016.

Dinesh, S., P. Kumaran, S. Mohanamurugan, R. Vijay, D. Lenin Singaravelu, A. Vinod, M. R. Sanjay, Suchart Siengchin, K. Subrahmanya Bhat, and S. Siengchin. (2020). Influence of wood dust fillers on the mechanical, thermal, water absorption and biodegradation characteristics of jute fiber epoxy composites. *Journal of Polymer Research* 27 (1):1–13. doi:10.1007/s10965-019-1975-2.

Dos Santos, J. C., L. A. de Oliveira, L. M. G. Vieira, V. Mano, R. T. Freire, and T. H. Panzera. (2019). Eco-friendly sodium bicarbonate treatment and its effect on epoxy and polyester coir fibre composites. *Construction and Building Materials* 211:427–36. doi:10.1016/j.conbuildmat.2019.03.284.

Ezeokpube Greg C., Okoronkwo George O, Onodagu Peter D. (2021). Natural fiber reggressors effects on physical and strength properties responses of bidirectional finger root fiber reinforced epoxy composites, *Journal of Inventive Engineering and Technology* (JIET), A Publication of the Nigerian Society of Engineers, Awka Branch. Vol. 1, Issue 5, pp. 1-15. @ Nigerian Society of Engineers, Awka Branch.

Ezeokpube Greg C., Okoronkwo George O, Onodagu Peter D. (2021). Strength properties analysis of biomimetic natural wire weed fiber reinforced polymer composite honeycomb plates, *Journal of Inventive Engineering and Technology* (JIET), A Publication of the Nigerian Society of Engineers, Awka Branch, Vol. 1, Issue 5, pp. 16-28. @ Nigerian Society of Engineers, Awka Branch.

Flynn, J., A. Amiri, and C. Ulven. (2016). Hybridized carbon and flax fiber composites for tailored performance. *Materials & Design* 102:21–29. doi:10.1016/j.matdes.2016.03.164.

George O. Okoronkwo, Kizito Chidozie Ibe, Simeon I. Bright. (2022). Composite response comparative analysis, modeling, validations, and regressors effects on ramie fibre reinforced polyester material strength properties, *Journal of Inventive Engineering and Technology* (JIET), A Publication of the Nigerian Society of Engineers, Awka Branch. Vol. 2, Issue 3, pp. 19-39. @ Nigerian Society of Engineers, Awka Branch.

George O. Okoronkwo, Kizito Chidozie Ibe, Simeon I. Bright. (2022). Application of ANN and RSM on the strength properties of alkali mercerized hybrid ramie-isora fibre reinforced biodegradable composites, *Journal of Inventive Engineering and Technology* (JIET), A Publication of the Nigerian Society of Engineers, Awka Branch. Vol. 2, Issue 3, pp. 40-61. @ Nigerian Society of Engineers, Awka Branch.

Ilyas, R. A., S. M. Sapuan, M. R. Ishak, and E. S. Zainudin. (2019). Sugar palm nanofibrillated cellulose (Arenga pinnata (Wurmb.) Merr): Effect of cycles on their yield, physic-chemical, morphological and thermal behavior. *International Journal of Biological Macromolecules* 123:379–88. doi:10.1016/j.ijbiomac.2018.11.124.

Jebadurai, S. G., R. D. E. Raj, V. S. Sreenivasan, and J. S. Binoj. (2021). Coccinia grandis stem fiber polymer composite: Thermal and mechanical analysis. *Iranian Polymer Journal* 30 (4):369–80. doi:10.1007/s13726-020-00896-4.

Jenish, I., S. G. Veeramalai Chinnasamy, S. Basavarajappa, S. Indran, D. Divya, Y. Liu, M. R. Sanjay, and S. Siengchin. (2022). Tribo-mechanical characterization of carbonized coconut shell micro particle reinforced with Cissus quadrangularis stem fiber/epoxy novel composite for structural application. *Journal of Natural Fibers* 19 (8):2963–79. doi:10.1080/15440478.2020.1838988.

Jothibasu, S., S. Mohanamurugan, R. Vijay, D. Lenin Singaravelu, A. Vinod, and M. R. Sanjay. (2020). Investigation on the mechanical behavior of areca sheath fibers/jute fibers/glass fabrics reinforced hybrid composite for light weight applications. *Journal of Industrial Textiles* 49 (8):1036–60. doi:10.1177/1528083718804207.

Kureemun, U., M. Ravandi, L. Q. N. Tran, W. S. Teo, T. E. Tay, and H. P. Lee. (2018). Effects of hybridization and hybrid fibre dispersion on the mechanical properties of woven flax-carbon epoxy at low carbon fibre volume fractions. *Composites Part B: Engineering* 134:28–38. doi:10.1016/j.compositesb.2017.09.035.

Madhu, P., M. R. Sanjay, A. Khan, A. A. Otaibi, S. A. Al-Zahrani, S. Pradeep, S. Siengchin, P. Boonyasopon, and S. Siengchin. (2020). Hybrid effect of PJFs/E-glass/Carbon fabric reinforced hybrid epoxy composites for structural applications. *Journal of Natural Fibers* 19 (10):3742–52. doi:10.1080/15440478.2020.1848724.

Mahakur, V. K., S. Bhowmik, and P. K. Patowari. (2022). Machining parametric study on the natural fiber reinforced composites: A review. *Proceedings of the Institution of Mechanical Engineers, Part C: Journal of Mechanical Engineering Science* 236 (11):6232–49. doi:10.1177/09544062211063752.

Mohana Krishnudu, D., D. Sreeramulu, and P. V. Reddy. (2020). Alkali treatment effect: Mechanical, thermal, morphological, and spectroscopy studies on abutilon indicum fiber-reinforced composites. *Journal of Natural Fibers* 17 (12):1775–84. doi:10.1080/15440478.2019.1598917.

Nagappan, S., S. P. Subramani, S. K. Palaniappan, and B. Mylsamy. (2022). Impact of alkali treatment and fiber length on mechanical properties of new agro waste Lagenaria Siceraria fiber reinforced epoxy composites. *Journal of Natural Fibers* 19 (13):6853–64. doi:10.1080/15440478.2021.1932681.

Najafi, M., S. M. R. Khalili, and R. Eslami-Farsani. (2014). Hybridization effect of basalt and carbon fibers on impact and flexural properties of phenolic composites. Iranian. *Iranian Polymer Journal* 23 (10):767–73. doi:10.1007/s13726-014- 0272-5.

Okoronkwo G. O**.,** Ifegbo A., N. (2021). The effects of regressors on tensile strength responses of rhus fiber reinforced thermoset composites, *Oriental Journal of Science and Engineering* (OJSE), Vol.2, Issue 1, pp. 58-70. @Chukwuemeka Odumegwu Ojukwu University (COOU), Uli, Anambra State, Nigeria.

Okoronkwo, G. O., Madu, K. E., Nwankwo, E., I. (2019). Analysis of fique fiber thermoset vinyl ester composite tensile and flexural strengths, *International journal of latest Engineering and Management Research* (IJLEMR), ISSN: 2455-4847, Volume 04, Issue 06, pp. 60-66. @ IJLEMR.

Ramesh, M., C. Deepa, M. Tamil Selvan, and K. H. Reddy. (2022). Effect of Alkalization on characterization of Ripe Bulrush (Typha Domingensis) grass fiber reinforced epoxy composites. *Journal of Natural Fibers* 19 (3):931–42. doi:10.1080/15440478.2020.1764443.

Ramesh, M., R. Bhoopathi, C. Deepa, and G. Sasikala. (2018). Experimental investigation on morphological, physical and shear properties of hybrid composite laminates reinforced with flax and carbon fibers. *Journal of the Chinese Advanced Materials Society* 6 (4):640–54. doi:10.1080/22243682.2018.1534609.

Ramesh, M., R. Logesh, M. Manikandan, N. S. Kumar, and D. V. Pratap. (2017). Mechanical and water intake properties of banana-carbon hybrid fiber reinforced polymer composites. *Materials Research* 20 (2):365–76. doi:10.1590/1980- 5373-mr-2016-0760.

Rangappa, S. M., S. Siengchin, J. Parameswaranpillai, M. Jawaid, and T. Ozbakkaloglu. (2022). Lignocellulosic fiber reinforced composites: Progress, performance, properties, applications, and future perspectives. *Polymer Composites* 43 (2):645–91. doi:10.1002/pc.26413.

RaviKumar, P., G. Rajeshkumar, J. Prakash Maran, N. A. Al-Dhabi, and P. Karuppiah. (2021). Evaluation of mechanical and water absorption behaviors of jute/carbon fiber reinforced polyester hybrid composites. *Journal of Natural Fibers* 19 (13):6521–33. doi:10.1080/15440478.2021.1924339.

Reddy, B. M., Y. V. Mohana Reddy, B. C. Mohan Reddy, and R. M. Reddy. (2020). Mechanical, morphological, and thermogravimetric analysis of alkali-treated Cordia-Dichotoma natural fiber composites. *Journal of Natural Fibers* 17 (5):759–68. doi:10.1080/15440478.2018.1534183.

Reddy, P. V., D. Mohana Krishnudu, P. Rajendra Prasad, and V. S. R. R. (2021). A study on alkali treatment influence on Prosopis juliflora fiber-reinforced epoxy composites. *Journal of Natural Fibers* 18 (8):1094–106. doi:10.1080/ 15440478.2019.1687063.

Reddy, R. S., D. Mohana Krishnudu, P. Rajendra Prasad, and P. V. Reddy. (2020). Alkali treatment influence on characterization of Setaria italica (Foxtail Millet) fiber reinforced polymer composites using vacuum bagging. (2020). *Journal of Natural Fibers* 19 (5):1851–63. doi:10.1080/15440478.2020.1788494.

Rizal, S., D. A. Gopakumar, S. Huzni, S. Thalib, H. P. S. Abdul Khalil, and H. Abdul Khalil. (2018). Interfacial compatibility evaluation on the fiber treatment in the Typha fiber reinforced epoxy composites and their effect on the chemical and mechanical properties. *Polymers* 10 (12):1316. doi:10.3390/polym10121316.

Sarasini, F., J. Tirillò, L. Ferrante, M. Valente, T. Valente, L. Lampani, P. Gaudenzi, S. Cioffi, S. Iannace, and L. Sorrentino. (2014). Drop-weight impact behaviour of woven hybrid basalt–carbon/epoxy composites. *Composites Part B: Engineering* 59:204–20. doi:10.1016/j.compositesb.2013.12.006.

Sarasini, F., S. D. J, C. Valente, T. Santulli, L. D. Touchard, F. Mellier, L. Lampani, P. Gaudenzi, L. Lampani, and P. Gaudenzi. (2016). Damage tolerance of carbon/flax hybrid composites subjected to low velocity impact. *Composites Part B: Engineering* 91:144–53. doi:10.1016/j.compositesb.2016.01.050.

Saravanakumar, S. S., A. Kumaravel, T. Nagarajan, and I. Ganesh Moorthy. (2014). Investigation of physico-chemical properties of alkali-treated Prosopisjuliflorafibers. *International Journal of Polymer Analysis and Characterization* 19 (4):309–17. doi:10.1080/1023666X.2014.902527.

Senthamaraikannan, P., S. S. Saravanakumar, V. P. Arthanarieswaran, and P. Sugumaran. (2016_. Physico-chemical properties of new cellulosic fibers from the bark of Acacia planifrons. *International Journal of Polymer Analysis and Characterization* 21 (3):207–13. doi:10.1080/1023666X.2016.1133138.

Sivaraman, B., N. Radhika, A. Das, G. Gopakumar, L. Majumdar, S. K. Chakrabarti, K. P. Subramanian, B. N. Raja Sekhar, and M. Hada. (2015). Infrared spectra and chemical abundance of methyl propionate in icy astrochemical conditions. *Monthly Notices of the Royal Astronomical Society* 448 (2):1372–77. doi:10.1093/mnras/stu2602.

TG, Y. G., S. Jawaid, S. Siengchin, M. Mavinkere Rangappa, S. Siengchin, and M. Jawaid. (2022). Mechanical and thermal properties of flax/carbon/kevlar based epoxy hybrid composites. *Polymer Composites* 43 (8):5649–62. doi:10.1002/pc. 26880.

TG, Y. G., V. Siengchin, S. MR, S. Kushvaha, M. R. Sanjay, and S. Siengchin. (2021). A new study on flax-basalt-carbon fiber reinforced epoxy/ bioepoxy hybrid composites. *Polymer Composites* 42 (4):1891–900. doi:10.1002/pc.25944.

Tran, T. P. T., J. C. Bénézet, and A. Bergeret. (2014). Rice and Einkorn wheat husks reinforced poly (lactic acid)(PLA) biocomposites: Effects of alkaline and silane surface treatments of husks. *Industrial Crops and Products* 58:111–24. doi:10.1016/j.indcrop.2014.04.012.

Tranchard, P., S. Duquesne, F. Samyn, B. Estebe, and S. Bourbigot. (2017). Kinetic analysis of the thermal decomposition of a carbon fibre-reinforced epoxy resin laminate. *Journal of Analytical and Applied Pyrolysis* 126:14–21. doi:10.1016/ j.jaap.2017.07.002.

Venkatasudhahar, M., P. Kishorekumar, and N. Dilip Raja. (2020). Influence of stacking sequence and fiber treatment on mechanical properties of carbon-jute-banana reinforced epoxy hybrid composites. *International Journal of Polymer Analysis and Characterization* 25 (4):238–51. doi:10.1080/1023666X.2020.1781481.

Vijay, R., A. Vinod, D. L. Singaravelu, M. R. Sanjay, and S. Siengchin. (2021). Characterization of chemical treated and untreated natural fibers from Pennisetum orientale grass-A potential reinforcement for lightweight polymeric applications. *International Journal of Lightweight Materials and Manufacture* 4 (1):43–49. doi:10.1016/j.ijlmm.2020. 06.008.

Vinod, A., J. Tengsuthiwat, Y. Gowda, R. Vijay, M. R. Sanjay, S. Siengchin, and H. N. Dhakal. (2022). Jute/Hemp bio-epoxy hybrid bio-composites: Influence of stacking sequence on adhesion of fiber-matrix. *International Journal of Adhesion and Adhesives* 113:103050. doi:10.1016/j.ijadhadh.2021.103050.

Yashas Gowda, T. G., A. Vinod, P. Madhu, M. R. Sanjay, S. Siengchin, and M. Jawaid. (2022). Areca/Synthetic fibers reinforced based epoxy hybrid composites for semi-structural applications. *Polymer Composites* 43 (8):5222–34. doi:10.1002/pc.26814.

Yatim, N. M., Z. Shamsudin, A. Shaaban, N. A. Sani, R. Jumaidin, and E. A. Shariff. (2020). Thermal analysis of carbon fibre reinforced polymer decomposition. *Materials Research Express* 7 (1):015615. doi:10.1088/2053-1591/ab688f.

Advanced Journal of Engineering and Scientific Applications (AJESA)

Research Paper Open Access

Available online at www.ajesa.com.ng Vol. 2 No.1, 2025. pp.59-73

Experimental Investigation of High Filler Loading of SiO_2 on the Mechanical and Dynamic Mechanical Analysis of Natural PALF fibre-Based Hybrid Composite

George O. Okoronkwo[1], Ibe Kizito Chidozie[2], Faloye Mayowa Emmanuel[3]

[1]Department of Chemical Engineering, Micheal Okpara University of Agriculture, Umudike, Abia State, Nigeria;
okoronkwo.george@mouau.edu.ng, ogeorgeonyeka@gmail.com

[2]Department of Civil Engineering, Micheal Okpara University of Agriculture, Umudike, Abia State, Nigeria
ibe.kizito@mouau.edu.ng

[3]Department of Civil Engineering, Micheal Okpara University of Agriculture, Umudike, Abia State, Nigeria
faloyemayow@gmail.com

Corresponding Author::ogeorgeonyeka@gmail.com

Abstract

This work aims to experimentally investigate high filler loading of on the mechanical and dynamic mechanical analysis of natural PALF fibre-based hybrid composite. The compression moulding process was used to fabricate the composite. To achieve the aforementioned goals, the blends were made using 25 % PALF and varied weight proportions (3wt. %, 6wt. %, and 9 wt. %) of nanoparticles. Tensile, bending, impact, interlaminar shear, shoreline D hardness, and dynamic mechanical analysis were all evaluated. SEM was used to examine the morphology of the materials, and an FTIR spectrometer was used to look for the presence of organic chemicals in fiber-reinforced composite materials. The findings show that adding 25 % PALF fiber and 6 % nanoparticles (D-type) to the epoxy polymer improved the thermal and mechanical properties of the composites. It can be attributed to the improved interaction and homogeneous dispersion of the fillers and epoxy polymers. Moreover, the water uptake parameters of all samples were studied. The findings showed that the inclusion of reinforcements boosts the water uptake of the composite significantly. The initial deterioration rate of the -incorporated hybrids is almost the same, at about 400°C, which is considerably greater than that of the beginning breakdown temperatures of PALF (300°C), according to the thermography study. This might imply that the fiber and polymers form a stronger bond, reducing polymer movement and increasing the thermo-stability of the combination.

KEYWORDS: PALF fiber, , Mechanical properties, Dynamic Analysis, FTIR, Water absorption

1. INTRODUCTION

In the current context, there is a growing desire for innovative composite materials with increased properties to meet distinct performance needs (Okoronkwo et al. 2022). The general approach for developing substances is the introduction of fillers and ber reinforcements to plastics. Polymers have expanded their possible applications in so many organizations due to their high resistance to corrosion, low price, and lightweight. Epoxy polymers have superior mechanical properties, good dimensional durability, and better heat resistance than other thermoplastic and thermoset polymers. Furthermore, when epoxy resins go through the hardening process, they become fragile. Brittleness is an indication of a serious problem that can be mitigated by the use of artificial filler or organic fiber ((Gholampour et al.2020); (Väisänen et al. 2017)). The enormous accomplishment of sturdy synthetic and natural

cloth merged in plastic is acknowledged and anchored. Nevertheless, these constant fiber-based polymeric plastic laminates have some disadvantages, such as debonding, which can be avoided by using nano or micro fillers instead of long fibers. Such constraints often constrain its application area and create a need for polymer plastic laminate to improve. Furthermore, significant growing worries and awareness of an eco-friendly and better ecosystem in society sharpened a deep belief in natural fiber and filler (Velmurugan et al. 2020). The use of various environmentally friendly and recyclable reinforcing materials, for example, leaves of plants, cotton, jute, wood powder, coir dust, axseed, wheat, grain, and so on, are encouraged. Rather than different efforts towards employing environmentally friendly and renewable polymers for commercial processes, a key disadvantage has been found in the thermo-mechanical properties. In recent years, the majority of polymer laminates were created using arti cial and organic textiles ((Sharma et al.2020); (Gouda et al. 2021); (Sanjay et al. 2018)). Of all regularly utilized biological fibers, pineapple leaf (PALF) fibers possess the greatest promise for usage as reinforcing in ber or powdered format to create a high-tensile, inexpensive, and recyclable biocompatible product. PALF fibers are multilayer fibers derived from pineapple leaves (Johny et al. 2023). PALF fibers are preferred over other natural fabrics due to their high cellulose content (70–85%), which leads to higher bending and tensile qualities than axseed, jute, sisal, and wool fibers. PALF has similar bending and twisting stiffness to jute fiber. PALF is widely available, has a low density, a good aspect ratio, as well as a small microbrillar inclination (Johny et al. 2023). (Ponnusamy et al. 2022) observed that PALF does have a high modulus and has a great potential for usage in the chemical industries. According to (Natrayan et al. 2022) the exposure to 30 phr PALF raised the compressive and tearing strengths of NBR laminate to 15 psi and 200 kN/mm, respectively. According to (Ponnusamy et al. 2022) the PALF may be eficiently employed in a polypropylene matrix. Despite a wide range of favorable qualities, PALF has lower impact strength than rice husk. To increase their qualities holistically, PALF as well as other fibers or fillers must be reinforced within a single polymer matrix. The combination of a rigid and moderately elastic fiber with an extreme load-to-failure fiber increases the fracture toughness of the resultant composite (Todkar et al. 2019). Furthermore, combining one kind of organic fiber with the other gives a noteworthy and workable option that leads to multipurpose composites having great creep and wear strength and better impact strength (G V et al. 2020). For instance, polymers with silicon dioxide (SiO_2) nanoparticles have outstanding physical, thermodynamic, as well as other characteristics. It should be noted that SiO2 nanoparticles are currently being investigated as potential replacements in polymeric matrices. (Lakshmaiya et al. 2022) conducted tensile and fracturing experiments using scattered silicon in an epoxy coating, finding that the inclusion of 5% nano llers might increase rigidity and breakage energies. Nano- SiO_2 is an ecologically friendly product with a composition comparable to basalt fiber. Due to its rich content, excellent eficiency, extensive surface area, tiny sizes, and high adsorption, it is extensively used in coatings, polymers, and chemicals, as well as other industries. (Natrayan et al. 2022) covered sandblasting iron using composite material made of micro- and nano- SiO_2 particles as well as an epoxy polymeric foundation, accordingly. In a saline spraying test, the composites were weathered. According to studies, nano- SiO_2 coatings are more corrosion-resistant than micro- SiO_2 coatings (Velmurugan et al. 2023). When compared to conventional epoxy coating, the impact resistance of hardened epoxy coating increased from 0.71 MPa to 0.93 MPa, a 20.2% rise, as well as the glass transition point from 200 ºC to 158 ºC, implying that nano- SiO_2 incorporation dramatically improved the damage tolerance and elevated heat resistance of the epoxy coating (Velmurugan et al. 2022). Several researchers have treated the surfaces of fibers with nano- SiO_2. (Maurya et al. 2022) used a sol-gel approach to transplant a SiO_2 covering with such a nano porosity architecture on the surfaces of PBO fibers. The adhesion strength among the altered PBO/ SiO_2 fiber and epoxy was discovered to be dramatically improved, the interface's shear force rose by 123.25%, and the hydrophobic nature also was highly improved. (Tang et al. 2017) created an aramid fiber insulation sheet by processing this with 1 wt. % of SiO_2. Both mechanical and electrical testing was performed on the aramid fiber insulation sheet before and following modifications. A significant interfacial impact between nano- SiO_2 and synthetic fibers was discovered, resulting in a 1% improvement in tensile strength, deformation at breaking, and dielectric breakdown power (Ponnusamy et al. 2022). As contrasted to untreated aramid insulation sheets, SiO_2-modi ed aramid fiber insulation paper improved by 7.5%, 10%, and 14%, respectively. The physical and dielectric characteristics of a carbon ber insulation sheet were enhanced as a result. Cheng et al. found that increasing the silica concentration improved the compression strength of glass-epoxy hybrids (Chai et al. 2022). The improved strength of concrete might be ascribed to improved interfacial adhesion caused by the scattered silica nanoparticles. Admittedly, few research projects have focused on the effect of laminate architectures as well as the role of inorganic nanoparticles such as SiO_2 particles on the characteristics of PALF composite materials based on epoxy. The purpose of this work was to establish the possibility of producing PALF/ SiO_2-based hybrid materials with varying filler weight proportions. To achieve the aforementioned goals, the mechanical and dynamic mechanical characteristics of the composites were investigated.

2. MATERIALS AND METHODS

2.1 Materials

2.1 Materials

In this investigation, artificial epoxy resin YD-535 LV as well as curing agent TH-725 were obtained from the C.K. pharmaceutical sector and employed as polymer matrices. PALF fibers acquired at Salam, Tamil Nadu, India, were used as reinforcing material in the production of synthetic epoxy composites. In this study, synthetic fillers such as SiO_2 (10 nm in particle size) were used. Figure 1 depicts photographs of reinforcements and fillers. Before using the PALF fiber its thoroughly washed with clean water and then treated with alkaline and silane solutions to enhance the interfacial bonding.

Figure 1. Photographic Images of (a) PALF fiber, (b) SiO_2 nanoparticles

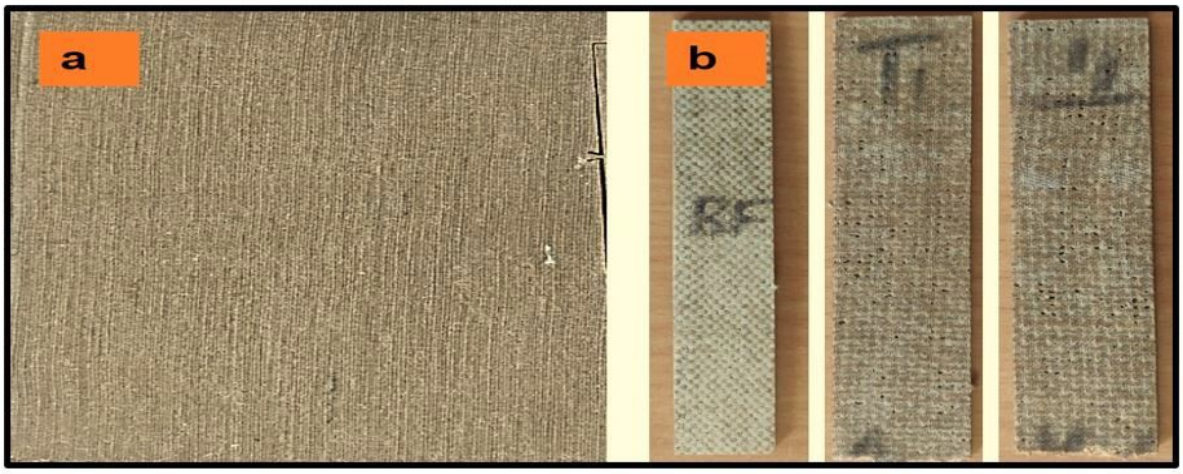

Figure 2. Fabricated composites of (a) Overall Plate, (b) Test specimen

2.2 Fabrication of Composite Laminate

The purchased PALF fibers were cleansed with running, pure tap water to wash away dirt and other foreign elements before being dried in the sunlight for 70 hours to eliminate any remaining wetness. The PALF fibers are chopped into little pieces and fed into standard slicing milling equipment to generate micro-particles of PALF fibers, which are then sieved through a 250-mesh screen. To use an electronic weight device, the epoxy polymers, curing agent, and reinforcing components were accurately weighed in varied weight proportions. The weight percentage for the manufacture of epoxy composite samples from PALF fiber and SiO_2 nanoparticles is shown in Table 1. Mechanical stirring was utilized to achieve homogeneous particulate distribution inside the resin. To prevent sudden drying, the combined liquid was promptly transferred to the mould and permitted to drain for real curing. To lower the interior water content, the created sample was poured into the mould and transported to the burner, which was set to 70°C (after drying). Figure 2 shows the image of fabricated and tested composite samples.

Table 1 Composite Fabrication based on the weight ratios of fiber/ fillers

Sl. No	Sample Symbol	Sample Descriptions	Weight % of Epoxy resin	Weight Ratio of PALF	Weight % of SiO_2
1	A	Pure Epoxy	100	-	-
2	B	Epoxy/PALF	75	25	–
3	C	Epoxy/PALF/SiO_2	72	25	3
4	D	Epoxy/PALF/SiO_2	69	25	6
5	E	Epoxy/PALF/SiO_2	66	25	9

2.3 Composite Fabrication

These involve:

2.3.1 Mechanical Properties

Tensile testing was carried out to measure the tensile strength of a manufactured epoxy-based polymeric hybrid composite. By the ASTM D 3039 standards, the sample was made into a rectangle with measurements of 25 mm in width, 250 mm in length, and 3 mm in thickness. This study was carried out at a crosshead velocity of 1 mm/min until the breakage was achieved. The three-point bending specimen was generated in Comtech's universal tester by the ASTM D790 standards for three-point bending tests. The deformation of an epoxy-based hybrid composite during compressive stresses was determined until the sample broke or cracked. All experimental materials had their bending movement and loading evaluated by the apparatus. The dimensions of the reinforced epoxy laminate sample for this study are 12.7 mm wide, 128 mm long, and 3 mm thick. The ASTM D2344-84 standards were employed to evaluate the fracture characteristics of polymers using interlaminar testing. Sections of epoxy composite samples were cut at 18 mm in length, 6 mm in width, and 3 mm in thickness. The assessment includes a spanning length of thirty mm and a speed of one millimeter per minute. The fracture toughness of epoxy polymeric composites is defined as their ability to absorb power from such an impact force in the context of a smooth surface that centers on strains. The izod impact test was carried out by the ASTM D 256 standards. Deformation durability testing equipment was used to assess the Shore D hardness of epoxy polymeric composites. An indenter was pushed against the reinforced hybrid composite sample until the bottom section of the indenter made total contact with the lamination. The polymeric characteristics can affect' hardness, which is indicated using the hardness indenter. The experiment was carried out at three different spots on the lamination, and the mean toughness was computed.

2.3.2 Thermal Stability

TGA testing was performed on epoxy hybrid composites in a nitrogen environment at temperatures ranging from 30 to 800ºC. Utilizing derivative thermal images, weight loss was evaluated, and leftover charcoal concentration was investigated at 700 ºC. The scanning electron microscopy technique was used to examine the surface structure of a hybrid composite. Before this, all of the specimens were covered with auricular dust. The hybridization interaction among the PALF ber matrix and SiO_2 nanoparticles was shown using Fourier transform infrared spectroscopy.

2.3.3 Moisture Absorption

The water uptake research for epoxy composite materials was performed by the ASTM D 570 specification. The specimen was dried in a furnace for a specific period at a specific temperature (60ºC), and its original weight was determined. The resulting epoxy-hybrid materials were then submerged in water for 60 days at ambient temperature. Following immersion, specimens were retrieved, extra water was wiped away using a towel, and they were measured again. The difference in weights between the beginning and final weights was recorded.

3. RESULTS AND DISCUSSION

3.1 FTIR characterization

The existence of organic compounds in fiber-reinforced epoxy composites was investigated using an FTIR spectrometer. The substituents of a composite's constituents were determined using FTIR. This substituent was identified using the FTIR attenuated whole reflection (ATR) equipment. The wavelength spectrum of the equipment was 500 – 4000 cm^{-1}. The transparency setting was used to capture the FTIR spectrum. Figure 3 depicts the FTIR spectroscopy of the PALF composite. An O-H group's feature was noticeable among the intensities of 3200 and 3550 cm^{-1}. Peaks for C-H extending and C = O extending are located at 2801–2850 cm^{-1} and 1601–1650 cm^{-1}, respectively. The wavelength region 1200 – 1300 cm^{-1} in the Figure 3 reveals C-H binding. The spectral analysis of PALF ber had changed following hybridization with SiO_2 nanoparticles. The bending vibration of N-H groupings

around 2800 cm^{-1} was widened, perhaps due to interactions of hydrogen bonds among SiO2 nanoparticles and PALF fiber (Kavya et al. 2021). Trend shifts from 1793 to 1798 cm^{-1} as well as 3640 to 3680 cm^{-1}, correspondingly, guarantee the presence of the hydroxyl group among -OH and -C = O. The vibrating wavelength of Si-OH changes from 3923 to 3969 cm^{-1}, indicating the presence of silicon in the epoxy. It was possible to determine that there were substantial contacts between the SiO_2 nanoparticles and the PALF fiber. So, these contacts might be diverse, including the previously stated hydrogen atoms and cytotoxic processes, in addition to electrostatic attraction among SiO_2 nanoparticles and PALF fiber (Hoque et al. 2018).

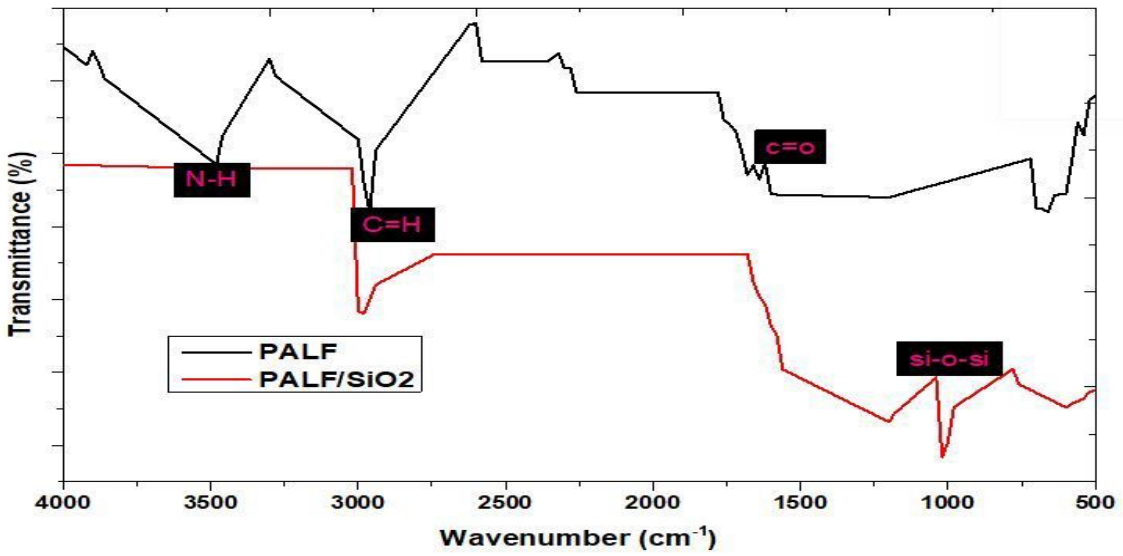

Figure 3. FTIR analysis of PALF and PALF/ SiO_2 based hybrid composites

3.2 Mechanical Properties

These are:

3.2.1 Tensile behavior

Many studies have shown that strengthening polymeric materials with such a low weight percentage of ller materials and natural materials yields the best mechanical characteristics. The cited comment has been in favor of D-type specimens. It was anticipated that combining a 6 wt. % SiO_2 composite with natural fiber would improve the mechanical characteristics of hybrid composites. As shown in Figure 4, each of the hybrid composites (C-type, D-type, and E-type) had higher tensile strength and modulus than the A and B-type. Even though contrasted with pure resin, hybrids laminate C, D, and E-type demonstrated 13.25 %, 23.369 %, and 20.36 % increases in tensile strength as well as 32.65 %, 45.62 %, and 40.12 % increases in elastic strength. This improvement in both modulus and tensile strength was made feasible by the hybrid composite's proper dispersion of 6 wt. % SiO_2, which facilitated eficient load transmission, as reported earlier by investigators (Natrayan et al. 2018). Moreover, the high adhesiveness of the alkali-silane-modified PALF fiber as well as the epoxy composite results in excellent binding at its contact point. Esters, hydrophobic interactions, and copolymer (NH-CO) production might occur during the metaphase between the PALF fiber and the basic matrices. Its collective effects of the nano- SiO_2 fillers and processed PALF fiber guarantee that the combination has good strength. As a result, for the previously indicated scenario, significant hybridization is being found. The tensile strength of the composites decreased as the SiO_2 concentration increased (over 6 wt. %). This is really due to the build-up of ller particles in the epoxy. This might be because SiO_2 nanoparticles accumulated on the fiber surface and caused numerous flaws, like fractures. Once the tension load was applied to the fiber, the fractures spread widely and spread from the handling to the fiber surface, leading to several maximum stress points on that surface and speeding fiber breakage.

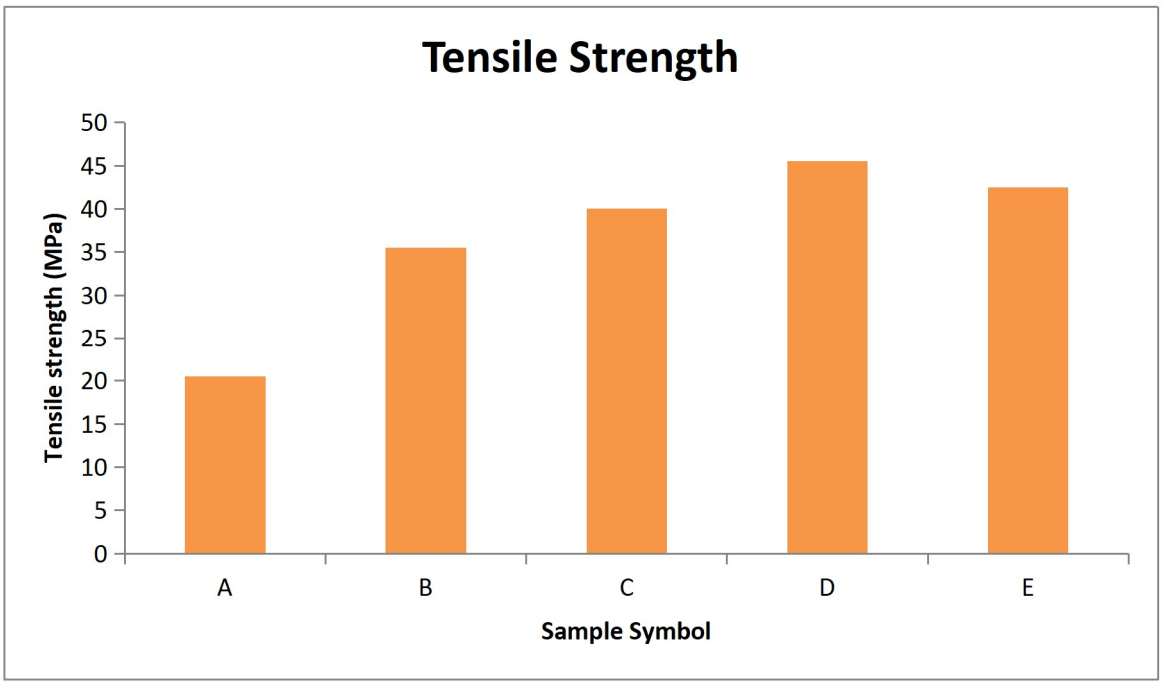

Figure 4(a). Tensile strength of PALF/ SiO_2-based hybrid composites

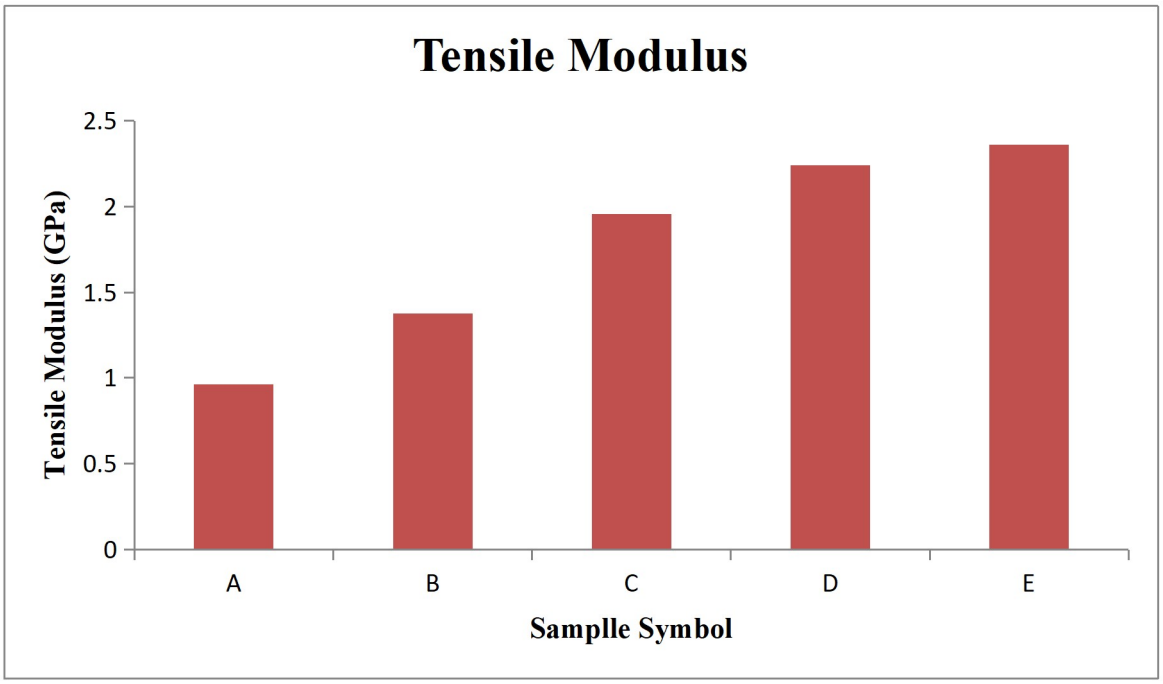

Figure 4(b). Tensile Modulus of PALF/ SiO_2-based hybrid composites

3.2.2 Flexural Behaviour

Figure 5 depicts the flexural behavior of epoxy as well as all-hybrid composites. Surprisingly, all of the materials show the same trend for bending modulus and strength as they do for tension characteristics. Flexural characteristics of PALF/ SiO_2-derived hybrid materials C, D, and E are greatly enhanced as compared to regular epoxy. The bending strengths rose by 30 %, 42 %, and 45 % in bio-composites such as C-type, D-type, and E-type, respectively. This increase was caused by the efficient load transfer across matrices to reinforcements as a consequence of the strong esters, hydroxyls, and nylon binding interactions among PALF fiber and resin, as well as the good distribution of nanocrystalline silicon dioxide. It had also been predicted that nano SiO_2 would have minimized the gap between the strengthening PALF fiber and matrix. This finding is in contrast with (Hamid et al. 2019). The E-type of all materials had the maximum flexural strength (58.96 MPa) and elasticity (2.79 GPa), whereas the A-type had the least strength properties at 26.32 MPa and elasticity of 0.85 GPA. Tensile property trends were also detected for flexural characteristics, indicating a favorable hybridized impact. A high adhesion/interaction between the PALF fiber and

epoxy contact, as well as the addition of nanocrystalline SiO_2, results in improved load transmission. Furthermore, as previously reported, superior SiO_2 dispersal and distance decrease among PALF ber and epoxy matrices contacts should have had an important impact in boosting load transmission from matrices to PALF fiber.

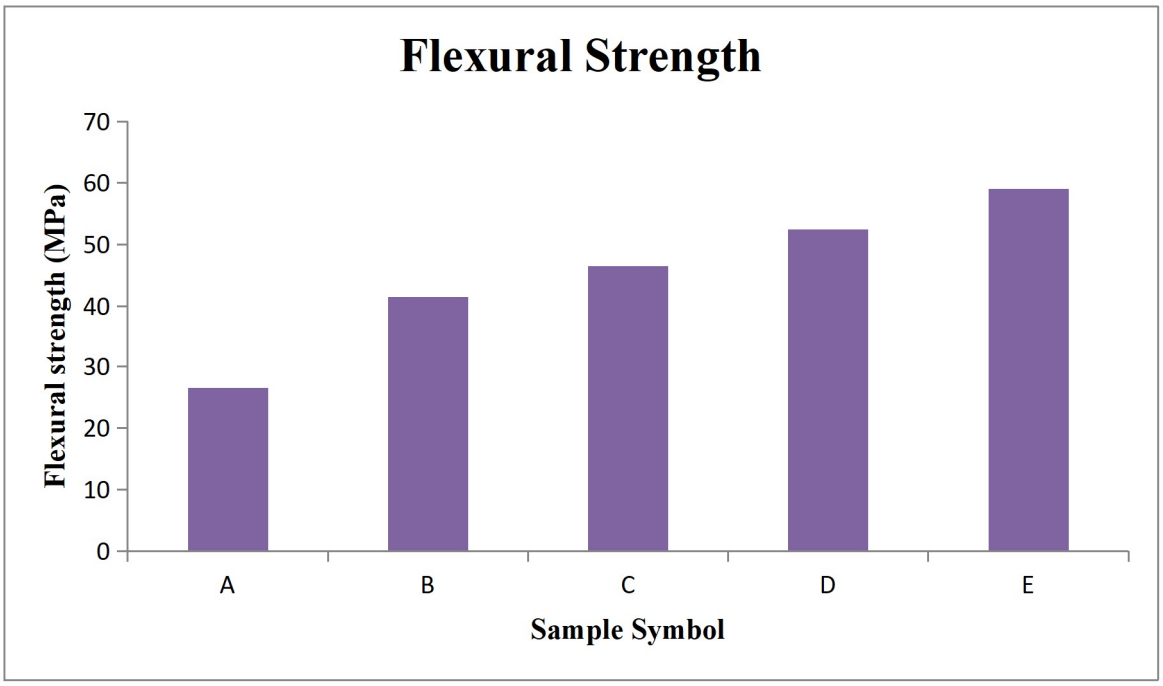

Figure 5(a): Flexural strength of PALF/ **SiO_2**-based hybrid composites

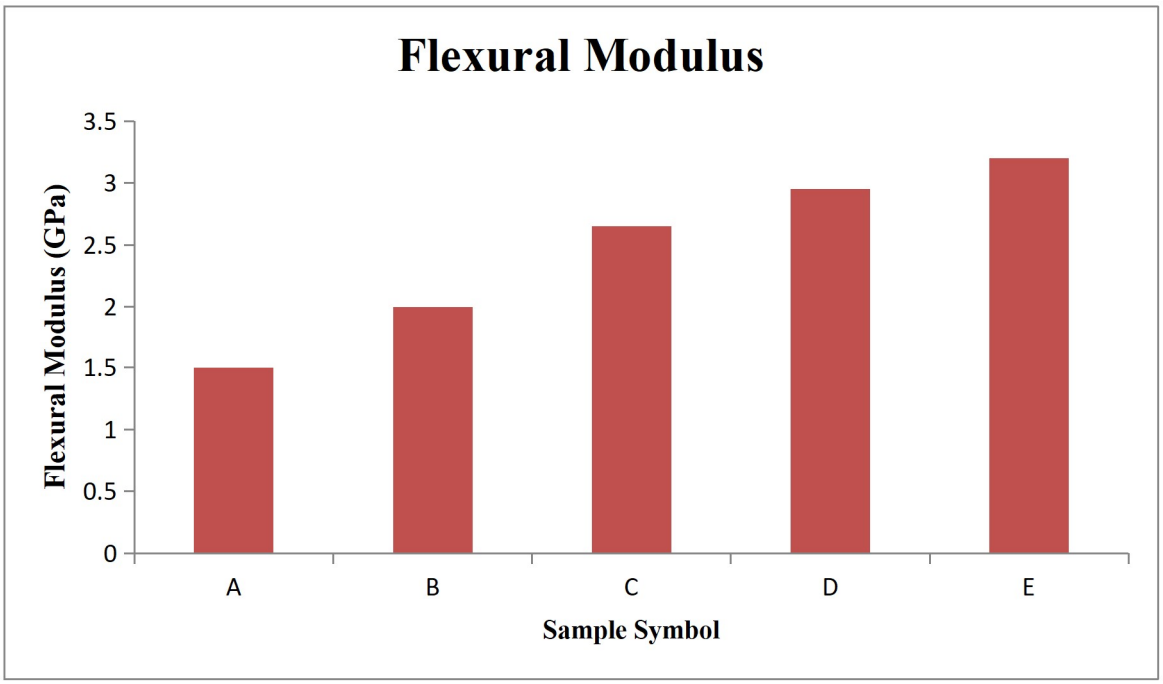

Figure 5(b): Flexural Modulus of PALF/ **SiO_2**-based hybrid composites

3.2.3 Interlaminar Shear strength

For instance, the interlaminar shear of an elastomeric polymeric matrix is vulnerable to the formation of voids and interfacial adhesion between the filler and the polymers. The produced composites were tested for resistance against inter-laminar strength properties. Figure 6 depicts the inter-laminar shear strength parameters of the manufactured epoxy composites. The sample D-type has a greater strength property of 27.12 MPa among different kinds of manufactured epoxy hybrid materials, whereas the sample B-type has a lesser strength property of 20.36 MPa. It can be accomplished by including nanoscale SiO_2 fillers. The additional fillers were securely supported by PALF fibers,

resulting in strong binding (Lakshmaiya et al. 2022). Inter-laminar shear force improved as the interaction among fillers and polymers improved. The presence of gaps and holes in the manufactured composites causes the hybrid composites to deteriorate faster, lowering the strength properties of the composites. The emergence of additional fractures and voids in B-type hybrids lowered inter-laminar shear capacity, and other researchers have seen comparable decreases ((Maurya et al. 2021); (Sormunen et al. 2019)).

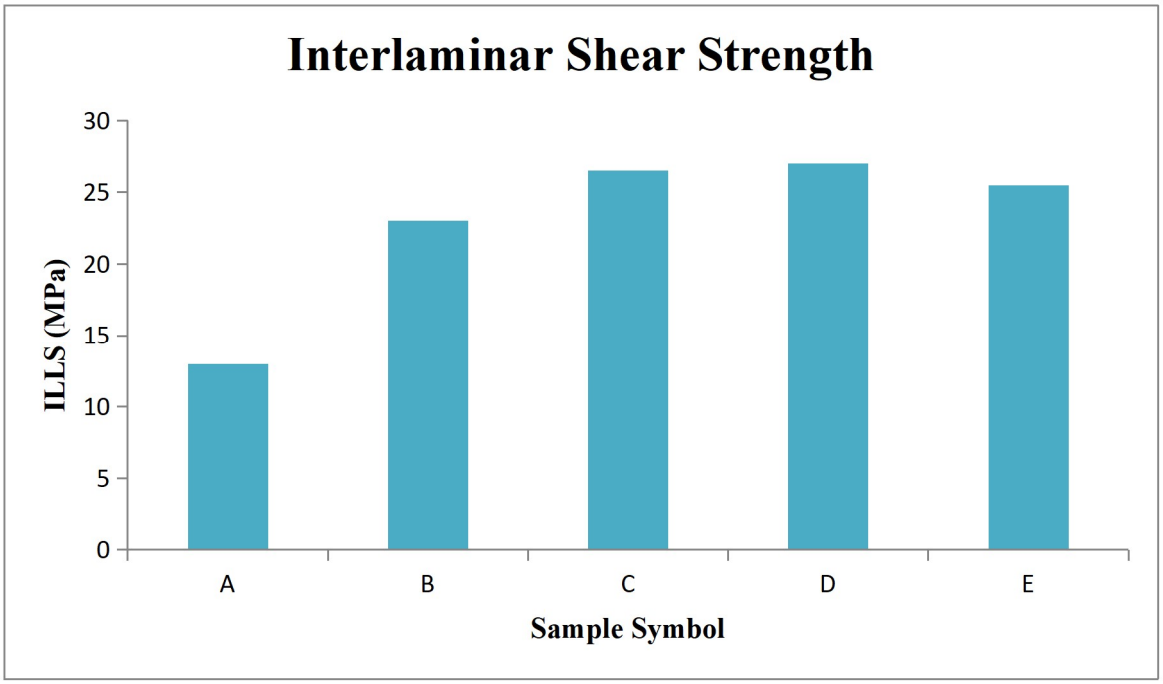

Figure 6: Interlaminar shear strength of PALF/ SiO_2-based hybrid composites

3.2.4 Impact and Hardness Properties

An automated Izod impact tester was used to measure the fracture toughness of epoxy composite samples. Figure 7 depicts the fracture toughness of epoxy polymer hybrid composites as a function of the presence of SiO_2 nanoparticles. Figure 7 shows that the fracture toughness of the D and E-type composites has increased and reached the highest level of 6.32 and 5.24 kJ/m^2, respectively, which would be higher than the A, B, and C-type composites. The impact resistance of the polymer binder has also been determined to match the stiffness of the polymer system. The inclusion of 6% SiO_2 nanoparticles increased the stiffness of the epoxy-reinforced hybrid because SiO2 connects several different epoxy networks via -COOH and -OH structural features. Additionally, the inclusion of filler particles reduces the fracture toughness of the epoxy-reinforced hybrid by increasing the filler particle concentration (Sitticharoen et al. 2016). The fortification from pressing in the sample is referred to as the characteristic Shore D toughness. The shoreline D hardness values of the produced epoxy composite samples are shown in Figure 7. This specimen's Shore D toughness is mostly determined by stiffness. In this study, both the outer and interior sections of the SiO_2 sample were made of PALF fiber, and the SiO_2 nanoparticles became tougher. In comparison to hybrid composites, sample D does have the maximum value of Shore D toughness of 73.21, and similar findings were also investigated by Bharath et al. In comparison to hybrid composites, sample B (without filler) does have a smaller value of Shore D toughness at 41.36 owing to the decreased rigidity of PALF fabric.

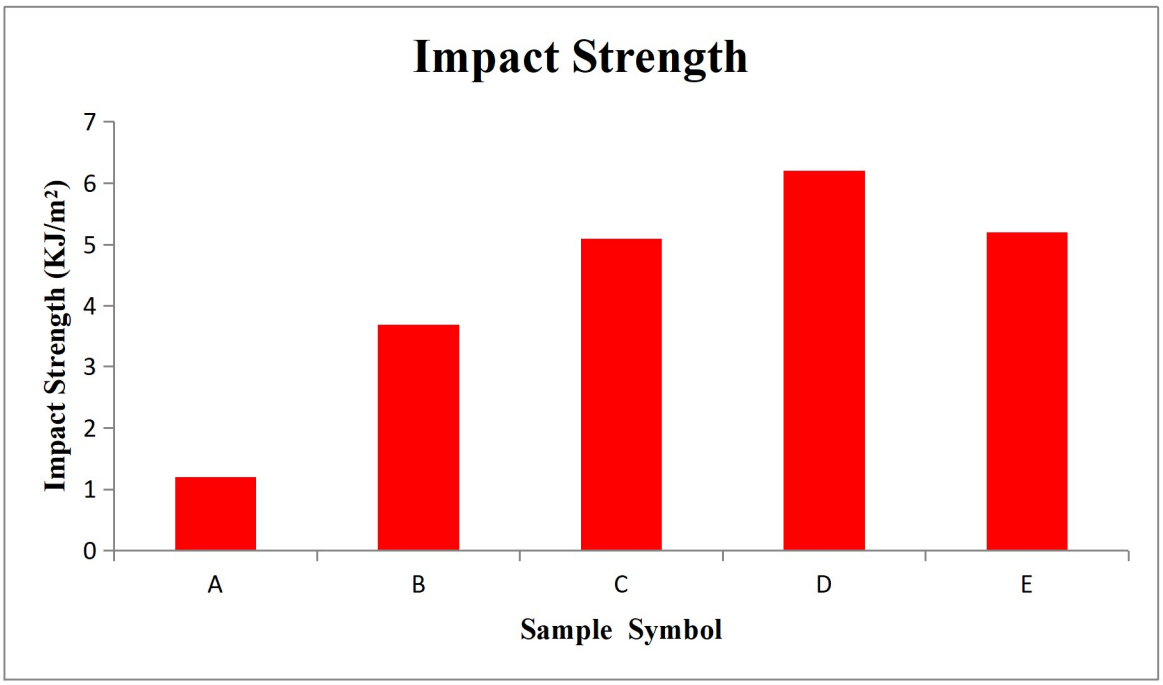

Figure 7(a) : Impact strength of PALF/ SiO_2-based hybrid composites

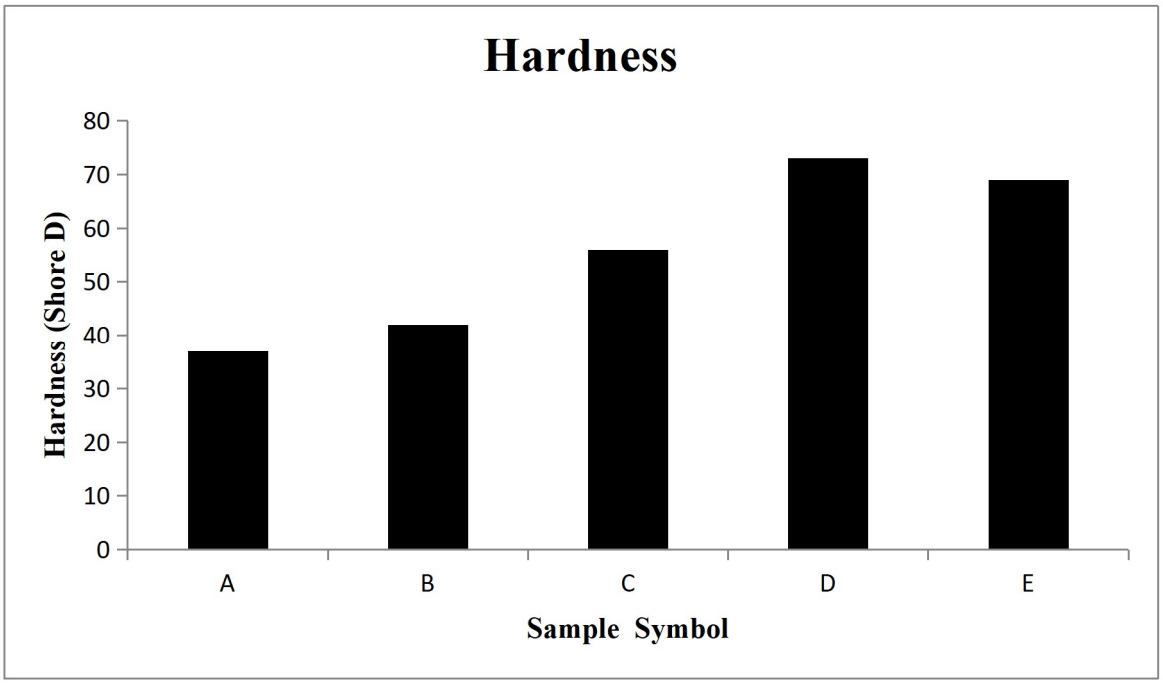

Figure 7(b): Hardness property of PALF/ SiO_2-based hybrid composites

3.2.5 Microstructural Analysis

The surface morphology of A, B, C, D, and E-type blends is shown in Figure 8. The PALF was strongly linked with the polymers in the PALF-reinforced epoxy (Figure 8(a)), as well as the rupture that developed throughout the fibers. This might be owing to the fundamental features of moisture absorption. Since PALF includes around 70% cellulose. Figure 8 (b) shows the SEM characterization of the composite's D type fractured tension reinforcement. PALF fibers and nanocrystalline SiO2 have been thoroughly entrenched in the epoxy, and the fibers have been coated and moistened with polymer. There aren't any visible cavities or gaps among the basic matrix and fiber. The direction of fibers within the matrices is crucial, as they seem to be dispersed equally at all four edges of the matrices (Natrayan et al. 2022). Effective binding at the intersection of PALF fiber, SiO_2, and epoxy matrices results in excellent fiber and polymeric contact. The surface morphology was also found to be rough, with branching, bending cracking, and cracked locking. These properties were also investigated in the particulate epoxy sphere. The failure mode of the 9 wt. % SiO_2 and 25% PALF-reinforced epoxy polymers appeared coarse, and more particles appeared to have deboned

from the polymers, as seen by the voids surrounding the fillers. Figure 8(c) also showed the existence of a basis for filler to accumulate. The concentration of SiO_2 nanoparticles acted as a carrier of failures, potentially reducing the material properties even more.

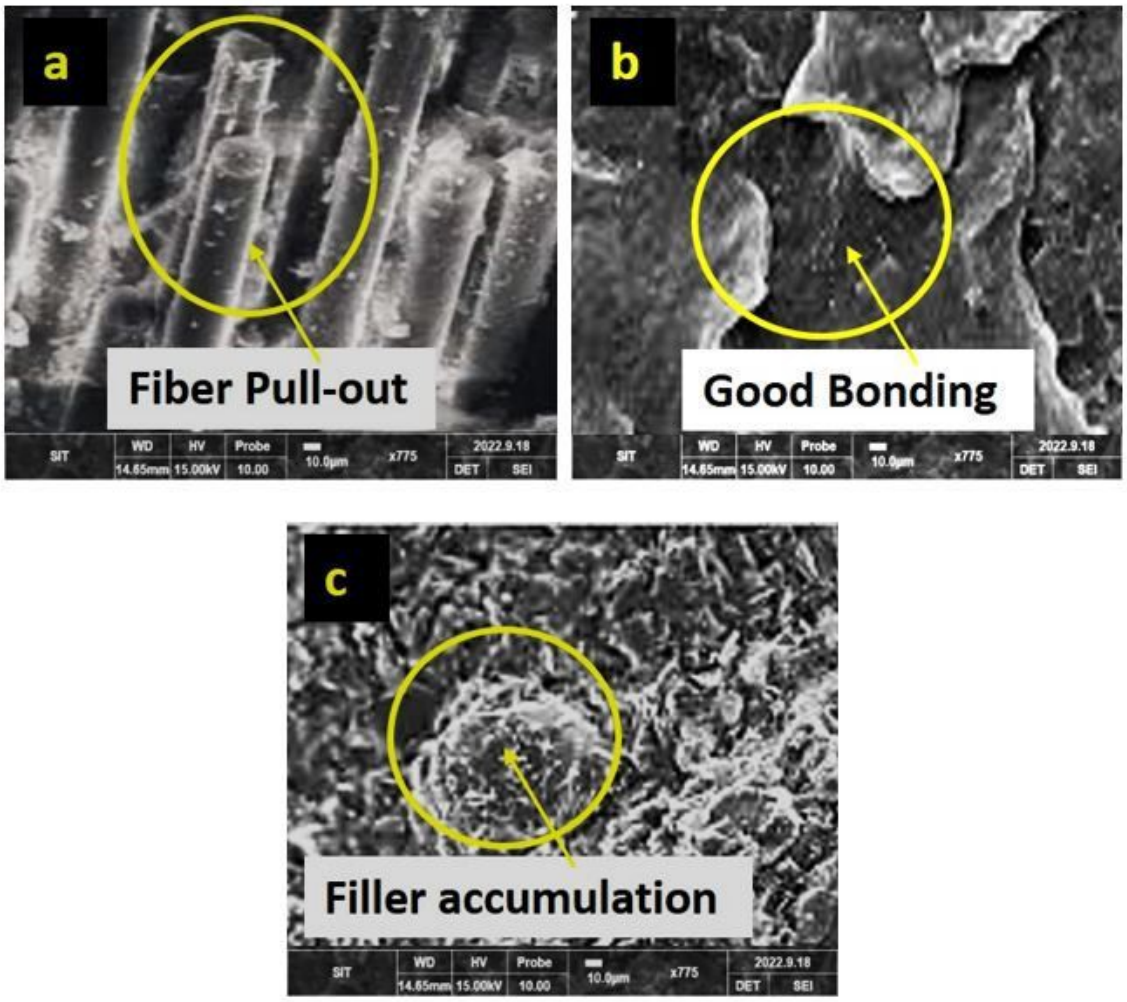

Figure 8: Micro-structural Images of (a) PALF, (b) PALF/6 wt. % of SiO_2, (c) PALF/9 wt. % of SiO_2 -based hybrid composites

3.3 Dynamic Mechanical Analysis

They are:

3.3.1 Storage Modulus

Figure 9 illustrates the DMA curves of PALF materials and SiO_2-based hybrid materials. Figure 9 also explains the storage modulus profiles of materials with a different weight proportion of SiO_2 filer. The maximum storage modulus at 30 ºC is 6 wt. % SiO_2/PALF. This seems to be owing to the composite's higher interfacial compliance, which limits the movement of polymeric chains and leads the contact between the fibers and the matrix to transfer greater loads, raising the rigidity of a material. The higher the loss ratio, the greater the amount of energy wasted by contact between the matrix and reinforcement.

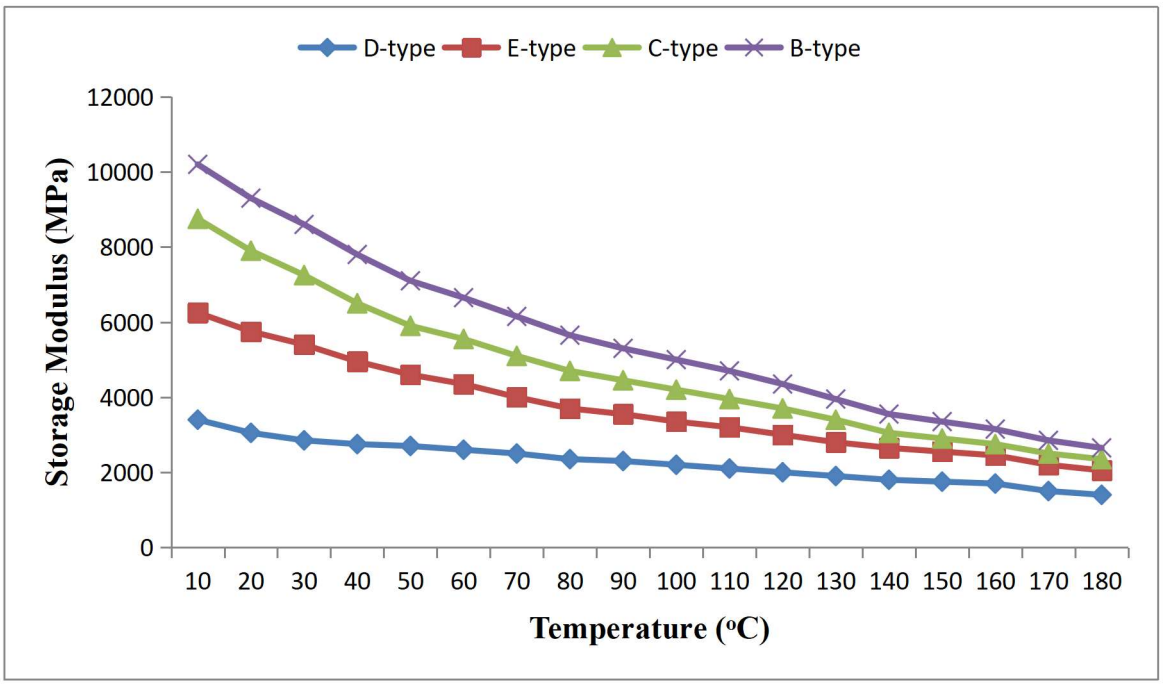

Figure 9. Storage Modulus of PALF/ SiO_2-based hybrid composites with a different weight ratio of filler content

3.3.2 Loss Modulus

The proportion of loss modulus to storage modulus is equivalent to the value of the dissipation factor, which makes it an essential metric when evaluating the mechanical behavior of fiber-reinforced materials. Figure 10 depicts the tan curve of a mixture before and after alteration. The change in temperature graphs in the image demonstrates that the enhanced composite's temperature of glass transition (Tg) is generally rising. With a SiO_2 level of 6 wt. %, the Tg of a hybrid increases by 20°C to 156.6°C when compared to the PALF material. When the degree of polymerization changes from a glassy to a rubbery condition as the temperature increases, the polymer moves substantially higher cohesion and friction barriers, which leads to greater energy loss, a worse storage modulus, and increased failure. The contact of a SiO_2/PALF composite with a weight of 6 % has a high adhesion property, a strong capacity to control the motion of an adhesive long sequence, as well as a low coecient of friction energy usage. As a result, its storage modulus diminishes rapidly, as does the amplitude of tan. Whenever the SiO_2 levels are excessive (9 wt%), aggregates on the fiber surface impede resin-fiber interaction, and interfacial bonding is poor, leading to greater energy dissipation (Chai et al. 2022).

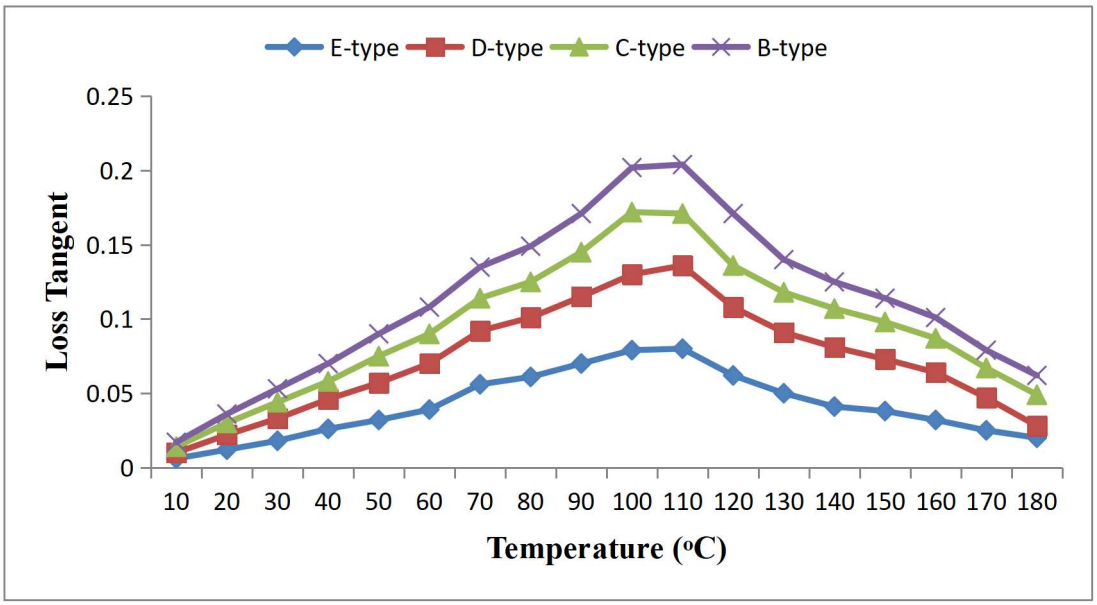

Figure 10. Loss Modulus of PALF/ SiO_2-based hybrid composites with a different weight ratio of filler content

3.4 Thermogravity Analysis

TGA is commonly used to assess the thermo-stability of materials. As seen in Figure 11, materials breakdown may be split into two phases: moisture and impurity breakdown (0 – 300 C), as well as resin condensation and degradation (300 – 600 ºC). Because the mass decrease induced by moisture and impurity breakdown represents around 5 % of the overall mass, the temperatures equivalent to 95% of a starting weight are referred to as the original degradation temperature (Natrayan et al. 2022). Because the breakdown temperatures of PALF fiber and SiO_2 are substantially greater than 600°C, the decrease in quality materials beyond 400°C is entirely due to resin combustion and deterioration. Figure 11 reveals that the rst degradation rate of the SiO_2-incorporated composites is nearly the same, at around 400°C, which is significantly higher than the starting decomposition temperature of PALF (300°C). This could indicate that the fiber and polymer get a stronger bond, which reduces the polymer's mobility and increases the mixture's thermo-stability. Also, the remaining weight of the composite changes drastically at 600°C. PALF, 3 wt. % SiO_2, 6 wt.% SiO_2, and 9 wt.% SiO_2 had residual masses of 60 %, 62 %, 56 %, and 50 %, respectively. Since the SiO_2 concentration is insufficient to be disregarded, we assume that the majority of the remaining section is made up of PALF fiber. The PALF fiber concentration in hybrids with 3 wt. % SiO_2 and 6 wt.% SiO_2 is lower compared to PALF. The possible explanation for this could be that the SiO_2 framework includes decreased interaction deficiencies, the closely packed framework between the ber and the epoxy allows the polymer to invade the fiber, the resin content is comparatively enhanced, as well as the fiber content is comparatively lowered, and the PALF fiber content is 9 wt.% SiO_2, which might be attributable to aggregation on the fiber surface, but also precludes the efficient approach of fiber and matrix, culminating in so many deficiencies and holes in the specimen.

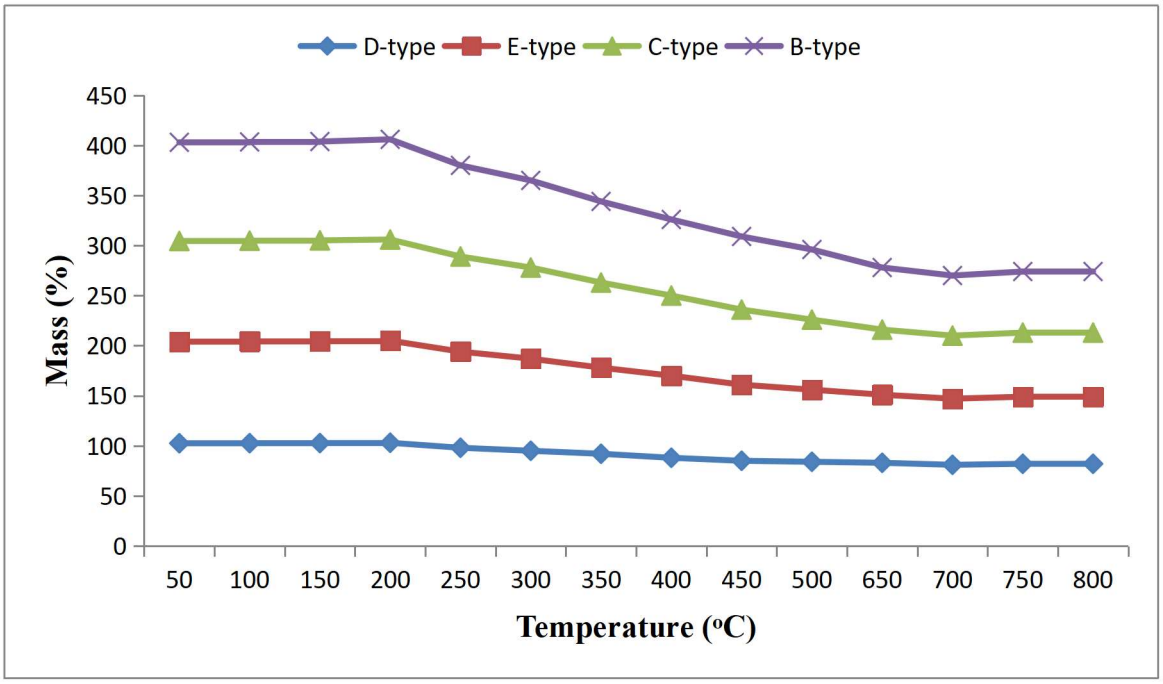

Figure 11. Storage Modulus of PALF/ SiO_2-based hybrid composites with a different weight ratio of filler content

3.4 Moisture Absorption Behaviour

Figure 12 depicts the water absorption properties of PALF and PALF/ SiO_2 polymer composites. It is mostly determined by Fickian diffusion. Moisture content is critical for all living things. It also becomes absorbed after 60 days. For all epoxy composite samples, both the maximal water usage and the beginning time for moisture absorption increased. Water uptake qualities of composite resin are examined using factors such as immersion time, filler-to-polymer ratio, processing technologies, filler, and matrix characteristics in a given environmental condition. The hydrophilic properties of leaf fibers are mainly accountable for this moisture absorption. Moisture is mostly utilized by the additives found in polymer composites strengthened with lignocellulosic biomass, such as PALF. Because the epoxy resin is hydrophobic, its moisture consumption may be decreased. Likewise, the water uptake behavior of SiO_2 nanoparticle-loaded PALF epoxy hybrid lamination is lower than that of PALF hybrids. The SiO_2 nanocrystals reduce the vacancy fraction of the composites, resulting in a reduction in water uptake capacity (Velmurugan et al. 2022). Moisture resilience is improved in the altered composites.

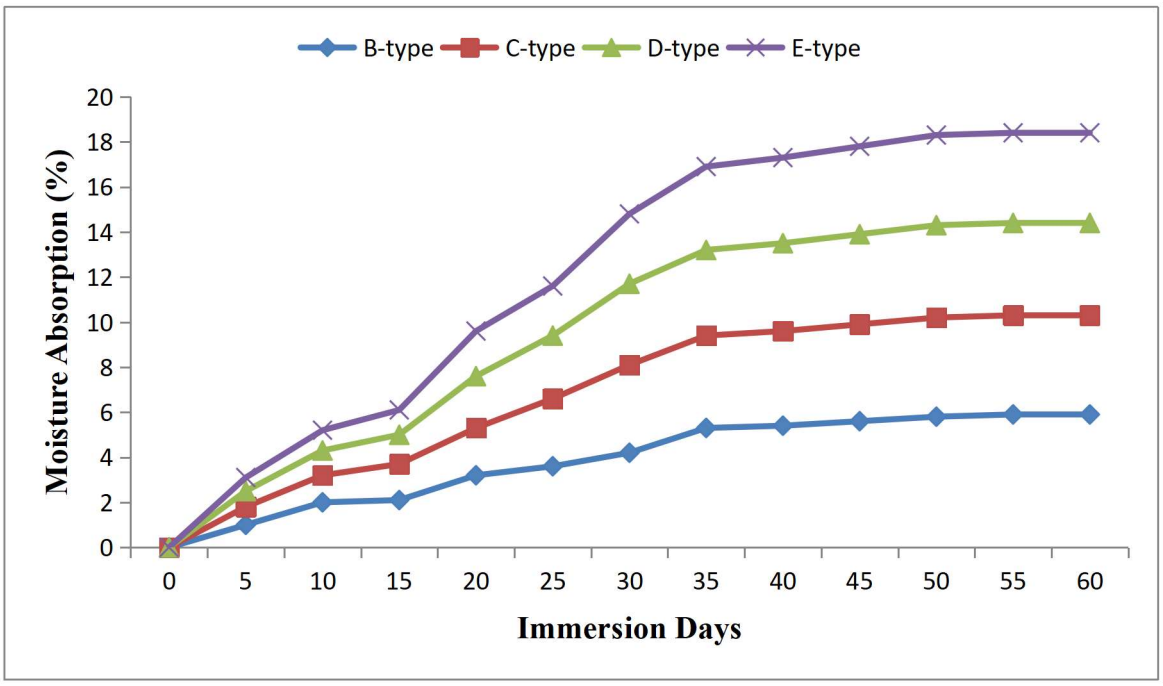

Figure 12. Storage Modulus of PALF/ SiO_2-based hybrid composites with a different weight ratio of filler content

4. CONCLUSION

PALF fiber reinforced with varied weight proportions of SiO_2 filler-based hybrid composites were generated in this experiment, and the composites were tested for mechanical characteristics such as tensile, bending, hardness, ILSS, impact strength, and dynamic mechanical analysis. The following conclusions were drawn from the findings: The bending vibration of N-H groupings around 2800 cm^{-1} was widened, perhaps due to interactions of hydrogen bonds among SiO_2 nanoparticles and PALF fiber. Trend shifts from 1793 to 1798 cm^{-1} as well as 3640 to 3680 cm^{-1}, correspondingly, guarantee the presence of the hydroxyl group among-OH and -C = O. The vibrating wavelength of Si-OH changes from 3923 to 3969 cm-1, indicating the presence of silicon in the epoxy. Among the five different types of composites i.e A, B, C, D and E types, the D-type composite (25 wt.% of PALF with 6 wt.% of SiO_2 filler) reveals high tensile (46.18 MPa) and E-type (25 wt.% with 9 wt.% SiO_2) composites reveals high flexural (58.96 MPa) strength. Even though contrasted with pure resin, hybrids laminate C, D, and E-type demonstrated 13.25 %, 23.36%, and 20.36% increases in tensile strength as well as 32.65 %, 45.62 %, and 4012 % increases in elastic strength. The flexural strengths rose by 30 %, 42 %, and 45 % in bio-composites such as C-type, D-type, and E type, respectively. This increase was caused by the efficient load transfer across matrices to reinforcements as a consequence of the strong esters, hydroxyls, and nylon binding interactions among PALF fiber and resin, as well as the good distribution of nanocrystalline silicon dioxide. The sample D-type has a greater ILSS property of 27.12 MPa among different kinds of manufactured epoxy hybrid materials, whereas the sample B-type has a lesser strength property of 20.36 MPa. Inter-laminar shear force improved as the interaction among fillers and polymers improved. According to the SEM analysis the failure mode of the 9 wt. % SiO_2 and 25 % PALF-reinforced epoxy polymers appeared coarse, and more particles appeared to have deboned from the polymers, as seen by the voids surrounding the fillers. According to TGA results the rst degradation rate of the SiO_2-incorporated composites is nearly the same, at around 400°C, which is significantly higher than the starting decomposition temperature of PALF (300°C). This could indicate that the ber and polymer get a stronger bond, which reduces the polymer's mobility and increases the mixture's thermostability. The water uptake behavior of SiO_2 nanoparticle-loaded PALF epoxy hybrid lamination is lower than that of PALF hybrids. Declarations Authors' contributions Velmurugan G: Conceptualization, Writing an original draft, Methodology.

Conflict of interest

The authors declare that there is no conflicting interest in the publication of this paper.

Acknowledgements

This paper was not supported by any financial grant from granting bodies. The authors really appreciate by acknowledging Engr. Dr. George. O. O. for his active inputs and contributions needed for the outcome of this publication financially and otherwise.

References

Gholampour, A., Ozbakkaloglu, T .(2020). A review of natural fiber composites: properties, modification and processing techniques, characterization, applications. Springer US

Väisänen, T., Das, O., Tomppo, L .(2017). A review on new bio-based constituents for natural fiber polymer composites. Journal of Cleaner Production 149:582–596. https://doi.org/10.1016/j.jclepro.2017.02.132

Velmurugan, G., Babu, K .(2020). Statistical analysis of mechanical properties of wood dust filled Jute fiber based hybrid composites under cryogenic atmosphere using Grey-Taguchi method. Materials Research Express 7:. https://doi.org/10.1088/2053-1591/ab9ce9

Sharma, M., Sharma, R., Chandra Sharma, S .(2020). A review on fibres and fillers on improving the mechanical behaviour of fibre reinforced polymer composites. Materials Today: Proceedings 46:6482–6489. https://doi.org/10.1016/j.matpr.2021.03.667.

Gouda, K., Bhowmik, S., Das, B .(2021). A review on allotropes of carbon and natural filler-reinforced thermomechanical properties of upgraded epoxy hybrid composite. Reviews on Advanced Materials Science 60:237–275. https://doi.org/10.1515/rams-2021-0024

Sanjay, M. R., Madhu, P., Jawaid, M .(2018). Characterization and properties of natural fiber polymer composites: A comprehensive review. Elsevier B.V.

Johny, V., Kuriakose Mani, A., Palanisamy, S .(2023). Extraction and Physico-Chemical Characterization of Pineapple Crown Leaf Fibers (PCLF). Fibers 11:5. https://doi.org/10.3390/ b11010005

Todkar, S. S., Patil, S. A .(2019). Review on mechanical properties evaluation of pineapple leaf bre (PALF) reinforced polymer composites. Composites Part B: Engineering 174:106927. https://doi.org/10.1016/j.compositesb.2019.106927

G V, K B, L IF .(2020). Optimization on Mechanical Behavior of Hemp and Coconut Shell Powder Reinforced Epoxy Composites Under Cryogenic Environment Using Grey-Taguchi Method. SSRN Electronic Journal. https://doi.org/10.2139/ssrn.3654034

Velmurugan, G., Siva Shankar, V., Kalil Rahiman, M .(2023). Effectiveness of silica addition on the mechanical properties of jute/polyester based natural composite. Materials Today: Proceedings 72:2075–2081. https://doi.org/10.1016/j.matpr.2022.08.138

Tang, C., Li, X., Yin, F., Hao, J .(2017). The performance improvement of aramid insulation paper by nano SiO_2 modification. IEEE Transactions on Dielectrics and Electrical Insulation 24:2400–2409. https://doi.org/10.1109/TDEI.2017.006560

Ponnusamy, M., Natrayan, L., Patil, P. P .(2022). Multiresponse Optimization of Mechanical Behaviour of Calotropis gigantea/Nano-Silicon-Based Hybrid Nanocomposites under Cryogenic Environment. Adsorption Science and Technology. https://doi.org/10.1155/2022/4138179

Chai, R., Zhu, W., Li, Q .(2022). Effect of Basalt Fiber Content on Mechanical and Tribological Properties of Copper-Matrix Composites. Metals 12:. https://doi.org/10.3390/met12111925

Kavya, H. M., Bavan, S., Yogesha, B .(2021). Effect of coir fiber and inorganic filler on physical and mechanical properties of epoxy based hybrid composites. Polymer Composites 42:3911–3921. https://doi.org/10.1002/pc.26103

Hoque, M. B., Hossain, M. S., Nahid, A. M .(2018). Fabrication and Characterization of Pineapple Fiber Reinforced Polypropylene Based Composites. Nano Hybrids and Composites 21:31–42. https://doi.org/10.4028/www.scienti c.net/nhc.21.31

Natrayan, L., Kumar, P. V. A., Baskara Sethupathy, S .(2022). Water Retention Behaviour and Fracture Toughness of Coir/Pineapple Leaf Fibre with Addition of Al_2O_3 Hybrid Composites under Ambient Conditions. Adsorption Science and Technology 2022:. https://doi.org/10.1155/2022/7209761

Hamid, N. H., Hisan, W. S. I.W. B., Abdullah, U. H .(2019). Mechanical properties and moisture absorption of epoxy composites mixed with amorphous and crystalline silica from rice husk. BioResources 14:7363–7374. https://doi.org/10.15376/biores.14.3.7363-7374

Lakshmaiya, N., Ganesan, V., Paramasivam, P., Dhanasekaran, S .(2022). Influence of Biosynthesized Nanoparticles Addition and Fibre Content on the Mechanical and Moisture Absorption Behaviour of Natural Fibre Composite. Applied Sciences (Switzerland) 12:.https://doi.org/10.3390/app122413030

Maurya, A. K., Gogoi, R., Manik, G .(2021). Mechano-chemically activated y-ash and sisal fiber reinforced PP hybrid composite with enhanced mechanical properties. Cellulose 28:8493–8508. https://doi.org/10.1007/s10570-021-03995-4

Sormunen, P., Kärki, T .(2019). Recycled construction and demolition waste as a possible source of materials for composite manufacturing. Journal of Building Engineering 24:100742. https://doi.org/10.1016/j.jobe.2019.100742

Sitticharoen, W., Chainawakul, A., Sangkas, T., Kuntham, Y .(2016). Rheological and mechanical properties of silica-based bagasse-fiber-ash-reinforced recycled HDPE composites. Mechanics of Composite Materials 52:421–432. https://doi.org/10.1007/s11029-016-9594-z

Natrayan, L., Kumarm, P. V. A., Baskara Sethupathy, S .(2022). Effect of Nano TiO2Filler Addition on Mechanical Properties of Bamboo/Polyester Hybrid Composites and Parameters Optimized Using Grey Taguchi Method. Adsorption Science and Technology. https://doi.org/10.1155/2022/6768900

Natrayan, L., Kumar, P. V.A., Kaliappan, S .(2022). Optimisation of Graphene Nano filler Addition on the Mechanical and Adsorption Properties of Woven Banana/Polyester Hybrid Nanocomposites by Grey-Taguchi Method. Adsorption Science and Technology. https://doi.org/10.1155/2022/1856828

Velmurugan, G., Siva Shankar, V., Natrayan, L .(2022). Multi-response Optimization of Mechanical and Physical Adsorption Properties of Activated Natural Fibers Hybrid Composites. Adsorption Science & Technology, 1–16. https://doi.org/10.1155/2022/1384738

George O. Okoronkwo, Kizito Chidozie Ibe, Simeon I. Bright. (2022). Application of ANN and RSM on the strength properties of alkali mercerized hybrid ramie-isora fibre reinforced biodegradable composites, *Journal of Inventive Engineering and Technology* (JIET), A Publication of the Nigerian Society of Engineers, Awka Branch. Vol. 2, Issue 3, pp. 40-61. @ Nigerian Society of Engineers, Awka Branch.

Ezeokpube Greg C., Okoronkwo George O, Onodagu Peter D. (2021). Natural fiber reggressors effects on physical and strength properties responses of bidirectional finger root fiber reinforced epoxy composites, *Journal of Inventive Engineering and Technology* (JIET), A Publication of the Nigerian Society of Engineers, Awka Branch. Vol. 1, Issue 5, pp. 1-15. @ Nigerian Society of Engineers, Awka Branch.

Ezeokpube Greg C., Okoronkwo George O, Onodagu Peter D. (2021). Strength properties analysis of biomimetic natural wire weed fiber reinforced polymer composite honeycomb plates, *Journal of Inventive Engineering and Technology* (JIET), A Publication of the Nigerian Society of Engineers, Awka Branch, Vol. 1, Issue 5, pp. 16-28. @ Nigerian Society of Engineers, Awka Branch.